Master’s Programme in Water and Environmental Engineering

Benchmarking and smart control in Finnish sewerage pumping stations

My Chu

Master’s Thesis
2023

Aalto-yliopisto
Aalto-universitetet
Aalto University

Author My Chu

Title of thesis Benchmarking and smart control in Finnish sewerage pumping station

Programme Master's Programme in Water and Environmental Engineering

Thesis supervisor Prof. Riku Vahala

Thesis advisor(s) Prof. of Practice Markus Sunela

Collaborative partner Fluidit Oy

Date 31.05.2023 **Number of pages** 84 + 16 **Language** English

Abstract

Sewerage system avoids flood and pollutants being discharged into the environment, which presents considerable economic, social, and environmental impacts. Due to the worldwide energy crisis and climate change from urbanization, the current network capacity and control will not be sufficient. Hence, we need better control for the pumping stations to satisfy future requirements. The goal of the work is to create an overall picture of the current Finnish sewerage systems and evaluate the effectiveness and applicability of smart control in reducing energy consumption and flooding.

The study was conducted in two phases: benchmarking and smart control solutions. In the first phase, the performance of the wastewater system in general and pumping stations specifically in five water utilities (HS-Vesi Oy, Porvoon Vesi, Kurikkan Vesihuolto Oy, Kouvola Vesi, and Tuusulan Vesi) was analyzed with their hydraulic performance and flood-risk assessment, therefore pointing out the opportunities for improvement. Following this, several pumping station chains were selected for applying smart control. The second phase was to develop a suitable wet well's level control algorithm based on two principles: variable speed drive and feedback PID controller.

The results indicated that the infiltration rate of the Finnish sewerage network was on an average level and the energy efficiency was on a fair to poor level, according to studies from other countries and based on the assessment standards. Yet, there is an opportunity to apply energy-recover equipment in the future. When comparing the five studied sites, Kurikka and Porvoo had lower infiltration rates, while Kouvola and Hämeenlinna had higher energy efficiency.

The proposed level control worked at its best during conditions that have high total inflows, in combination with more suitable pump selections. More thorough research should be done in the future on the energy-saving potential of using variable speed drives in combination with level control. The level control performance in overflow reduction was restricted to a definite level based on the network capacity. When the total network capacity has been utilized, additional storage is suggested to store the overflows.

Keywords Sewer network, energy efficiency, energy balance, overflows, level control, friction loss, pumping station, variable speed drive

Contents

Preface

I would like to express my gratitude to all the partners for entrusting me with this project.

Firstly, I want to mention my sincere recognition for Fluidit Ltd. Company. I owe many thanks to my advisor, CTO Markus Sunela for his guidance and support anytime I need him. His patience and feedback taught me much valuable knowledge and also important insights into the industry. Warm thanks to CEO Timo Ranta-Pere and Co-founder Kalervo Aho for creating the amazing thesis opportunity to elevate my expertise for my future career. I would also like to give a big acknowledgment to Mika Kuronen for coordinating the project, keeping up everything on track, and interacting with the clients. Along with Mika's advice in my thesis process, I am also very grateful to have Janne Väyrynen and Pedro Almeida, who are always willing to give me a hand, answering all of my questions nicely and in the easiest way to understand. Moreover, I want to show appreciation to Lauri Rantala for always being there, not only for helping with my work-related problems but also for your moral support and thoughtfulness. Thank you Moein for your answers regarding the storm network. It was such a pleasure to work with everyone and learn from the best experts.

Secondly, Aalto University contributed significantly to the instruction, planning, and execution of this educational program as well as the creation of this master's thesis. I would like to express my sincere gratitude toward my supervisor Prof. Riku Vahala for his tutoring during this thesis.

Special thanks to the five water utilities that provide the data used and access to their sewer network models: HS-Vesi Oy, Porvoon Vesi, Kurikkan Vesihuolto Oy, Kouvola Vesi, and Tuusulan Vesi. A huge thank to Maa- ja vesitekniikan tuki ry for your financial support during the finalizing phase.

Lastly, I want to thank my family, especially my mother and grandmother, for their encouragement and support during my overseas studies. There were many tough points in the thesis writing process, and I am very grateful to have my friends by my side to keep me sane. Thank you, Jasmin, Chacha, Carla, and Gabe for your accompany on the Aalto campus and for improving my thesis presentation.

Symbols and abbreviations

Symbols

$\boldsymbol{h}$ or $\boldsymbol{H}$	height or depth
$\boldsymbol{l}$ or $\boldsymbol{L}$	length
$\boldsymbol{\mu}$	coefficient
A	area
$\boldsymbol{q}$ or $\boldsymbol{Q}$	flow rate
$\boldsymbol{h}$	pump head
$\boldsymbol{I_S}$	sewer slope
$\boldsymbol{I_R}$	friction slope
$\boldsymbol{S}$	slope of the energy line
$\boldsymbol{n}$	Manning's roughness coefficient
$\boldsymbol{R_h}$	hydraulic radius
$\boldsymbol{c}$	coefficient depending on the friction properties of the pipe
$\boldsymbol{d}$	diameter
$\boldsymbol{f_v}$	resistance number
$\boldsymbol{\varepsilon}$	coefficient of pipe roughness
$\boldsymbol{h_L}$	local loss
$\boldsymbol{k}$	resistance factor
$\boldsymbol{v}$	velocity
$\boldsymbol{N}$	pump rotational speed
$\boldsymbol{P}$	power
$\boldsymbol{g}$	gravitational constant
$\boldsymbol{\eta}$	pump efficiency
$\boldsymbol{\rho}$	density
$\boldsymbol{E_s}$	specific energy
$\boldsymbol{G}$	gravitational constant
$\boldsymbol{K_P}$	constant proportional gain
$\boldsymbol{K_i}$	constant integral gain
$\boldsymbol{K_d}$	constant derivative gain
$\boldsymbol{e}(\boldsymbol{t})$	error at time t

Abbreviations

EPA	Environmental Protection Agency
I/I	Infiltration and inflow
JVP	Jäteveden pumppaamo – wastewater pumping station
NLS	National Land Survey of Finland
PAS	Performance Assessment System
PID	Proportional-Integral-Derivative automatic control method
PVC	Polyvinyl chloride
SYKE	Suomen ympäristökeskus - Finnish Environmental Center
WWTP	Wastewater treatment plant

1 Introduction

The sewerage system operation is to avoid overflow and pollutants being discharged into the environment, which presents considerable social, economic, and most importantly, environmental impacts. A sufficient drainage system is needed for establishing a safe urban environment. Thus, optimizing the design of sewage pumping stations system and sewage pipe network layouts is of considerable practical significance and economic value.

Due to climate change, the frequency of heavy rainfall or snowmelt will be increased, while urbanization and the capacity of current sewerage facilities will not be sufficient for draining (United Nations, 2014). Moreover, the existing simple on-off control of the pumping station based on only start-up and shut-off depth will lead to an overloaded situation in extreme weather and causing floods. Besides, wastewater treatment plant mostly has a fixed maximum capacity and cannot control or predict disturbances such as rainfall, hence, sudden massive inflow will be partly bypassed the environment and damage the biological system (Ganora et al, 2017).

There have been numerous attempts to reduce energy consumption and costs associated with sustainable water use because of the global energy crisis and the need to lower greenhouse gas emissions. One of the critical and cost-effective solutions is to optimize pump scheduling and recover excessive energy whenever feasible (Marinaki and Papageorgiou, 2005). The wastewater system needs to adapt and consider innovative approaches because energy is lost not only in pumping stations but also in the system structure due to pipelines and exfiltration.

There are countless drawbacks to the currently available control system. With the hydrological model, the parameters need to be calibrated and it often requires a massive amount of data. Yet, in return, the error can be minimized but cannot be avoided. According to Marinaki and Papageorgiou (2005), nonlinear optimal control is the most effective approach with its capability in predicting inflow, process nonlinearities, and constrain, however, the sophisticated codes cause problems for the real-time optimal solution. On the other hand, multivariable regulators, based on simpler codes, have issues when operating in a large-scale network because of dimensionality and its linear programming approach (Marinaki and Papageorgiou, 2005). Physical-based methods, however, can be more effective and simpler to implement. For example, a case in Portugal using real-time control with a PID feedback controller (Pereira, 2019) based on WWTP capacity and measurement data at the pumping station. The wastewater will be divided and treated in different WWTP based on different scenarios. However, the system needs accurate sensors and one of the most drawbacks is that it can be very complex to tune, location-specific, and can create difficulties for developers, hence needing more research.

1.1 Goals, research questions and scope

The first goal of the thesis is to create an overall picture of the Finnish sewer pumping station's energy consumption by studying the measurements of energy and cost efficiency of pressurized sewers and comparing the hydraulic design performance in different locations based on the topography, network capacity, and weather. Defining the smart control methods' effectiveness in controlling floods and reducing energy consumption, as well as evaluating their practicalities in implementation is another goal of this study.

The main objectives are described in the following research questions:

Phase 1 questions:

How is the current performance of the pumping station and sewer network of the studied area, compared to other utilities?

1. Which locations in the area is flood-prone that require higher control to prevent future crisis? Which station can be allowed to have floods?
2. Which stations in the area consume lots of energy? Besides, which have low energy efficiencies, high head losses, and unsuitable pump models that need further improvement?

Phase 2 questions:

How can energy consumption and overflow be reduced by changing the pumping schedule of a specific pumping station chain and maximizing the network capacity?

1. What is the capacity limit of a specific network concerning wastewater treatment plant intake and different storm intensities to avoid flood?
2. What are the suitable pumping rate and pump models considering the rotational speed, efficiency, and pumping scheme?

The scope of the research is limited to the currently existing network and the data provided by the five utilities which took part in the project: HS-Vesi Oy (Hämeenlinna regions), Porvoon Vesi, Kurikkan Vesihuolto Oy, Kouvola Vesi, and Tuusulan Vesi. The latest sewer network models with their network information system (NIS) are given for analysis, together with the measurement of customers' water use, pumping station flow rate, and approximately measured pumping station flow rates and energy use if applicable. The statistical analysis will not deliver a conclusion beyond the provided data and the suggested pumping control will not propose additional construction to the network.

1.2 Thesis structure

The thesis structure is divided into seven chapters. The first chapter provides the background, targets, and scope of this study. In the second chapter – the literature review, the background information of the sewerage network with their hydromechanics terminology was introduced as an overview. The chapter also gives an outline of the energy balance in the sewer system, the sanitary overflows, and the pumping station control methods.

The research process and the methods utilized for each step of the research are illustrated in Chapter 3 to describe the study's methodology. Each analysis is discussed and explained, as well as the study location and data sources. The analysis is divided into two phases: analyzing Finnish sewerage networks performance based on the five sites under study, and then evaluating the efficacy of the suggested smart control technique based on the energy-saving and overflow reduction potential.

In Chapter 4 and Chapter 5, the results of benchmarking phase for all five water utilities and smart control methods optimization applied in three regions are shown. Following, Chapter 6 delivers a thorough discussion of the results. An overall evaluation of the Finnish sewer system is made along with the comparison between the five studied sites. The takeaways from Chapter 4 and Chapter 5 are pointed out and explained. Chapter 6 begins with a discussion of the study's uncertainties and concludes with suggestions for future studies.

Finally, the conclusion is summed up in Chapter 7.

2 Literature review

Urban drainage systems have an important role in the planning and development of cities as they manage the waste discharged into the environment. The sewer system is designed to collect wastewater through pipes to a centralized treatment location. The sewage system must be properly maintained to prevent infiltration, inflow, or exfiltration from happening within the collection path (Karttunen, 2004). In the following sections, the sewer system components, hydromechanics and relevant background information for the study such as the energy balance, sanitary overflows, and pumping station control method will be presented.

2.1 Sewer network components

A sewer network comprises a set of elements that take place in different processes, for instance, storing the wastewater volume in the storage unit or the transportation of pipes and the merging of flow in the nodes. In the following subsections, the main elements are described with their core function and impact on the system generally.

2.1.1 Pipes

The network contains a series of pipes with drainage outlets that connect the lines of the individual facilities to the group network. Wastewater can be transported by gravitational flow or using a pumping station when gravity flow is not possible due to topography difficulties through pressurized lines (Walski, 2004). There are various sets of pipe materials for wastewater collecting purposes, which can be used in different conditions, such as ductile iron, concrete, plastic, and vitrified clay (EPA, 2000). Plastic pipe in general and polyvinyl chloride (PVC) specifically is chiefly used for wastewater systems and high-pressure pipes, which has proven its high durability and stiffness properties as well as resistance to highly aggressive substances (Uponor, 2014). Likewise, in recent years, polypropylene has been increasingly used in sewer networks due to its high impact resistance and good temperature resistance.

2.1.2 Pumping station wet well

The wet wells in pumping stations are modeled through the continuity equation comprising the presently stored water in the tank, adding the incoming flow to the reservoir and extracting the pumped flow from the reservoir and the possible overflow.

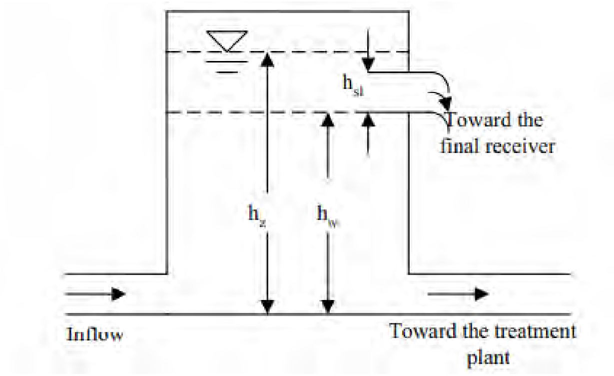

Figure 1: Reservoir capacity (Marinaki and Papageorgiou, 2005)

The overflow and water level of the reservoir relationship is shown in equation (1), along with the visualization for the variables in Figure 1:

$$q_{over} = \begin{cases} 0, if\ h_z - h_w \leq 0 \\ \frac{2}{3}\mu_P\sqrt{2g}(h_z - h_w)^{3/2} l_w\ (Poleni\ formula), if\ h_z - h_w \leq h_{sl} \\ \mu_T\sqrt{2g}(h_z - h_w - h_{sl}/2)^{1/2} A\ (Toricelli\ formula) \end{cases} \quad (1)$$

where:
h_w is the weir's height (m).
h_{sl} is the height of the slot over the top of the weir (m).
l_w is the weir's length (m).
μ_P is an overflow coefficient (Poleni formula).
μ_T is a coefficient for the flow under pressure from the slot (Toricelli formula) $(\mu_T = (2/3)\mu_P\sqrt{2})$
A is the slot's area (m^2) ($A = h_{sl}\ l_w$).

2.1.3 Nodes

The transmission and combining of flows take place at the network connections, which represent the manholes in reality. Propagation and merging are the two types of nodes that can be recognized. The propagation node has one incoming link and one outgoing flow for connecting sewers with different geometry. Hence, the inflow and outflow of the node are the same. On the other hand, merging nodes are where more than one incoming flow merges into one outgoing flow. Therefore, the sum of incoming flows is the outgoing flow from the nodes. (Marinaki and Papageorgiou, 2005)

2.1.4 External Inflows

The flow into a sewer system can be divided into flow components. The sum of flow is called wet weather flow (WWF) and includes all the water that goes into the sewer system. The WWF can be divided into the flow that only appears due to precipitation, the rainfall-derived inflow and infiltration (RDII), and the base wastewater flow (BWF). The latter can be further divided into dry weather flow (DWF) and groundwater infiltration (GWI). DWF is caused by water consumption by residents, which is often the same as potable water consumption measured by water meters. (EPA, 2008)

2.1.5 Treatment Plants

Before releasing the sewer into the environment, the sewage will be treated in a facility in which a combination of various processes such as physical, chemical, and biological treat the wastewater and remove pollutants, called a sewage treatment plant. With the preliminary treatment, coarse materials can be easily removed from screening, grit, and grease removal. Following, primary treatment or so-called sedimentation tanks will remove a large portion of suspended solids and organic matter. Biological processes are utilized to get rid of the remaining soluble organic material, excessive phosphorus, and nitrogen by using microorganisms, creating biological floc or biofilm. Lastly, tertiary treatment includes biological nutrient removal, disinfection, and removal of micropollutants such as environmentally persistent pharmaceutical pollutants. (Davis, 2020)

After being treated to remove and neutralize potentially harmful components following the regulatory standards, the effluent is then discharged to the local waterways or reused for other suitable purposes. Nonetheless, there will be specific situations where the incoming water flow rate goes beyond the treatment plant limit capacity, which leads to partially untreated wastewater being released to the nearby streams. This discharge type is defined as an unauthorized release or wastewater bypass (Weyrach et al., 2010). The release occurs when a sanitary sewer overflows from a plugged collection system or pumps untreated wastewater out of a manhole to a nearby ditch, usually due to rain or snowmelt that creates this inundated area. On the other hand, a bypass of wastewater from an outfall is authorized by the facility's permit which cannot cause effluent limit exceedance. The sewer bypass can be diverted around a clarifier or dichlorination system (Minnesota Pollution Control Agency, 2020).

2.2 Hydromechanics

In the study of pumping and pipe flow, the consideration is based on hydrodynamics – the motion of a fluid and the forces generated by the motion. The section will present the most important terms needed and related to wastewater network model formation. The quantities needed for the energy consumption and efficiencies analysis are defined from hydromechanics equations.

2.2.1 Flow mechanism

The foundation for the mathematical modeling of the hydrodynamic link element is the Saint-Venant equation. From the equation, the dynamic behavior of the flow in the sewer system is accurately modeled, taking into account the friction and inertia of the flowing liquid and backward phenomena (Labedie et al., 1980). The first continuity equation shows the mass conservation of the liquid:

$$\frac{\partial F(h)}{\partial h}\frac{\partial h(x,t)}{\partial t}+\frac{\partial q(x,t)}{\partial x}=0 \quad (2)$$

where:

$q(x,t)$ is the flow (m^3 /s) at location x (m) along the sewer axis at time t

$h(x,t)$ is the depth of sewer flow (m) at location x (m) along the sewer axis at time t

$F(h)$ is the cross-sectional area of flow (m^2)

The second Saint-Venant equation includes the momentum equation:

$$\frac{1}{g}\frac{\partial v}{\partial t} + \frac{v}{g}\frac{\partial v}{\partial x} + \frac{\partial h}{\partial x} = I_S - I_R \tag{3}$$

where:
I_S is the sewer slope
I_R is the friction slope $I_R = cq^2R(h)^{-4/3}F(h)^{-2}$
g is the gravitational acceleration (m/s²)
$\frac{\partial h}{\partial x}$ is the slope of the water's surface
$\frac{v}{g}\frac{\partial v}{\partial x}$ expresses the influence of the change of the energy height along the sewer (when the flow is rapidly changing in space)
$\frac{1}{g}\frac{\partial v}{\partial t}$ expresses the influence of the time-change of the velocity (when the flow is locally changing rapidly over time, the flow is stationary)

In the sewerage system, there are two flow subcategories, which are open flow and pipe flow. While in open channel flow, the liquid is affected by atmospheric pressure, the pipe flow takes place in a closed environment. Since in the pipe flow, the tube needs to be filled with liquid, it is applied in pressure lines. By contrast, the gravitational tubes are usually only partially full, hence, the case is open channel flow. (Munson et al., 2005)

Head losses occur inside the pipes depending on several factors such as the flow rate, the diameter, material, and length of the pipe. The magnitude of flow losses should be determined since it holds an important role in estimating the pipe size and pump head. Manning, Hazen-Williams, and Darcy-Weisbach are the three most common equations for figuring head losses in sewer networks.

The Manning equation stated below is used exclusively for open-channel flow:

$$Q = \frac{1}{n}AR_h^{2/3}S^{1/2} \tag{4}$$

where:
n is Manning's roughness coefficient (-)
S is the slope of the energy line (m/m)
A is the cross-sectional area of the flow (m²)
R_h is the hydraulic radius (m)
Q is the flow rate (m³/s)

Head loss in pressurized lines can be determined by two formulas, both approaches have their pros and cons, explained in Table 1. To begin with, the empirically based Hazen-Williams formula is presented in the following:

$$h_v = L \cdot \sqrt[0.54]{\frac{Q}{0.278 \cdot c \cdot d^{2.63}}} \tag{5}$$

where:
L is pipe length (m)
Q is the flow rate (m³/s)

c is the coefficient depending on the friction properties of the pipe. The coefficient can vary depending on the pipe material and the age of the material. The value is experimentally determined, however, for plastic pipe, the value is about 130 to 150.

Head loss from the Darcy-Weisbach formula, which is more physically based and preferred in Europe, can be more accurate than the Hazen-Williams formula, that only applied to water in a turbulent flow. While water's temperature and viscosity are not accounted for in Hazen-Williams, Darcy-Weisbach can be applied to determine the pipe's head loss for any Newtonian fluid in all flow regimes. (Walski et al., 2007). The Darcy-Weisbach can be shown below:

$$h_v = f_v \cdot \frac{L}{d} \cdot \frac{v^2}{2g} \tag{6}$$

$$\frac{1}{\sqrt{f_v}} = -2log(\frac{2.51}{R_e\sqrt{f_v}} + \frac{\varepsilon/d}{3,7}) \tag{7}$$

where:

L is pipe length (m)

d is the inner diameter of the cable (m)

f_v is the resistance number, which can be obtained from equation (5)

ε is the coefficient of pipe roughness.

Local losses:

Various local factors affecting fluid flow, such as pipe inlets, outlets, valves, pipe size changes, and pipe angles, cause local losses. Compared to losses from flow, local losses are often small. If the flow rate changes, it can be expressed below:

$$h_L = k(\frac{{v_1}^2}{2g} - \frac{{v_2}^2}{2g}) \tag{8}$$

where:

h_L is the local loss (m)

k is the resistance factor

v_1 and v_2 is a higher flow rate and a lower flow rate correspondingly.

Head loss

The pump head, known as the total dynamic head (TDH) in Figure 2, is the difference in suction to the discharge point of the pump. A pump's function is to provide the additional energy required to overcome head losses and height variations. The static height (Figure 2), or geodetic head, is the amount of head required to create the real elevation difference between the water level in the trench and the highest point of the discharge pipe. Hence, as demonstrated by Walski et al. (2007), the system head curve is created by adding the additional head required to make up for head losses to the static head.

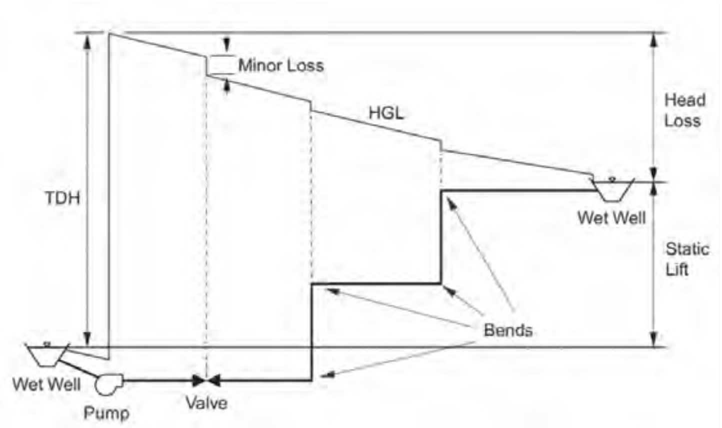

Figure 2: Hydraulic grade line for a pumped system (Walski et al., 2007)

Throughout a pump cycle, the static head between a pumping station and its discharge point will alter continuously. The typical method for defining the geodetic head when dimensioning a pump is to utilize the average water level between the start and stop. Determining the proportion of elements in the total head is needed to ensure the appropriate pump fits the necessary geodetic head in a pump installation or pumping station. (Nasik, 2010)

Surcharge methods

For learning the hydrological process, Storm Water Management Model (SWMM) software is widely utilized to analyze the sewer network. In hydromechanics, the surcharge is the condition that the sewer is flowing fully under a pressurized condition. There are two surcharge methods mainly used to handle this specific situation in the SWMM model simulation: Preissmann SLOT and EXTRAN.

Both surcharge methods are based on the Saint Venant equations, yet the pressurized flow is converted to synthetic open channel flow before applying the St. Venant formula in Preissmann SLOT (Wood and Heitzman, 1983). The EXTRAN approach uses the variation of the Surcharge Algorithm to update nodal heads (Wood and Heitzman, 1983) while the SLOT options will add a virtual top surface width to full flowing pipes so that pressurized flow can be treated similarly to unsteady flow in open channels in SWMM (Malekpour and Karnev, 2014). Each method has its disadvantages. EXTRAN does not employ discretization within conduits and has a long computational time because it needs a small routing time-step to maintain stability and flow continuity (Pachaly et al., 2021). Preissmann SLOT cannot maintain negative pressures regularly that might falsely diversify the flow regime disregarding the actual ventilation of the system. Moreover, numerical oscillation can happen in this method (Pachaly et al., 2020).

2.2.2 Theory of pump

Pumping stations are a component of sanitary sewage systems that raise gravity sewers from their lower location for pumping across drainage divides or for transferring sewage over long distances on flat land (Walski et al., 2007).

Pumps and pump motors
Numerous configurations are possible for pumping stations. A separate wet and dry well for storing wastewater and housing pumping equipment is often the most expensive station to build and is only utilized for large systems. In a dry well, floods can still occur even though the pump motors are above the flood level. Submersible pumps, on the other hand, are more typical. While wet-pit pump motors are situated at an elevation that won't be inundated and is connected by a shaft to the pumps below, submersible pump motors are likewise submerged. The design flow needs to be higher than the station's maximum anticipated inflow. Due to the capacity, the station should have several pumps. The most typical setup is a duplex system, in which typically one pump can maintain the design flow and the other supplementary pump will work with higher inflows. The appropriate motor type should be chosen in this regard. (Walski et al., 2007)

Centrifugal pump
Depending on the pump's functions and the pumped liquid, pumps have been classified corresponding to their basis of applications. According to Karttunen (2004, 25), dynamic and displacement are the two main groups. Centrifugal pumps are the most popular dynamic pumps used in wastewater pumping stations because they are cost-effective and have a good ability to transfer suspended particles (Walski et al., 2007). A rotating element (the shaft and impeller that transform mechanical energy into hydraulic energy) and a stationary element (the casing, casing cover, and bearings) make up the pump. The impeller can have a single inlet or double suction and can be either radial-flow, axial-flow, or a mix of the two (Spellman, 2003).

Variable speed pump system
A variable-speed pump is a pump coupled to a variable-speed drive or controller such that the voltage of the pump motor is varied by rotating the motor rotation, as opposed to a centrifugal pump, which typically has a set rotational speed and impeller diameter (Walski et al., 2007). The characteristic curve of the pump will change as the speeds change. The use of variable-speed pumps improves process control, lowers maintenance costs, and saves energy (Hydraulic Institute, 2004) where there are significant system head changes for a given flow rate, such as in a sewer force main with many pumps. Pullin (2009) claimed that it is economically practical to manage the pumps' speed when dynamic losses make up more than 50% of the total losses.

Yet, there have been noted that installing a variable speed pump does not reduce the system energy consumption in every case, not to mention some reported an increase in energy consumption. The increase in energy usage can be caused by two reasons, partial impeller clogging – extending the run times because of longer operational cycles, and operation of the pump's best efficiency point, which results in systems with a high static head percentage. (Flygt, 2013). It is noted that the flow rate in the pressurized pipes affects the force main sedimentation level as well as the energy consumption, where the two are contradictive, as shown in Figure 3 below. In short, the low pumped flow reduces energy usage, however, increases the risk of sedimentation. Hence, variable speed pumping should not allow fluid velocity to go below the limit to avoid the issue, for instance, the recommended value is 0.7 m/s (Fair, 1968).

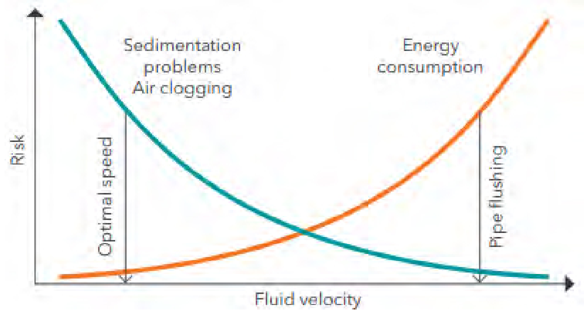

Figure 3: Fluid velocity effects on sedimentation and energy consumption (Flygt, 2013)

With a 20% margin to manage under-voltage and overload scenarios, the motor in wastewater pumping applications should be able to supply the impeller with the full torque necessary to cope with any potential clogging issues. Therefore, a variable speed drive that can generate nominal torque at startup and maintain double the nominal torque at its maximum working speed for at least one second is required.

Affinity laws:
By altering the rotational speed of the centrifugal pump, affinity rules are used to control its performance. In practice, when a pump's rotational speed changes significantly, the pump's efficiency must be taken into account (Halonen, 1987). The flow rate for a specific point on the pump's characteristics changes as the rotational speed does, and at the same time, the head changes as the square of the speed, and the power changes as the cube of the speed, as shown in the following equations:

$$\frac{Q}{Q_f} = \frac{N}{N_f} = n \tag{9}$$

$$\frac{h}{h_f} = \left(\frac{N}{N_f}\right)^2 = n^2 \tag{10}$$

$$\frac{P}{P_f} = \left(\frac{N}{N_f}\right)^3 = n^3 \tag{11}$$

where:
Q is pump flow (m³/s) and Q_f is flow at full speed (m³/s)
N is the rotational speed of the pump (rpm) and N_f is the rotational speed of the pump at full speed (rpm)
n is the ratio of pump speed to full speed
h is the pump head (m)
h_f is the pump head at full speed (m)
P is the power (kW) and P_f is the power at full speed (kW)
(Karassik, 1998)

2.2.3 Energy efficiency

Pumping systems consist of the pump, its motor, piping, valves, and instrumentation. The energy and materials used by a system depend on the design of the pump, the installation, and the process condition. The correct sizing of the pump represents the most significant economic opportunity to reduce energy consumption. (Ruuskanen, 2007). The power that is delivered to the water from the pump, hydraulic power P_H, is defined as below (Wirzenuis, 1978):

$$P_H = \rho g Q H \tag{12}$$

where:
ρ is the volumetric mass density of water (kg/L)
g is the gravitational constant (m²/s)
Q is the flow rate of the pump (L/s)
H is the head of the pump (m)

The electrical power that is delivered to the motor can be defined as input power P_E. Brake power, or so-called shaft power P_S, is determined as the power given to the pump from the motor:

$$P_S = \frac{P_H}{pump\ efficiency} \tag{13}$$

A centrifugal pump's total efficiency is the sum of its mechanical, volumetric, and hydraulic components. Losses in the stuffing box, bearing frame, and mechanical seals are included in the mechanical efficiency. In the case of semi-open impellers, vane clearances, balancing holes, and leaks through wear rings are all included in the volumetric efficiency calculation. Hydraulic efficiency, the main consideration despite the mechanical and volumetric losses, takes into account liquid friction as well as additional losses in the volute and impeller. (Evans, 2012). The centrifugal pump and induction motor both just have two main parts that the designer can change. It is the rotor and the stator in the case of the motor. (Walski et al., 2007). The motor efficiency of the pump is determined by calculating the ratio between the input power and the brake power at the working point:

$$\eta_M = \frac{P_S}{P_M} \tag{14}$$

The pump efficiency can be determined from the hydraulic power and the brake power:

$$\eta_P = \frac{P_H}{P_S} \tag{15}$$

Overall, the wire-to-water efficiency can be expressed as follows based on the ratio of hydraulic power to input power:

$$\eta_{TOT} = \frac{P_H}{P_E} = \eta_P \cdot \eta_M \cdot \eta_{VSD} \tag{16}$$

(Wirzenuis, 1978).

Specific energy:

The quantity of energy required to pump a specific liquid volume is known as specific energy. The value cannot be used as the reference for comparison between other pumping systems without accounting for system differences because it is valid only for the specific pump system for which it was calculated (Bulu, 2018).

$$E_s = \frac{energy}{volume}\left[\frac{kWh}{m^3}\right] = \frac{h}{\eta}\rho g \cdot \frac{1}{3600000}\left[\frac{kWh}{m^3}\right] \quad (17)$$

where:
E_s is the specific energy (kWh/m^3)
h is the total head delivered from the pump (m)
η is the total efficiency of the pump (%)
ρ is the density of the fluid (kg/m^3)
G is the gravitational constant (m/s^2)

2.3 Energy balance

The energy balance of the entire system will produce a deeper understanding of energy-intensive components and identify measures to increase efficiency. Even though wastewater collection and transport consume roughly 6% of the total energy usage in this utility (Loureiro et al., 2020), improvement opportunities should be defined. The assessment supports the tactical level of management that points out the interventions in subsystems. The analysis also helps to capture the network at the operational level of management, critical subsystems can have their service improved by specific modification according to demand profiles. Hence, the energy-balance scheme is studied to estimate the percentage of intrinsic and external energy components coming in and out of the system, based on energy efficiency and different inflows components such as domestic, infiltration, and rainwater. (Jorge et al., 2021)

Unlike water supply system that mainly consists of pressurized pipes and has a higher chance to recover their energy through turbines at excessive pressures (Marchis et al. 2014), the use of energy recovery equipment is more challenging due to the fluid liquidity, containing possible solid materials and typical having low heads with high flow rates (Berger et al., 2013). Nevertheless, to visualize the energy balance of the system, the potential in reducing capital costs and optimizing the system's hydraulic design is significant.

Based on Jorge et al.'s studies (2014), the scope of the energy balance assessment only focuses on the transportation of the sewage and excludes the treatment steps. With the difference in weather conditions and the available data of flow measurement, network information, and energy components, the energy balance can be calculated with different maturity levels, layouts, and operation levels. First of all, the macro-level assessment can be used to estimate the energy consumption in the system with authorized and undue inflows. Following, the meso-level evaluation consists of the elevation-associated energy such as energy created by gravitational flow, together with the wasted energy components such as energy inefficiencies, friction losses, and local head losses. The micro-level assessment can be handled with a fully calibrated model, allowing for the formulation of enhancement measures at the tactical level of management as well as the identification of the system's primary inefficiencies.

Table 1. Energy balance (Jorge et al., 2021)

<table>
<tr><th colspan="2">Energy inflows</th><th colspan="3">Energy outflows</th></tr>
<tr><td rowspan="6">Total inflow **intrinsic energy E_I** (associated with gravity flow)</td><td rowspan="2">$\boldsymbol{E_{IAI}}$
Inflow intrinsic E associated with due inflows</td><td rowspan="6">Total inflow **intrinsic energy E_I**</td><td rowspan="2">Dissipated energy $\boldsymbol{E_{ID}}$</td><td>Inefficiencies in energy recovery equipment $\boldsymbol{E_{IDT}}$ (= 0)</td></tr>
<tr><td>Pipe friction, head losses $\boldsymbol{E_{IDL}}$</td></tr>
<tr><td rowspan="4">$\boldsymbol{E_{IUI}}$
Inflow intrinsic E associated with undue inflows</td><td rowspan="2">Energy associated with exceedance volume $\boldsymbol{E_{IEV}}$</td><td>Not consume energy $\boldsymbol{E'_{IEV}}$</td></tr>
<tr><td>Potentially consume energy $\boldsymbol{E''_{IEV}}$</td></tr>
<tr><td colspan="2">System downstream energy $\boldsymbol{E_{IDE}}$</td></tr>
<tr><td colspan="2">Recovered energy $\boldsymbol{E_{IRE}}$</td></tr>
<tr><td rowspan="3">Total **external energy** (electrical) $\boldsymbol{E_E}$</td><td>$\boldsymbol{E_{EAI}}$
External E associated with due inflows</td><td rowspan="3">Total **external energy** $\boldsymbol{E_E}$</td><td rowspan="2">$\boldsymbol{E_{ED}}$
Dissipated energy</td><td>$\boldsymbol{E_{EDE}}$
Due to inefficiencies in electro-mechanical equipment</td></tr>
<tr><td rowspan="2">$\boldsymbol{E_{EUI}}$
External E associated with undue inflows</td><td>$\boldsymbol{E_{EDL}}$
Due to pipe friction and local head losses</td></tr>
<tr><td colspan="2">Elevation-associated energy $\boldsymbol{E_{EE}}$</td></tr>
</table>

In terms of energy going in and out of the system boundary, the energy balance can be divided into the total energy influx and outflux. The sum of the total influx of intrinsic energy E_I and external energy E_E is the total energy influx utilized in the system for transportation. Total external energy E_E is the energy provided by the pumping stations, whereas total intrinsic energy E_I is the energy connected to the free surface flow (E_{IAI} and E_{IUI}). The outflux energy presents the energy loss by the system, including total intrinsic energy E_I refers to the system's downstream pipe friction and head losses, as well as the energy E_E associated with exceedance volumes that are not connected to energy-consuming components. On the other hand, total external energy can be broken down into elevation-associated energy (E_{EE}), which represents losses during the pumping of wastewater to the delivery point, and dissipated energy (E_{EDE} and E_{EDL}), which refers to mechanical losses and energy loss as a result of equipment inefficiency.

2.4 Sanitary sewer overflows

Despite having separate networks for sewage and rainwater, separated sewer systems can still be vulnerable to excessive precipitation. Sanitary sewer overflows (SSOs) happen when the flow in the system exceeds the capacity of the conveyance system, causing untreated sewage to be discharged into the environment before reaching a wastewater treatment plant. As a result, deteriorating water infrastructure raises the risk of flooding (EPA, 2016a). Due to rainfall-induced infiltration and in-flow (RDII) entering the sewer system, SSOs can happen during dry weather conditions, but they are more frequently linked to wet weather occurrences (EPA, 2000).

Sewer system overflows (SSOs) can happen for several causes, including bad weather, blockages and breakage in the sewer pipes, incorrect system operation and maintenance, and vandalism (EPA, 2016a). Surcharging causes an SSO when the hydraulic grade line rises to a point where the system is exposed to the environment when the flow exceeds the pipe's capacity. If flows are greater than the pumping capacity of the station or the hydraulic capacity of the headworks, a conveyance system may overflow at a pump station or treatment facility. As stated by EPA (2000), surcharging and backups can be made worse by reduced pipe capacity brought on by blockages (grease, debris, etc.), broken pipes, or joint failure. Additionally, SSOs happen when RDII and input result in a peak flow in the sewer that is greater than the capacity. Extraneous flow that enters the sewage system directly through connections is referred to as infiltration and inflow (l/l), as does infiltration during periods of heavy rainfall. RDII happens when stormwater runoff prompts a quick groundwater recharge near sewers, and the resulting water subsequently seeps into the system through broken pipes, faulty pipe joints, or damaged manhole walls. Peak wet weather flow, according to EPA (1995), varied between 3.5 and 20 times the typical dry weather flow. A metric that can be used to predict whether a sewer system will overflow is the ratio of peak rainy weather flow to average dry weather flow. The overflow typically grows with a ratio of 4 to 5, though how often it happens varies depending on the particulars of the system.

These incidents raise concerns because pathogen-filled raw sewage is released into the environment. Jahai et al. (2017) claim that when SSO incidents contaminate public areas and seas, people may be in danger of coming into contact with untreated sewage when enjoying themselves in open waters, consuming contaminated fish or shellfish, drinking contaminated water, or coming into contact with contaminated flood waters. In September 2000, after a million-gallon SSO event into Goodwin Hollow Creek, an underground stream that fed multiple springs and served as the source for private water wells, residents of Springfield, Missouri, and nearby areas received drinking-water alerts (EPA 2000).

Regular sewer system maintenance, eliminating I/I to reduce peak flows, improving conveyance and treatment capacity, and building more wet weather storage and treatment facilities are all ways to lower sanitary sewer overflows. Constructing overflows that exist in separate sanitary sewer systems is another short-term measure to reduce the harm to property and health hazards brought on by other overflows, such as basement flooding. A surcharged sewer has the potential to leak raw sewage into nearby groundwater and other areas through open joints. To lessen harm to the building, constructed overflows may also be installed at pumping stations and treatment plant headworks. (EPA 1995)

In Finland, ice jams are a unique phenomenon of rivers in cold climates that restrict flow and raise water levels, which can result in flooding and property damage (Aaltonen and Huokuna, 2017). Hence, when the water level is rising in seas and rivers where the overflow pipe is connected, water can start to flow backward into the sewer system (Wapro, 2020). Therefore, backflow prevention devices should be applied to avoid accidents.

2.4.1 Flood risk map

As claimed by SYKE (2016), flood risk mapping is necessary to identify potential flood-prone locations and to help with land use planning, rescue efforts, and communication. Large amounts of input data are needed to create reliable hazard maps, including information on the existing hydro-technical infrastructure and how it functions as well as spatial data (such as information on land use, digital terrain models, and cross sections of rivers). To simulate how flooding spreads throughout the landscape, these data are fed into hydrological and hydrodynamic models (Fischer and Stanchev, 2022). Information on the elements that are susceptible to floods, such as data on the population and social infrastructure, is required to develop flood risk maps.

Morante-Carballo (2022) asserts that there are various techniques for analyzing and estimating the risk of flooding. The empirical approaches, which needed accuracy in calibration and data validation but were simple to use and supported other modeling tools, were one of the first methodologies. Following, hydrodynamic models concentrate on simulating the motion of the flow in 1D, 2D, and 3D using mathematical models. Furthermore, although the simplified conceptual models also use mathematics, they don't need to be precise in terms of flow dynamics and have the smallest computational cost.

2.5 Pumping station control methods

The optimal operation of a sewer network implies that overflow should not take place anywhere in the network and the system consumes energy efficiently. A structure for real-time control of sewer networks that combines high efficiency, low implementation cost, and reduce substantial overflows can be composed of many control layers. Due to the direct consideration of input forecasts, process nonlinearities, and limitations, nonlinear optimum control is the most effective method. Based on significantly simpler computation codes, multivariable regulators can approximate the effectiveness of nonlinear optimal control. The "curse of dimensionality" makes it challenging to use dynamic programming methodologies on large-scale networks, even while linear programming may not take into account the nonlinearities of the process. However, developing and maintaining expert systems, fuzzy control, or heuristic techniques is more difficult and time-consuming. (Marinaki and Papageorgious, 2005)

A control system is a single device or a group of connected devices that manages, commands, or controls the behavior of devices or systems. Systems for controlling machinery or equipment are utilized in industrial production. (Goodwin et al. 2000). Among two common classes of the control system: open-loop and closed-loop, the latter system, also called the feedback control system, is more widely used, and operates due to its accuracy. While the output of the open-loop does not affect the control action of signal input, the current output in the closed-loop approach is taken into consideration and corrections are made based on feedback. Hence, the system is highly effective in making corrections using a feedback mechanism. (Ellis, 2004)

2.5.1 PID Controller

A common control loop feedback mechanism in industrial control systems is the PID Controller, often known as a Proportional-Integral-Derivative controller. The size of the correction is proportional to the gap between the desired value (set point) and the measured value, and it is applied to the controlled variable (Ellis, 2004). Because the PID controller algorithm uses three distinct constant parameters, it is frequently referred to as three-term control:

$$u(t) = K_P e(t) + K_i \int e(t)dt + K_P \frac{de}{dt} \tag{18}$$

where:
K_P is the constant proportional gain
K_i is the constant integral gain
K_d is the constant derivative gain
$e(t)$ is the error at time t which is fed to the PID controller

The PID controllers were explained by Åström and Hägglund (1995). The value that is proportionate to the current error value is the output of the proportional term. The setpoint is approached further when the mistake is greater because the output value increases. The contribution of the integral term is inversely proportional to the magnitude and duration of the error. To get the integral, the instantaneous error must be added over time in order to get the cumulative offset (steady-state error), which should have been rectified earlier. Finding the error's slope over time and multiplying this rate of change by the derivative gain are the final steps in calculating the derivative of the process error.

In a nutshell, the time-variant feedback controller is as follows: 'P' depends on the present error, 'I' on the growth of past errors, and 'D' is a prediction of future errors based on the current rate of change. The weighted sum of these three actions is used to alter a control element, such as the placement of a control valve, the setting of a damper, or the design of a pump's rotational speed drive. (Ellis, 2004)

2.5.2 Wet well level control

Simple relay systems or solid-state controllers, such as specialized pump controllers and pump supervision units, can be used to start and stop pumps. Variable speed drives are frequently used as a means to control the speed of induction motors. PLCs (programmable logic controllers) are frequently used for larger, more complicated systems that require extensive specialized algorithms for the particular software. In order to correctly regulate the sequence and all pumps, a master controller is necessary. (Pohjola, 2006)

There are several pump sump level control methods to monitor the wet well level, preventing overfilling and subsequent pollution. Generally, the pump stations are operated at their pre-decided rotational speed and with an on-off mode where distinctive start and stop levels enable the wet well to fill and empty. One traditional method for variable speed operation is the constant level method (Figure 4). The water level is used as the reference input so that the frequency will be modified to maintain the constant level inside the wet well. For example, from James's study (2003), energy saving with constant level control of over 15% was achieved and pump cost saving would be contingent upon the used pump type. However, the method will waste energy as in low inflow situations, the pump is operated at too low speed and efficiency, not to mention the sedimentation risk in the pipes and partial pump clogging for non-self-cleaning pumps. (Flygt, 2013).

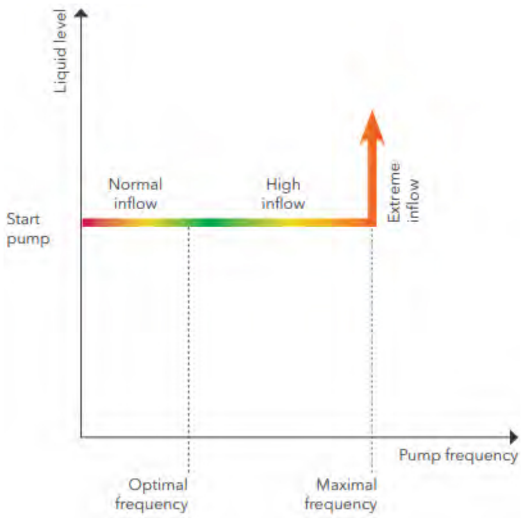

Figure 4. Traditional constant level control (Flygt, 2013)

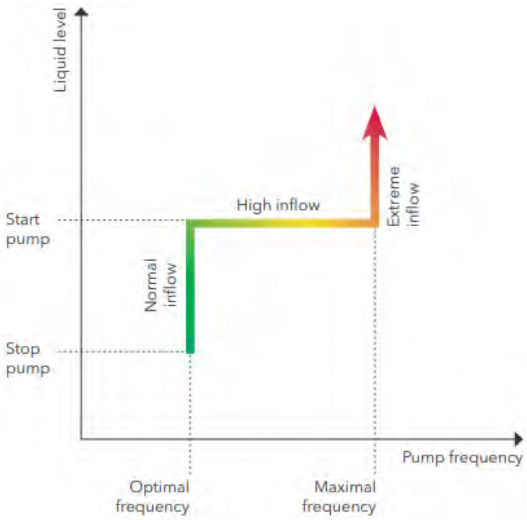

Figure 5. Optimal constant level control (Flygt, 2013)

Consequently, using a better optimal control that combines reduced speed and intermittent start-stop operation is the most energy-efficient approach for wastewater pump stations (Figure 5). It is vital to determine an appropriate distance between the start and stop levels to save energy for a sufficient time. The minimum energy frequency should be considered the optimal value to reduce energy consumption and maximize operational performance.

Similarly, Flygt (2013) continued introducing the variable level control (Figure 6) follows the same approach but is more advanced in the way that the inflow can be buffered to smoothen the pressurized flow, in other words, the velocity is proportional to the water level in the sump. As an illustration, the method had been used in a study by Fecarotta et al. (2018) to analyze an urban drainage system in Naples, Italy. By using optimal control, energy savings can range from an average of 32% to a maximum of more than 70% in the most convenient situation. The plant's features, including the inflow discharge and head loss, determine the amount of savings.

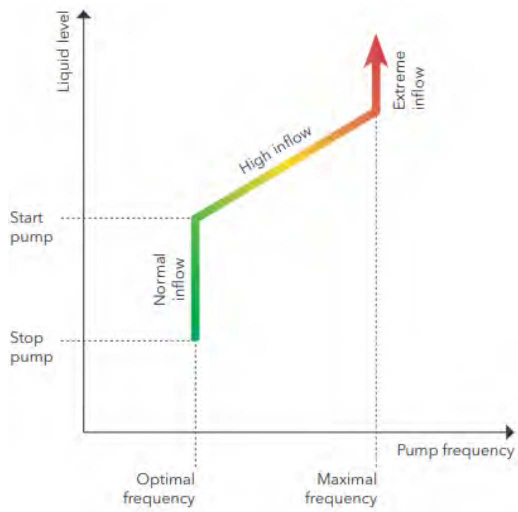

Figure 6. Variable level control (Flygt, 2013)

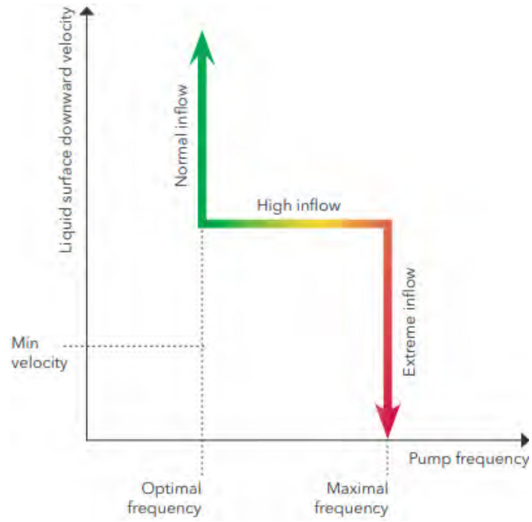

Figure 7. Minimum flow control (Flygt, 2013)

Last but not least, another widely used technique (Figure 7) is based on the use of the time-derivative of the wet well level: the normal on/off control is set at normal inflow with the best frequency, at higher inflow the pump speed will automatically increase to ensure the liquid surface velocity is equal to the minimum velocity, but the relation cannot be maintained at the extreme inflow.

3 Research material and methods

The study's main goals were to create and evaluate a general picture of the Finnish sewer pumping station based on five chosen water utilities and its performance improvement using the purposed control method. After the first phase which focuses on operation analysis, several pumping chains with low performance and likely overflow will be selected for the second phase. The results were studied using Fluidit Sewer 2.2, which is based on an extended version of OpenWaterAnalytic's version of EPASWMM simulator (5.1.13).

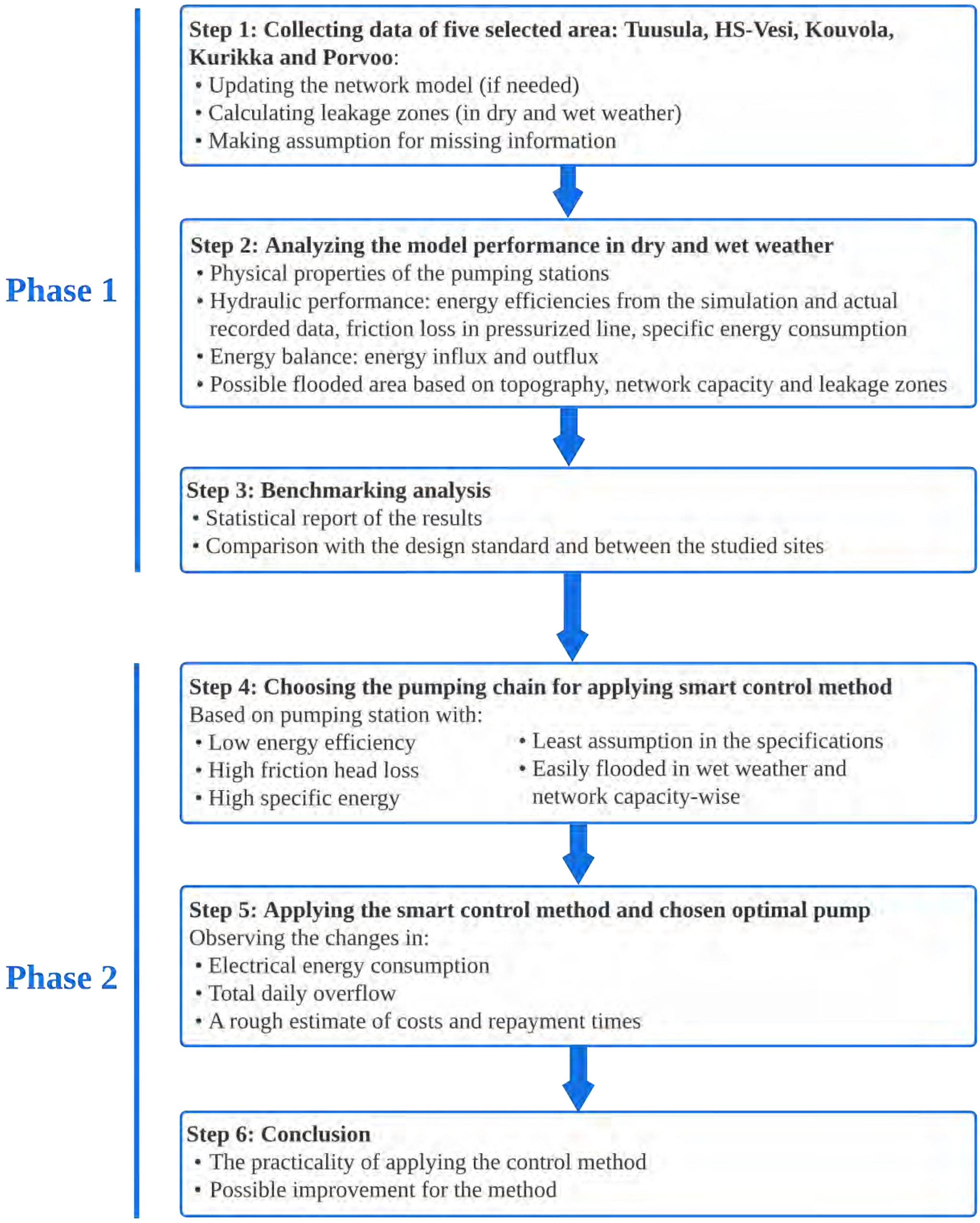

Figure 8. Research process

In Figure 8 above, the research process was demonstrated. The first step of the study was to update and complete the given information on the five water utilities for the model simulation. Next, the energy analysis was made in both dry and wet weather regarding the pumping station's physical properties (network length, pipe diameter, etc.), hydraulic performance (energy efficiency, friction loss in pressurized pipes, and specific energy consumption), and energy balances of the system. The inundation areas were also located based on flood-risk analysis. From the results, the conclusion for the benchmarking phase was established. Furthermore, from the first phase outcomes, the specific pumping chains were selected based on their low performance, hence, needed for the application of a smart control method and more suitable pump model. The benefit from the control was studied from the changes in energy consumption and overflows, with a rough estimation of cost in the end. The practicality of the control was then defined.

3.1 Data collection

The location of the studied areas in Finland can be found in Figure 9. The up-to-date network model was handled from 5 water utilities. In total, there were 9 different networks: HS-Vesi (Viiala, Toijala, Hämeenlinna), Porvoo, Kurikka, Kouvola, and Tuusula (Hyrylä, Jokela, Kellokoski). The summary information of the regions and their network can be observed in Table 2.

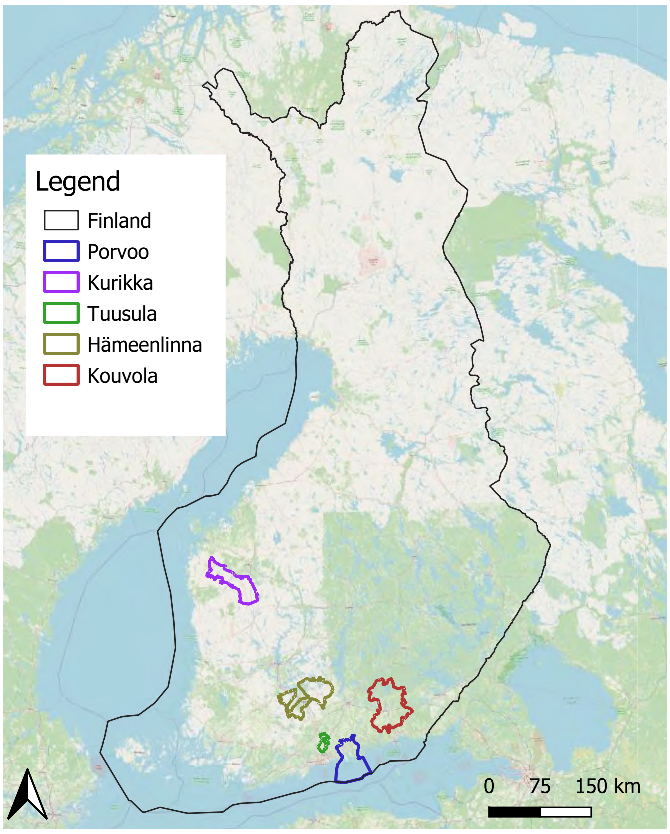

Figure 9. Location of five studied regions

Table 2. General information of the chosen studied regions

Name		Region area (km²)	Population	Network length (km)	Total inflows (m³/d)
HS-Vesi	Viiala	1 785	68 000	73	1 200
	Toijala			166	1 500
	Hämeenlinna			363	11 000
Kouvola		2 558	79 434	643	11 000
Kurikka		1 725	19 845	250	3 700
Porvoo		655	51 247	323	6 700
Tuusula	Hyrylä	219	40 427	162	4 400
	Jokela			78	2 400
	Kellokoski			28	6 600

The regional area in Table 2 was retrieved from the National Land Survey of Finland from dataset *Hallinnolliset aluejaot 1:10000* and the population was taken from Tilastokeskus (Statistics Finland's free databases) of the year 2022 – 2023. With the physical-based model, crucial information for pipe material, manhole elevation, customer demands, storage unit volume, pump definition, and its setting can be observed. The flow rate going out of the pump was estimated based on wet well measurement (the volume differences or the time needed to empty the well). The information from January 2019 to December 2022 for HS-Vesi and Porvoo, 2016 for Kurikka was given by the utilities to study the differences between dry and wet weather, while the infiltration rate was already available in the Kouvola and Tuusula models. Energy consumption measurements were additionally provided by Porvoo, Kurikka, and HS-Vesi in some of the main stations. The data was roughly estimated and did not include the heating and control system etc., which could be inaccurate. Besides, the provided HS-Vesi's estimated hourly electric use was not reliable and therefore cannot be included in the analysis.

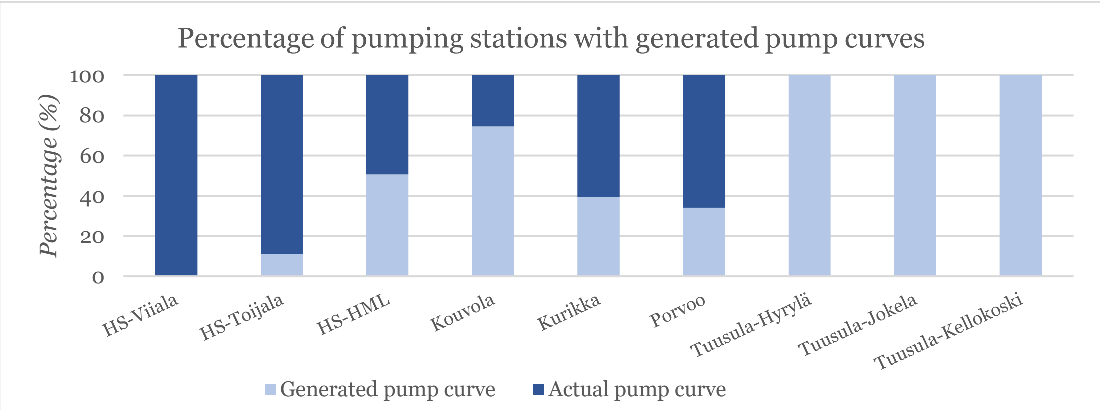

Figure 10. Percentage of pumping stations with Fluidit-generated pump curves

However, the network information is not complete and may contain errors, hence, the system needs updates and corrections. The missing invert elevation of some manholes and storage units was estimated based on the rationale for pipes slope in gravitational or pressurized line to create the complete sewer network, similarly with some storage unit volume (based on total customers' inflow demand of the area), the startup and shutoff pumping level, and the rim elevation assumed by using Digital Elevation Model (2 m grid) fetched from NLS of Finland. Most importantly, the pump definition was not documented in many parts of the networks, which were mainly small stations. In these cases, the pump head-flow curve was generated in Fluidit software, based on the pressurized pipe material and the elevation difference between the pump and the discharge point. The best efficiency of the generated pump was assumed to be 60%. The contribution of generated pump curve in the study can be observed in Figure 10. Commonly, main pumping stations were simulated with audited pump models.

3.2 Energy analysis

The simulations were run using the Preissmann SLOT surcharge method, Chezy-Manning for gravitational line, and the Darcy-Weisbach for pressurized pipes used as head loss formula. In this section, the energy analysis focused on the calculation of head loss in the pressure line, the energy efficiency the energy flux of the system in dry and wet weather.

3.2.1 Head loss in the pressure line

The friction loss of each pumping station was needed to determine stations with high friction loss percentages over a total head of over 50% that will benefit from the use of variable speed drive. Also, the friction loss percentage was important information for assessing the saving potential and looking for a better pump model in the location.

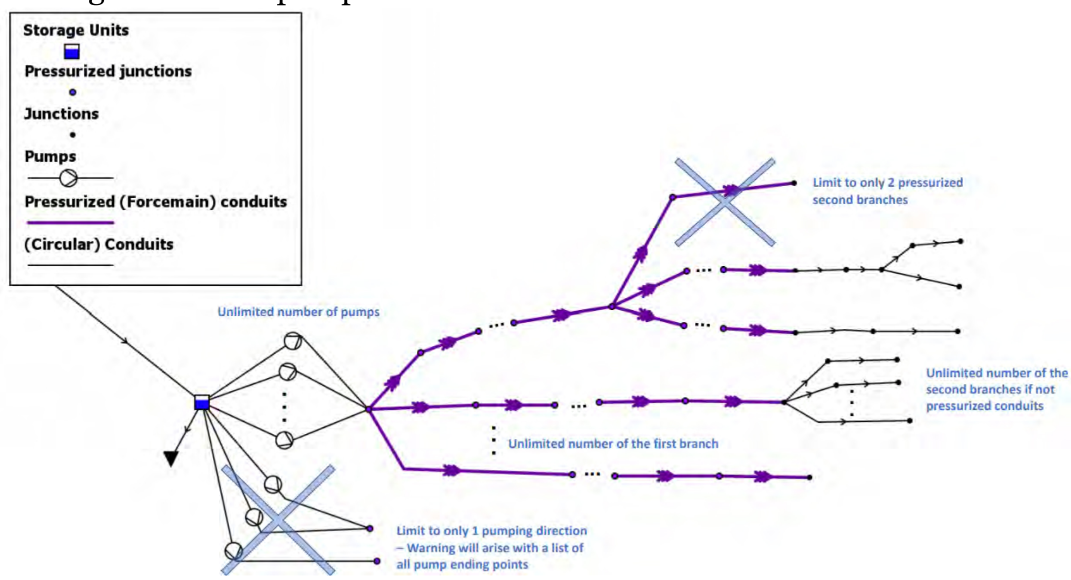

Figure 11. Limitation of Python algorithm

The friction loss of the pumping system was estimated with a Python algorithm built for the calculation since the friction loss cannot be retrieved directly for a pump from the Fluidit Sewer 2.2, for which only the total head result is available. The algorithm covers the situation when there are an unlimited number of pump components connected to one node, multiple numbers of first branches in the pressurized line, and an unlimited number of second branches if they are gravitational pipes. Thus, the warning will be raised when there is more than one ending point of the pump component and when there is another second pressurized branch (Figure 11).

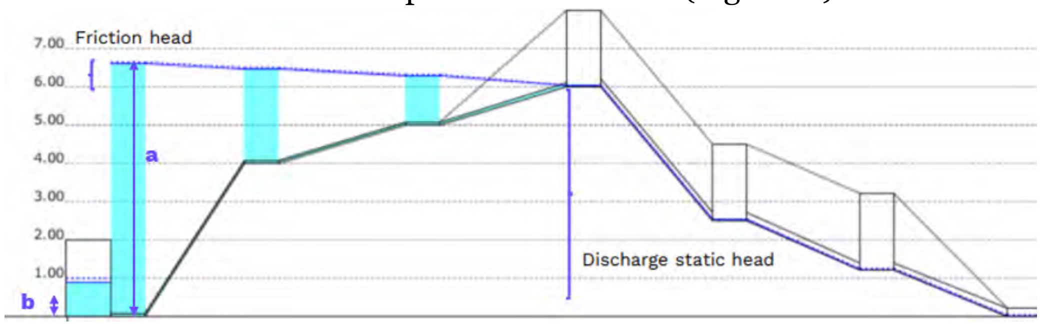

Figure 12. Friction head and discharge static head explanation

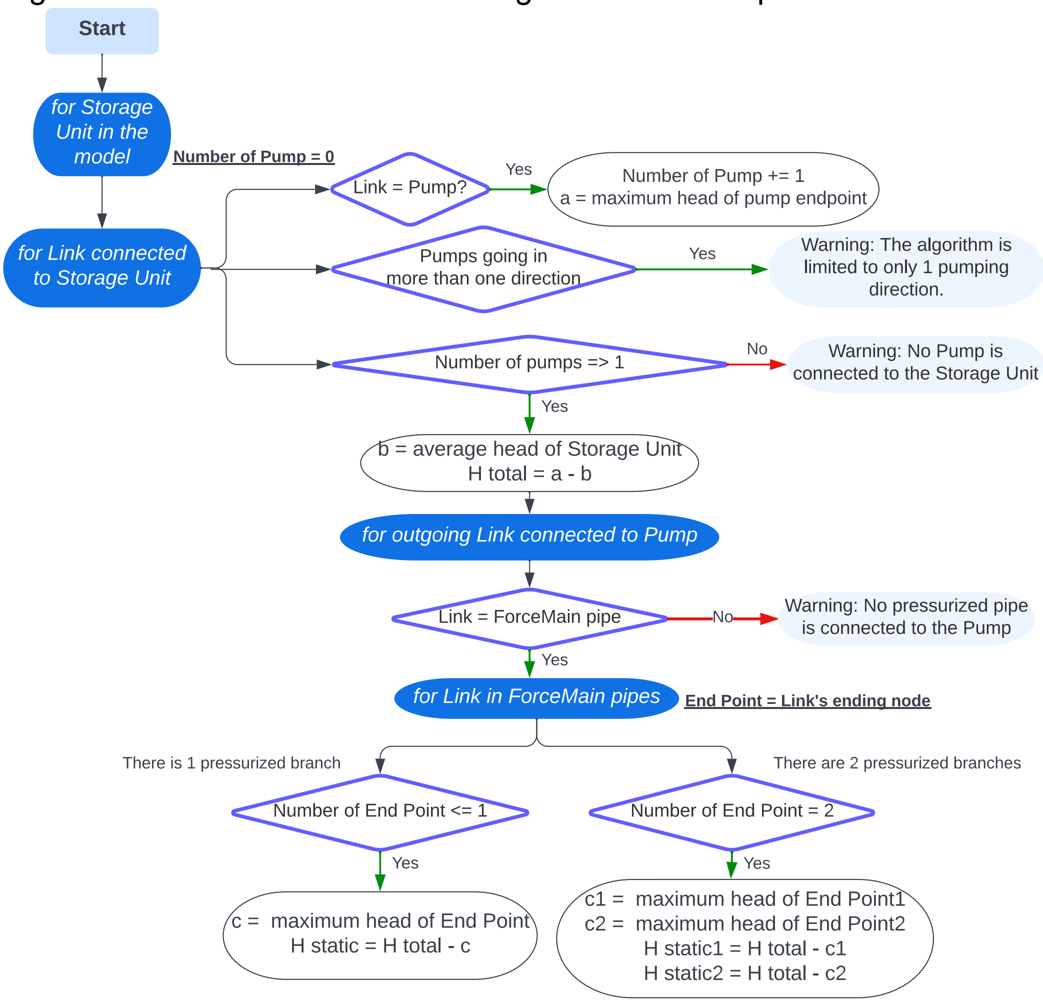

Figure 13. Friction loss calculation algorithm

The fundamental of the head loss calculation was based on Figure 2 (section 2.2.1), the friction loss is the difference between the total dynamic head and static head. The variables used in the calculation are shown in Figure 12. The maximum head of the pressure sewer discharge manhole (defined as $\boldsymbol{a}$ in Figure 12) and the pumping station wet well average head ($\boldsymbol{b}$) were applied in the Python algorithm diagram. As demonstrated in Figure 13, the friction loss was determined firstly by the recognition of the pressurized line and connected pump(s), then the calculation was made based on the corresponding average head of the storage unit and the maximum head of the pump ending point to get the total head. The difference between the maximum head of the discharge manhole and the total head was then the friction loss value.

3.2.2 Energy efficiencies

The energy efficiency of each pump was taken from Fluidit Sewer 2.2's *Electric Efficiency (average)* result. The value was calculated based on equation (15), with the default motor efficiency of 85% and default VSD efficiency of 95% when the pump motor power was not specified in the pump definition. Besides nominal energy efficiency, the flow-weighted efficiency was also taken into account in the analysis. The results were determined based on the nominal energy efficiency multiplied by the ratio of the total pumped volume in the station over the total volume of the whole system.

3.2.3 Energy balance

The analysis considers different inflow components: the consumer due inflows which are the revenue water and the undue inflows comprised of infiltrations such as groundwater in dry weather and rainwater in wet weather, so-called non-revenue water.

The total energy influx is the energy coming into the system and produced by the system for the transportation of effluent, which includes revenue water and non-revenue water. Total intrinsic energy refers to the energy associated with the free-surface flow, or gravitational flow. The result was the sum of the hydraulic energy of all gravitational pipes in the network. Constantly, the total external energy refers to the energy supplied by the pumping stations in pressurized flow. The result was obtained from the sum of all hydraulic energy of pump components connected to the station.

Following, the total energy outflux presents the energy loss by the system, comprising similar intrinsic and external terms as influx energy. Total intrinsic energy refers to the system's downstream pipe friction and head losses, as well as the energy associated with exceedance volumes (not connected to energy-consuming components). Total external energy can be divided into elevation-associated energy (losses when pumping the effluent to the delivery point) and dissipated energy due to the inefficiencies in the equipment. The inefficiencies energy was defined as the difference between the total electrical consumed energy and the hydraulic energy transferred into the water. The overall demonstration of the approach can be observed in Table 3.

Table 3. Energy balance approach

<table>
<tr><th></th><th colspan="2">Intrinsic energy</th><th colspan="2">External energy</th></tr>
<tr><td rowspan="2">Energy influx</td><td colspan="2">Gravitational energy produced</td><td colspan="2">Theoretical hydraulic energy to pump the sewage</td></tr>
<tr><td>Due: domestic consumption</td><td>Undue: groundwater (dry weather) and rainwater (wet weather)</td><td>Due: domestic consumption</td><td>Undue: groundwater (in dry weather) and rainwater (in wet weather)</td></tr>
<tr><td rowspan="2">Energy outflux</td><td colspan="2">Friction loss in gravitational pipes</td><td colspan="2">Friction loss in pressurized pipes</td></tr>
<tr><td colspan="2">Energy loss from overflows</td><td colspan="2">Energy losses from inefficiencies in pump motor, VSD, and hydraulic loss</td></tr>
</table>

3.3 Flood-risk analysis

Three different approaches were operated to locate the flood-risk point in the studied area, in order to choose the most probable overflow accident that can occur in the future.

Firstly, elevation maps were made with the worst-case flood scenario in heavy rainfall using SCALGO Live (SCALGO, 2023) and lake flood maps using ArcGIS Pro 3.0.0 (ArcGIS, 2023) based on the elevation difference. Ice jam problem that obstructs the flow and causes the lake water level to rise. As a result, significantly increased inflows will go to the collecting system, then overflow in locations with low capacity. The elevation map (2 m grid) was retrieved from the National Land Survey of Finland (NLS). The population data and industrial facilities information provided by Tilastokeskus/Statistic Finland were also included in the flood-risk map. The assumption of a severe scenario in which the water level would be increased significantly was based on the reported past accident (Table 4).

Table 4. Water level used in the flood-risk maps

Region	Past incident	Water level
HS-Vesi	According to HS (2019), the water in Hämeenlinna was 2.5 meters higher than the average in June 1899. Several streets were under water.	82.0 m
Kouvola	In the Kymenlaakso region, Kouvola is one of the areas prone to flooding surrounded by River Kymijoki (EBPI, 2012). The level used in the analysis was hypothetically assumed 2.5 m high than the average.	58.6 m
Kurikka	The river Kyrönjoki has a mean discharge of 43 m^3/s, which can increase to 500 m^3/s during the spring	92.0 m

	flooding season when the water level in the river can be more than 6 m higher than during dry periods (YLE, 2012). The map was made assuming the hypothesis when Lake Pitkämö surface level increased by 2 m, however, hardly occurs in reality since the artificial lake is tightly controlled.	
Porvoo	According to YLE (2004), the Porvoo River rise 2.5 m above its average level in some places.	70.5 m
Tuusula	No recorded past incidents since there is a regulation dam in Hyrylä. The level used in the analysis was hypothetically assumed 2.5 m high than Lake Tuusulanjärvi's average level.	40.3 m

Secondly, the network capacity was accessed in Fluidit Sewer 2.2. The active network model was re-simulated with higher demand multipliers to locate the point with low capacity and likely overflowing during peak days.

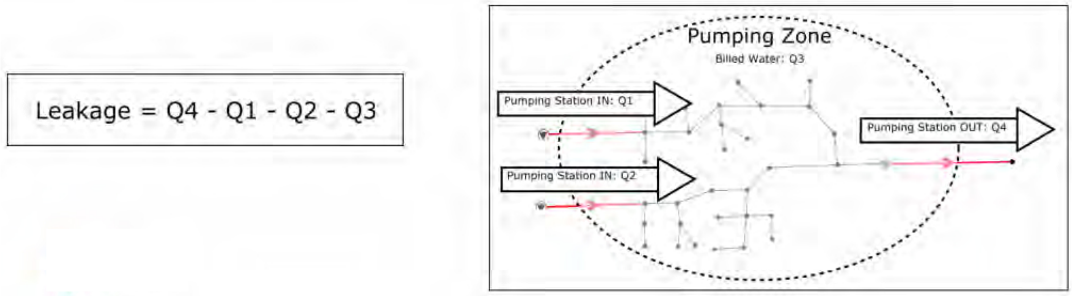

Figure 14. Infiltration rate calculation for pumping zone (Kuronen, 2022)

Lastly, the infiltration rate calculation of the zones was defined from the pumping station's outgoing and incoming flow estimation received from the water utilities. The method is shown in Figure 14: the network is divided into multiple zones and the leakage percentage can be determined from the change of the total incoming flow to the zone and the outgoing flow of the final pumping station. The dry weather and wet weather periods were chosen differently for each area as presented in Table 5.

Table 5. Infiltration rate

Region		**Dry weather and wet weather period**
HS-Vesi	Viiala	The dry weather from the daily average of the 14th of July to the 12th of October and wet weather from the daily average of the 15th of February to the 16th of May of 2019 to 2022.
	Toijala	
	Hämeenlinna	The dry weather from the daily average of the 1st of July to the 1st of September and wet weather from the daily average of the 1st of October to the 31st of October of 2019 to 2022.
Kurikka		The daily dry weather flow was calculated from the monthly average and minimum in the 2016 flow measurement, and the daily wet weather flow was calculated from the monthly average and maximum in the 2016 flow measurement.

Kouvola	The infiltration rate was defined initially from the given model, based on the flow measurement from 2019 to 2020.
Porvoo	Dry weather from the daily average of the 8th of June to the 15th of December and wet weather from the daily average of the 3rd of February to the 14th of May of 2020 to 2022.
Tuusula	The infiltration rate was defined initially from the models. All the modeled flows were multiplied by 1.3 for wet scenario.

3.4 Smart control method

The control method had been operated by using a Python script in Fluidit Sewer to control the pump operating parameters during the simulation. The Python Control Stations built-in support was utilized to allow hooking into the simulation and controlling the pumps.

3.4.1 Method explanation

The optimization algorithm was developed for water level control by adjusting the pump speed, such as VSD when put into application. The pump speed was changed by alternating the rotational speed of the pump accordingly to the desired set value of the wet well level. In such words, when the water level in the well is higher than the set point, water will be pumped at a higher speed to achieve the desired. In contrast, if the water level is lower than the set point, the pump will stop so that level will rise to the wanted value. Furthermore, at the higher level of control, when the water level of the downstream storage unit rises above the allowed limit, the connected upstream pumping station(s) will pump less water in order not to create overflow in the downstream section.

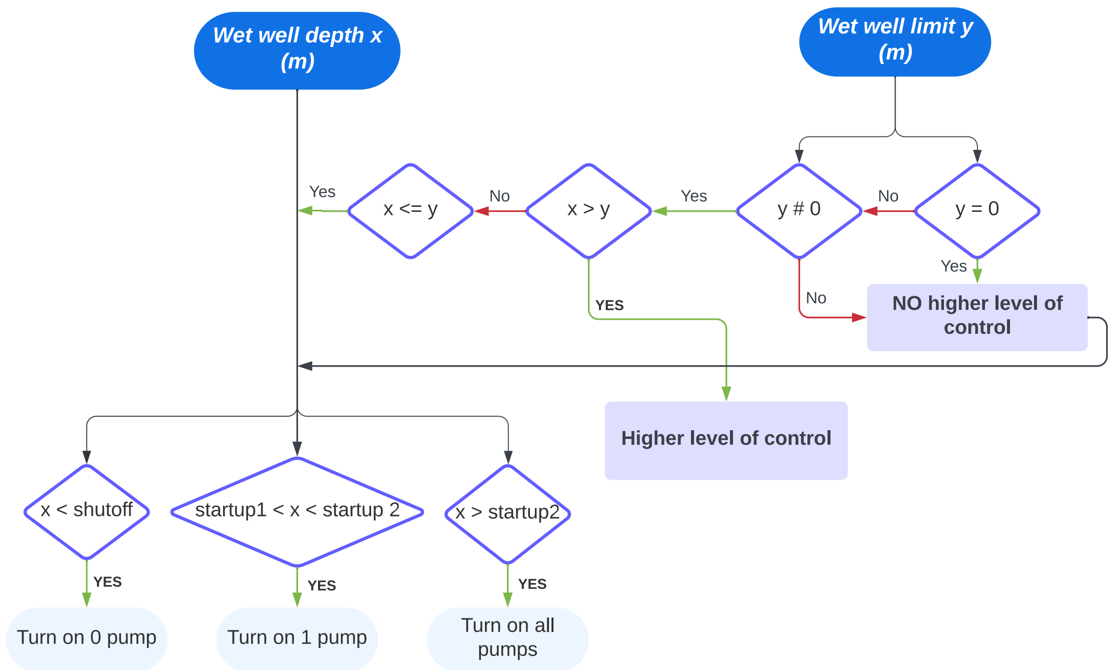

Figure 15. Influence of wet well's water level on pump rotational speed

As can be seen in Figure 15, several set points need to be considered in the controller. Firstly, the minimum frequency of the pump should be found. The rotation speed usually ranks from 0 to 50Hz, which is identified as 0 (0 Hz) to 1 (50 Hz) in the software. The minimum value should be chosen thoughtfully so that the pressurize line's velocity will not be below 0.7 m/s. The approach used was to create a simplified model containing only the chosen pump and then let the simulation run from setting 0 to 1 with time changing every hour. As a result, the flow rate of 0.7 m/s was checked to find out the lowest possible frequency. At different well water levels, the pump will perform differently, as explained in Table 6.

Table 6. Pump operation according to the wet well's water level

Water level	Pump operation
Shutoff	The pump stops when water goes below this level.
Startup1	One pump starts working at this level with minimum frequency.
Desired level	The pump's rotational speed will be altered from the minimum value to the maximum value of 1 to keep the wet well level at this rate.
Startup2	If the station has more than one pump, all other pumps start pumping when the current level is higher than this level.
Limit	For station(s) that are likely to flood, a higher level of control is applied: only stations with upstream pumping station connections will be assigned this value. When the water level goes above the limit, all other upstream stations will be controlled at *startup2* – 0.1 (m). Since the level is higher than the previous, more water can be retained and avoid flood in downstream.

The ***startup1*** level was set based on the previous pump setting of the network. The ***desired level*** was chosen to be as low as possible to save more storage for the flood situation. The ***startup2*** rate should not be higher than 1 meter from Z'1 level (the difference between the wet well bottom elevation and the previous discharge manhole), to prevent overflow to the upstream network. Similarly, the set ***limit*** value should be below the storage unit overflow pipe Z'2 (Figure 16), to minimize overflows discharged to environment.

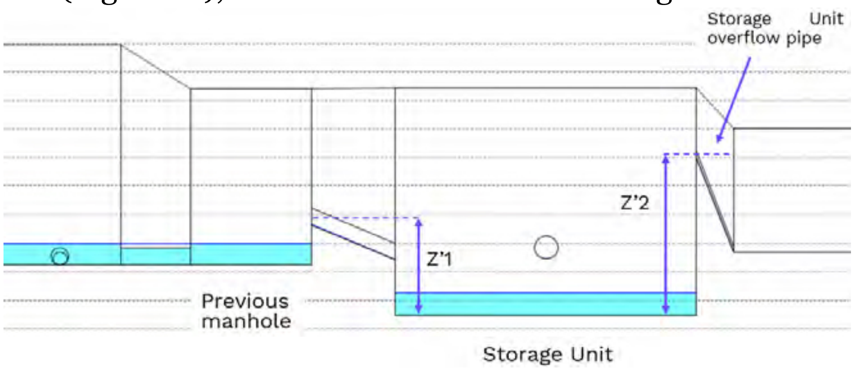

Figure 16. Elevation constraints in pumping station wet well

The pump setting in the smart control method was adjusted using a PID controller proportional (P) and integral (I) controls active. The constant proportional gain K_P was equal to 0.01 and the constant integral gain K_i was chosen to be 0.6. Without the higher level of control, the water level should be kept at the ***desired level***, while with a level of control, the level will be retained at a higher value, keeping only one pump running, as shown in Figure 17 in proportional control. The integral control would alter the output setting according to the variance between the previous setting and the new setting.

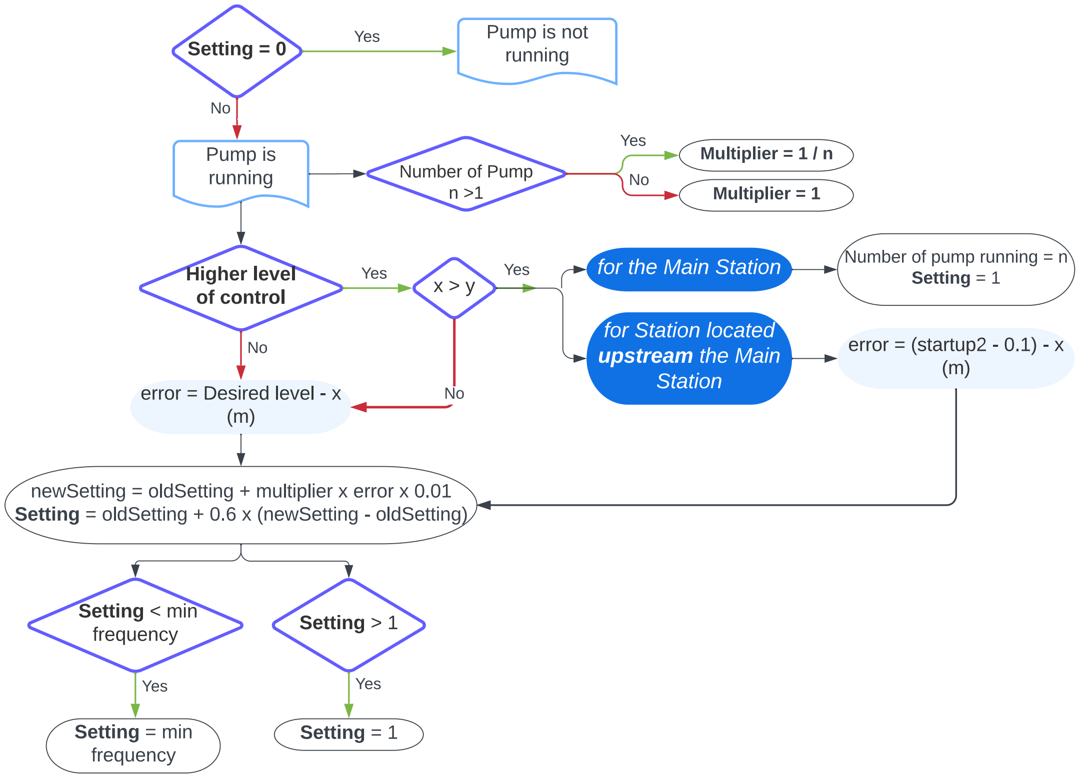

Figure 17. PID level control scheme

3.4.2 Selected pumping chains for the smart control method

The pumping chains for applying a smart control scheme were selected based on energy and flood risk analysis. Practically, pumping stations with high energy consumption due to large inflows but having low energy efficiency and high friction loss should be studied for choosing a more suitable pump. The optimal pump was selected using the Grundfos Product Selection website (Grundfos, 2023), using the existing nominal pump flow rate in the network, the total head, and friction head results which were calculated from the previous analysis. The capacity limit of the network was carried out using different overflow scenarios in Fluidit simulation and the easily flooded area was located using a flood-risk map. The network bottleneck was pointed out in three cases: using the peak scenario of wet weather, the hypothetical pipe blockage happening, and the backflow from overflow pipes. The region and its overflow-type case were chosen based on the utilities' insights and past accidents that happened on the sites, nonetheless, all scenario properties were made hypothetically:

- Peak scenarios: Viiala, Hyrylä
- Pipe blockages: Hämeenlinna, Porvoo, Jokela, Kellokoski
- Backflow from overflow pipes: Porvoo, Toijala

Based on previous analysis of the energy consumption, energy efficiency, and friction loss of each pumping station in the studied region, a more suitable pump to use for the case would be suggested. The optimal pump was chosen from Grundfos following the current flow rate of the network in dry weather, along with the calculated total head and friction head. In the following figures which present the pumping chain of each region, stations chosen for pump definition change were highlighted.

To observe the benefits, alternatives, and costs made by applying the proposed control method, the chosen pumping chain results of energy consumption and overflow volume will be compared in four circumstances:

- Current control, current pump
- Current control with optimal pump selection
- Level control using the current pump
- Level control with optimal pump selection

Based on the fit of the control and the positive improvements from the method and optimal pump changes, the corresponding cost for renewing selected pump(s) would be suggested to give an estimation of the repayment period for the utilities. The cost for yearly electric consumption was estimated with the assumption of 245 days for dry weather and 120 days for wet weather. Accordingly, the repayment period was defined to be the ratio of the suggested pump's cost with one-year maintenance expense and the reduction in yearly electrical energy consumption when applying the new pump.

HS-Vesi

The pumping chains chosen in Viiala, Toijala, and Hämeenlinna are shown in Figure 18, Figure 19, and Figure 20 respectively and their control setting is in Table 7, Table 8, and Table 9. Only pumping stations with bolded names in the figures will be selected for substituting better pump models.

Scenario 1 – Viiala region:

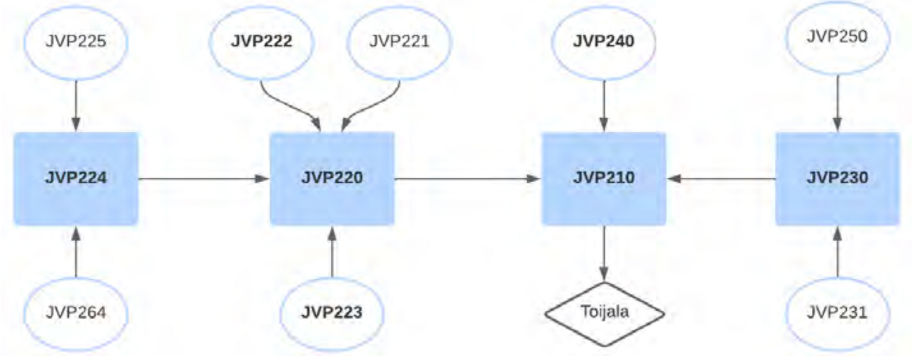

Figure 18. Viiala pumping station chain

The demand multiplier of 2.1 for the peak scenario on the 18th of April 2022 was applied. Without smart control, there will be an overflow in the overflow duct of pumping station JVP210.

Table 7. Control algorithm settings for Viiala

Station	shutoff (m)	star-tup1 (m)	level (m)	Z'1 (m)	Z'2 (m)	startup2 (m)	limit (m)	Minimum frequency (Hz)
JVP224	0.4	0.9	1.2	1.81	4.23	2.5	1.6	35
JVP225	0.4	1.4	1.0	2.0		3.1		35
JVP264	0.4	0.8	1.1	1.2		2.8		25
JVP220	0.4	0.9	1.2	1.36	3.60	1.4	1.6	27.5
JVP222	0.4	2.0	2.5	3.23		3.3		25
JVP223	0.4	1.1	0.9	1.20		2.5		20
JVP221	0.4	1.6	1.2	1.82		3.4		35
JVP210	0.4	0.9	1.2	0.89	2.78	1.4	1.6	35
JVP240	0.4	1.5	2.0	2.76		3.4		32.5
JVP230	0.4	0.8	1.0	1.03	2.98	2.1	1.2	20

Scenario 2 – Toijala region:

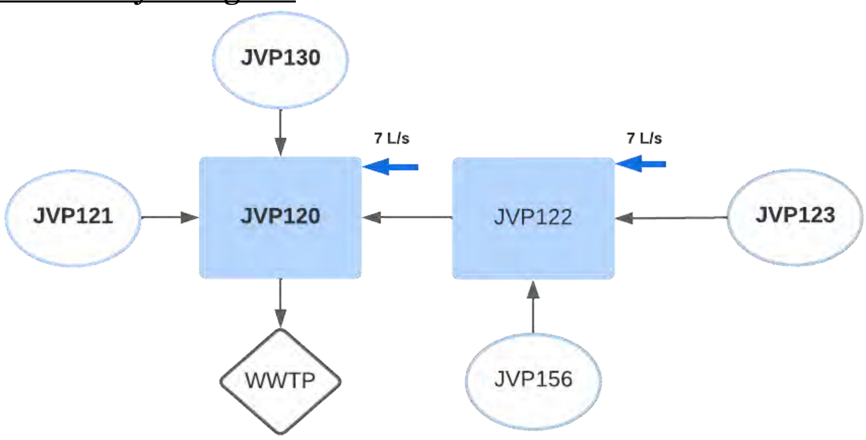

Figure 19. Toijala pumping station chain

Hypothetically, there will be backflow happening from overflow pipes in JVP122 (7 l/s) and JVP120 (7 l/s) with the leakage observed on the 18th of April 2022, there will be overflow in junction Junction-6729.

Table 8. Control algorithm settings for Toijala

Station	shutoff (m)	startup1 (m)	level (m)	Z'1 (m)	Z'2 (m)	startup2 (m)	limit (m)	Minimum frequency (Hz)
JVP120	0.4	0.6	0.9	0.65	3.0	1.2	1.4	20
JVP130	0.4	0.9	1.2	1.12	3.29	2.7		35
JVP121	0.4	0.9	1.2	1.71		3.0		35
JVP122	0.4	0.9	1.2	1.36	4.00	2.5	1.4	35
JVP123	0.4	0.9	1.2	2.0		3.0		40
JVP156	0.4	0.9	1.2	1.8		2.7		35

Scenario 3 – Hämeenlinna:

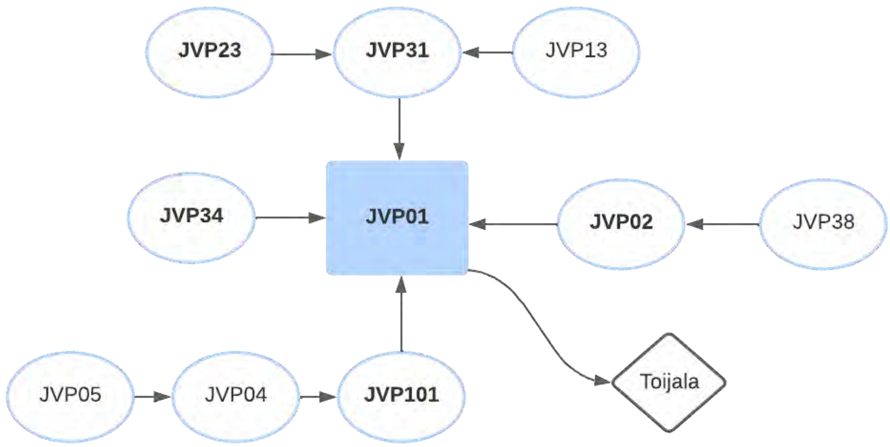

Figure 20. Hämeenlinna pumping station chain

Pipe blockage happened in the downstream pipe going from JVP01 from 6.00 to 8.30 in the average wet weather scenario. To minimize the overflow, JVP01 should be stopped at a certain time during transportation time, which was before the suction truck arrives. There will be overflow from the overflow pipe of JVP01.

Table 9. Control algorithm settings for Hämeenlinna

Station	shutoff (m)	startup1 (m)	level (m)	Z'1 (m)	Z'2 (m)	startup2 (m)	limit (m)	Minimum frequency (Hz)
JVP34	0.4	0.9	1.2	1.22	5.20	2.1	1.5	45
JVP01	0.3	0.7	0.9	3.87	2.80	1.0	2.0	30
JVP31	0.4	0.9	1.2	1.08	3.54	2.1	1.4	17.5
JVP23	0.4	0.9	1.1	0.98	5.35	2.0		35
JVP13	0.4	0.9	1.2	1.95	5.83	2.9		37.5
JVP101	0.4	0.9	1.2	2.06		3.0	1.4	30

JVP04	0.4	0.9	1.2	2.18		3.0	1.4	35
JVP05	0.4	0.7	1.0	1.01		2.0		35
JVP02	0.4	0.9	1.2	1.05	3.04	2.8	1.4	27.5
JVP38	0.4	0.9	1.2	1.05		2.0		35

Porvoo

The chosen pumping chain in Porvoo is presented in Figure 21. The whole chain was used in the study of the backflow scenario, with part of the chain (circled) being studied for the blockage scenario. The Porvoo's control setting can be found in Table 10. The pumping stations with bolded names in Figure 21 will be selected for better pump model replacement.

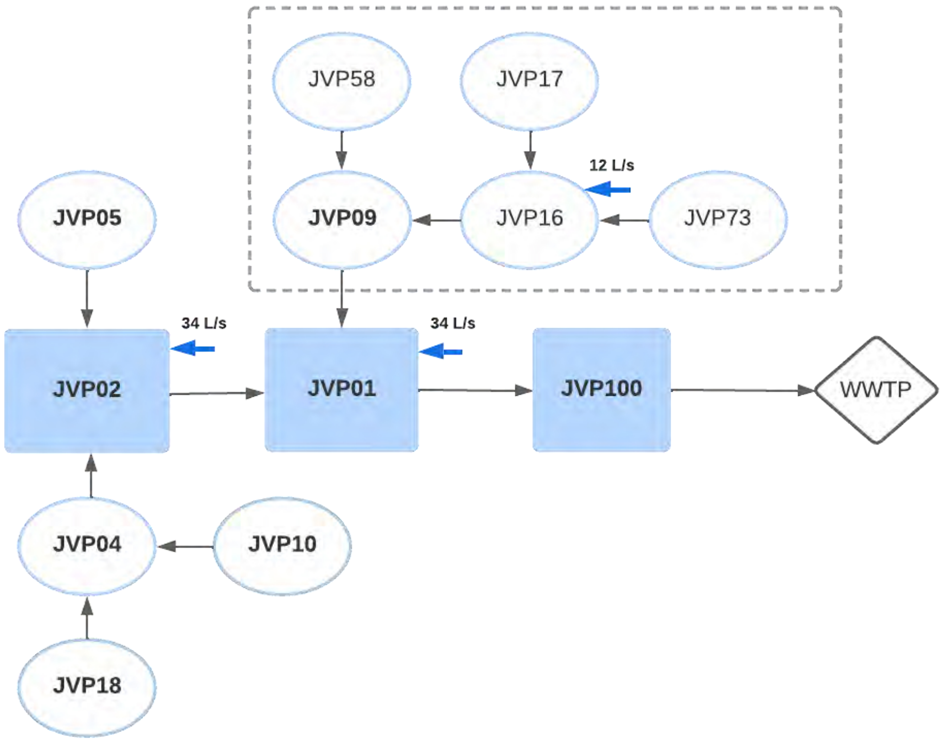

Figure 21. Porvoo chosen pumping chain

Scenario 1: Backflow in pumping stations

The backflow happened in JVP1, JVP2, and JVP16 with the flow rate shown below, in the average wet weather of multiplier 1.7. Overflow happens in the overflow pipe of JVP100, which is 39.4 m^3/d.

Scenario 2: Pipe blockage

Supposedly, there will be a blockage in the downstream pipe going from JVP09 from 6.00 to 8.00. The chosen pumping chain for this case is circled in the figure above.

Table 10. Control algorithm settings for Porvoo

Station	shutoff (m)	star-tup1 (m)	level (m)	Z'1 (m)	Z'2 (m)	star-tup2 (m)	limit (m)	Minimum frequency (Hz)
JVP2	0.5	0.9	1.2	1.89	4.68	2.6	1.4	20
JVP4	0.5	0.9	1.2	2.95	2.80	2.7	1.4	20
JVP5	0.5	0.9	1.2	2.08	3.00	2.9		30
JVP18	0.5	0.9	1.2	1.54	2.40	2.5		22.5
JVP10	0.5	0.9	1.2	2.51	4.51	3.0		35
JVP1	0.5	0.9	1.2	3.28	3.48	3.1	1.4	35
JVP9	0.5	0.9	1.2	1.77	3.14	2.6	1.4	35
JVP16	0.5	0.9	1.2	3.34	3.10	2.9	1.4	35
JVP73	0.5	0.9	1.2	2.11	2.20	2.1		35
JVP17	0.5	0.9	1.2	2.30	2.75	2.7		35
JVP58	0.5	0.9	1.2		2.75	2.9	1.4	35
JVP100	0.5	0.9	1.2	1.07	3.03	2.9	1.4	22.5

Tuusula:
The pumping chains chosen in Hyrylä, Jokela, and Kellokoski are shown in Figure 22, Figure 23, and Figure 24 respectively and their control setting is in Table 11, Table 12, and Table 13. Similar to other cases above, only bolded pumping stations in Figure 22, Figure 23, and Figure 24 will be chosen to replace with more suitable pump models.

<u>Scenario 1 – Hyrylä region:</u>

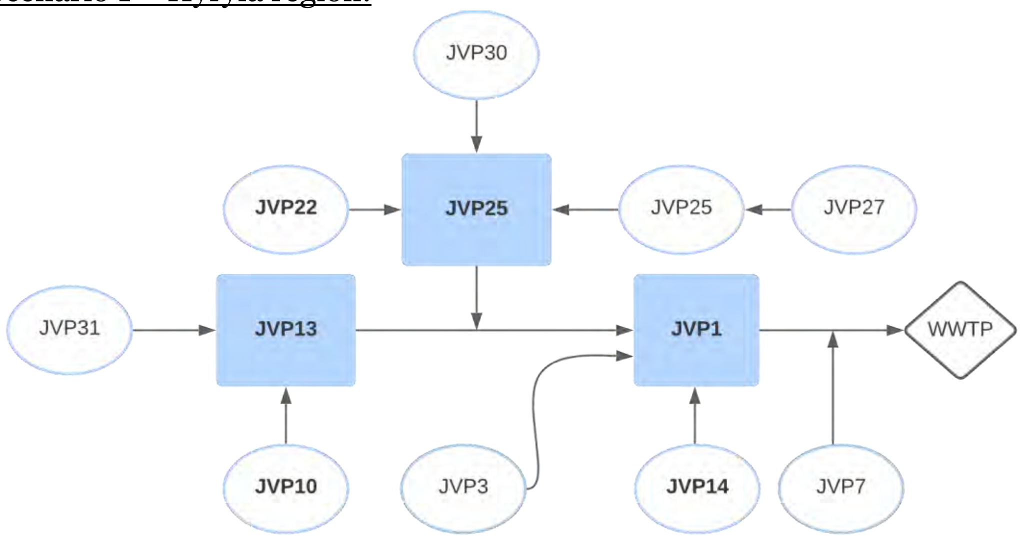

Figure 22. Hyrylä chosen pumping chain

A demand multiplier of 1.3 was set in the wet weather scenario. The total overflow of the whole network is 17 624 m^3/d.

Table 11. Control algorithm settings for Hyrylä

Station	shutoff (m)	startup1 (m)	level (m)	Z'1 (m)	startup2 (m)	limit (m)	Minimum frequency (Hz)
JVP25	0.5	0.9	1.2	1.42	2.2	1.4	17.5
JVP30	0.5	0.9	1.2	1.35	2.1		35
JVP26	0.5	0.9	1.2	1.11	2.0	1.4	35
JVP27	0.5	0.9	1.2	8.10	2.9		32.5
JVP22	0.5	0.9	1.2	1.10	1.9		40
JVP13	0.5	0.9	1.2	1.50	2.3	1.4	32.5
JVP10	0.5	0.9	1.2	1.14	2.0		20
JVP31	0.5	0.9	1.2	1.03	1.9		15
JVP3	0.5	0.9	1.2	2.04	2.8		35
JVP1	0.5	0.9	1.2	2.06	2.8	1.4	20
JVP14	0.5	0.9	1.2	1.03	1.9		22.5
JVP7	0.5	0.9	1.2	1.48	2.3		35

<u>Scenario 2 – Jokela:</u>

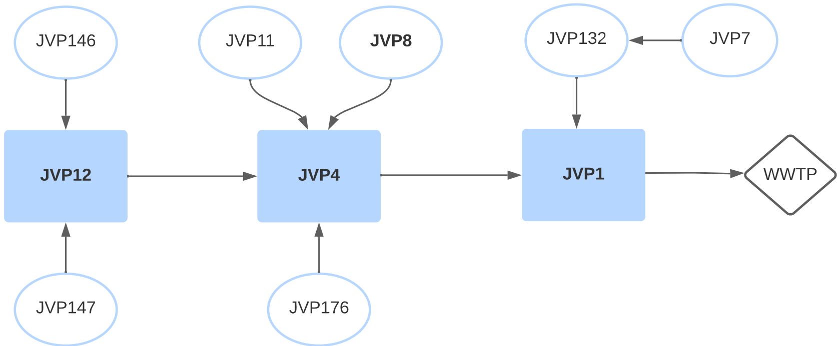

Figure 23. Jokela chosen pumping chain

A pipe blockage happened in the downstream pipe going from JVP1 from 6.00 to 8.00 in wet weather. Overflow occurs in the gravitational pipe going into JVP1 station.

Table 12. Control algorithm settings for Jokela

Station	shutoff (m)	startup1 (m)	level (m)	Z'1 (m)	startup2 (m)	limit (m)	Minimum frequency (Hz)
JVP12	0.5	0.9	1.2	1.05	2.1	1.4	40
JVP146	0.5	0.9	1.2	1.04	2.1		35
JVP147	0.5	0.9	1.2	1.31	2.4		35
JVP4	0.5	0.9	1.2	1.01	2.1	1.4	37.5
JVP11	0.5	0.9	1.2	2.08	3.0		32.5
JVP8	0.5	0.9	1.2	2.29	3.3		25

JVP176	0.5	0.9	1.2	1.12	2.2		35
JVP1	0.5	0.9	1.2	2.40	3.0	1.4	37.5
JVP132	0.5	0.9	1.2	1.03	2.1	1.4	30
JVP7	0.5	0.9	1.2	1.36	2.2		30

Scenario 3 – Kellokoski:

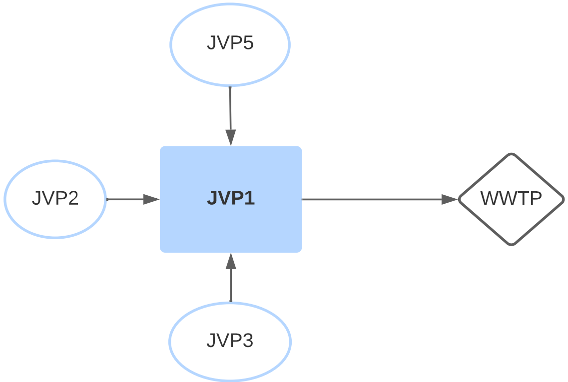

Figure 24. Kellokoski chosen pumping chain

There was pipe blockage in the downstream pipe going from JVP1 from 6.00 to 8.00 in dry weather using a multiplier demand of 1.3. Overflow in manholes had a total of 101 m^3/d.

Table 13. Control algorithm settings for Kellokoski

Station	shutoff (m)	startup1 (m)	level (m)	Z'1 (m)	startup2 (m)	limit (m)	Minimum frequency (Hz)
JVP1	0.5	0.7	0.9	2.22	1.0	1.5	37.5
JVP2	0.5	1.7	1.2	2.25	2.5		25
JVP3	0.5	1.7	1.5	1.61	2.5		20
JVP4	0.3	0.95	0.9	1.04	3.0		30
JVP5	1.5	2.0	1.8	1.05	2.6		30

4 Benchmarking results

In this section, the result regarding the flood risk and energy analysis will be presented in both average dry weather and wet weather. As can be seen from Table 14, the selected energy use parameters along with the calculated leakages were shown with the median values and the 60% confidence interval range. The leakage percentage in wet weather was 2 to 3 times higher than in dry weather. The energy efficiency and friction loss were relatively higher with larger inflows.

Table 14. The overall benchmarking values for the five studied sites

Parameter		Unit	Median	60% Confidence interval
Infiltration	Dry	%	18.9	22.8 – 27.2
	Wet	%	67.5	58.2 – 63.0
Specific electrical energy use in the pumping station		kWh/m^3	0.11	0.12 – 0.15
Electrical efficiency	Dry	%	35.2	31.9 – 33.0
	Wet	%	36.6	33.6 – 34.7
Pressurized pipe length		km	0.5	1.3 – 1.6
Pressurized pipe inner diameter		mm	136	166 – 170
Geodetic head	Dry	m	6.4	8 – 8.5
	Wet	m	6.7	8.5 – 9.0
Friction head	Dry	m	0.6	1.0 – 1.2
	Wet	m	0.7	1.4 – 1.6
Friction loss	Dry	%	10.3	17.4 – 19.0
	Wet	%	12.0	19.5 – 21.2

4.1 Flood analysis

The results of flood analysis are presented from the infiltration rate and flood-risk maps in this section.

4.1.1 Seasonal inflow variation

The sites were firstly divided into smaller zones for I/I rate calculation, which is presented in all regions as diagrams from Figure 25 to Figure 32 in dry and wet weather, except for Kellokoski because the network was relatively small. The percentage of infiltration in each zone is shown in the tables next to the diagrams (from Table 15 to Table 22). Kellokoski's I/I rate was 8.5% in dry weather and 41% in wet weather. Zones that include the chosen pumping chains for smart control in phase 2 were highlighted with red circles in the diagram of the Hämeenlinna region, Porvoo, and Tuusula sites.

HS-Vesi – Viiala

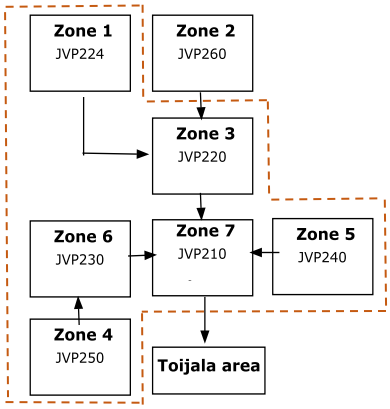

Figure 25. Viiala zones

Table 15. I/I percentage in Viiala

Zone	Dry	Wet
1	0.4 %	41 %
2	21 %	52 %
3	41 %	78 %
4	2 %	16 %
5	37 %	84 %
6	2 %	38 %
7	69 %	68 %

HS-Vesi – Toijala

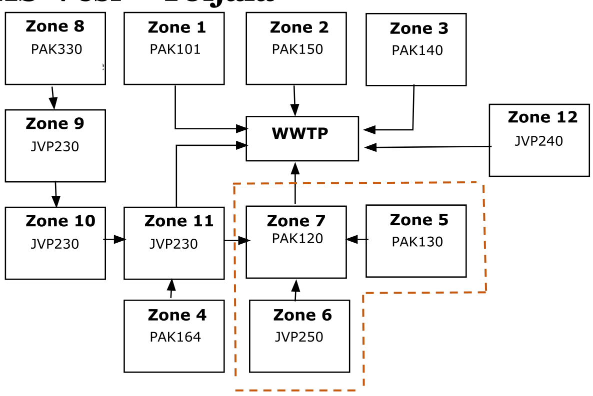

Figure 26. Toijala zones

Table 16. I/I percentage in Toijala

Zone	Dry	Wet
1	0 %	5.6 %
2	1 %	55 %
3	47 %	77 %
4	17 %	67 %
5	25 %	63 %
6	33 %	73 %
7	32 %	66 %
8	0.4 %	14 %
9	0.4 %	30 %
10	83 %	85 %
11	9 %	58 %
12	1.5 %	68 %

HS-Vesi – Hämeenlinna

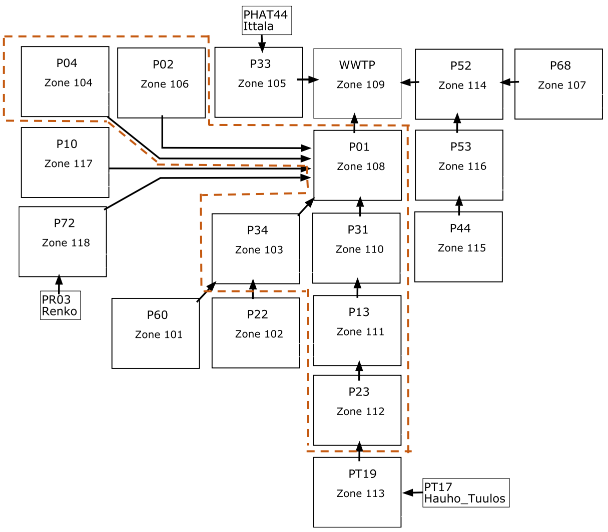

Figure 27. Hämeenlinna zones

Table 17. I/I percentage in Hämeenlinna

Zone	Dry	Wet
1	8 %	12 %
2	6 %	51 %
3	3 %	45 %
4	44 %	77 %
5	7 %	59 %
6	22 %	46 %
7	0 %	40 %
8	38 %	66 %
9	30 %	58 %
10	43 %	77 %
11	26 %	68 %
12	46 %	74 %
13	16 %	88 %
14	26 %	71 %
15	19 %	51 %

16	6 %	53 %
17	0 %	11 %
18	58 %	91 %

Porvoo

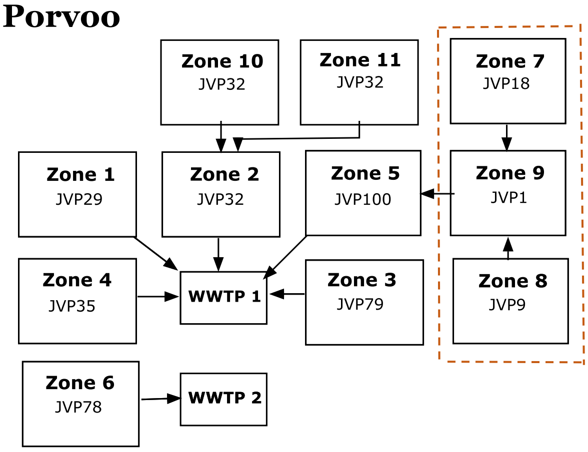

Figure 28. Porvoo zones

Table 18. I/I percentage in Porvoo

Zone	Dry	Wet
1	0 %	50 %
2	86 %	71 %
3	11 %	76 %
4	0 %	46 %
5	74 %	79 %
6	11 %	57 %
7	0 %	47 %
8	2 %	70 %
9	4 %	56 %
10	5 %	71 %
11	0 %	49 %

Kurikka

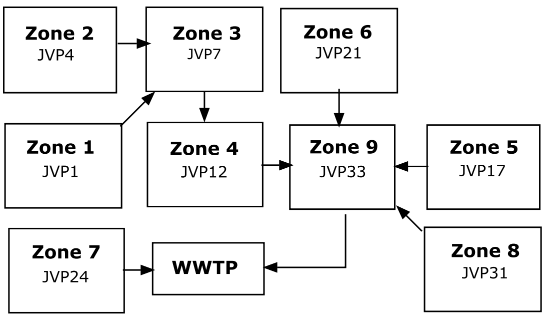

Figure 29. Kurikka zones

Table 19. I/I percentage in Kurikka

Zone	Dry	Wet
1	51 %	63 %
2	13 %	45 %
3	1 %	3 %
4	3 %	24 %
5	34 %	55 %
6	2 %	7 %
7	3 %	23 %
8	1 %	2 %
9	15 %	51 %
10	0.5 %	2 %
11	0.4 %	8 %
12	3 %	21 %

Kouvola

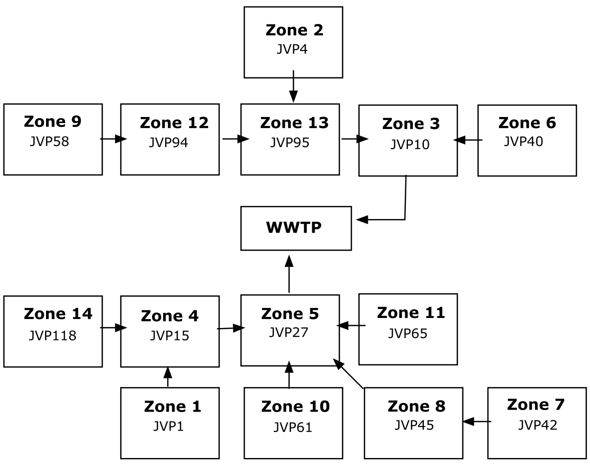

Figure 30. Kouvola zones

Table 20. I/I percentage in Kouvola

Zone	Dry	Wet
1	0 %	83 %
2	2 %	80 %
3	29 %	92 %
4	10 %	83 %
5	45 %	78 %
6	16 %	85 %
7	58 %	98 %
8	27 %	92 %
9	42 %	87 %
10	56 %	85 %
11	10 %	74 %
12	37 %	39 %
13	37 %	93 %
14	19 %	88 %

Tuusula – Hyrylä

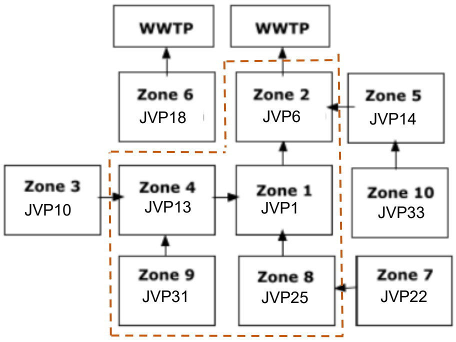

Figure 31. Hyrylä zones

Table 21. I/I percentage in Hyrylä

Zone	Dry	Wet
1	54 %	90 %
2	30 %	45 %
3	45 %	86 %
4	63 %	93 %
5	61 %	80 %
6	28 %	45 %
7	56 %	86 %
8	61 %	89 %
9	67 %	94 %
10	80 %	89 %

Tuusula – Jokela

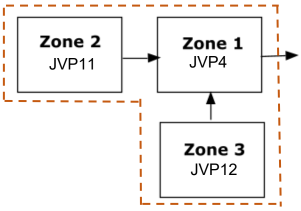

Figure 32. Jokela zones

Table 22. I/I percentage in Jokela

Zone	Dry	Wet
1	52 %	89 %
2	26 %	94 %
3	24 %	88 %

4.1.2 Flood-risk maps

The elevation maps and network capacity maps were created. However, due to confidentiality, the results are not presented in the thesis.

4.2 Energy analysis

The energy efficiencies, energy balances, and friction loss percentages will be studied for the overall energy analysis in dry and wet weather in this section.

4.2.1 Energy efficiencies

The best achievable efficiency from all pump efficiency curves used in the model was taken into account in the analysis. From Figures 33 and 34 below, the average efficiencies in dry and wet weather were compared with the average best efficiencies.

In Hämeenlinna regions, the average best efficiencies of all available pump curves in Viiala, Toijala, and Hämeenlinna were 36%, 44% and 52% respectively. The average best efficiency in Kurikka was in the similar range, which was 51.4%. The value was higher in Porvoo (57.5%), Kouvola (59%), and all Tuusula regions, which was 60% because all pump curves in this area were generated by Fluidit software.

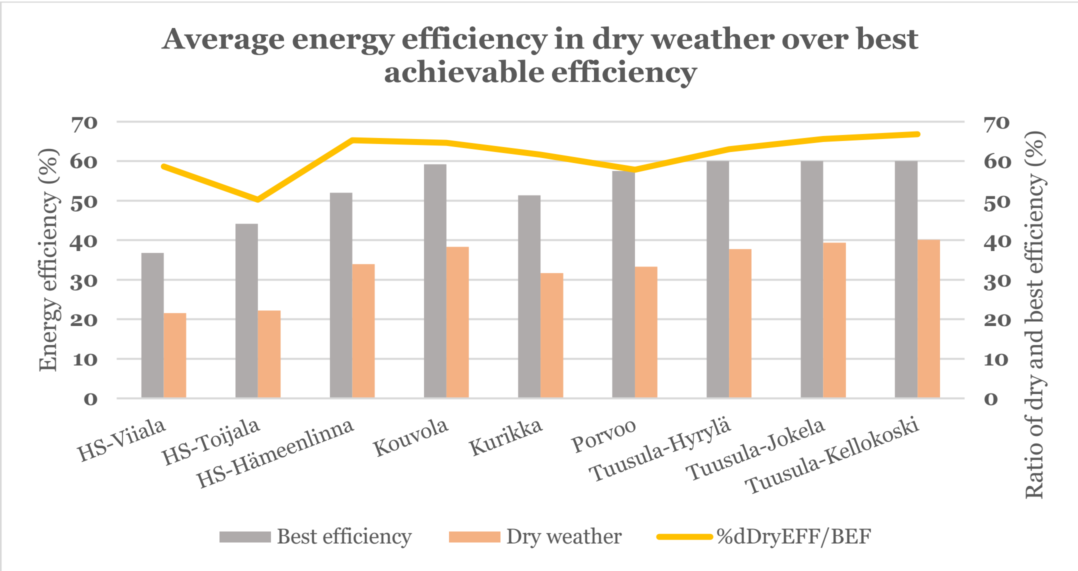

Figure 33. Average energy efficiency in dry weather over its best achievable efficiency

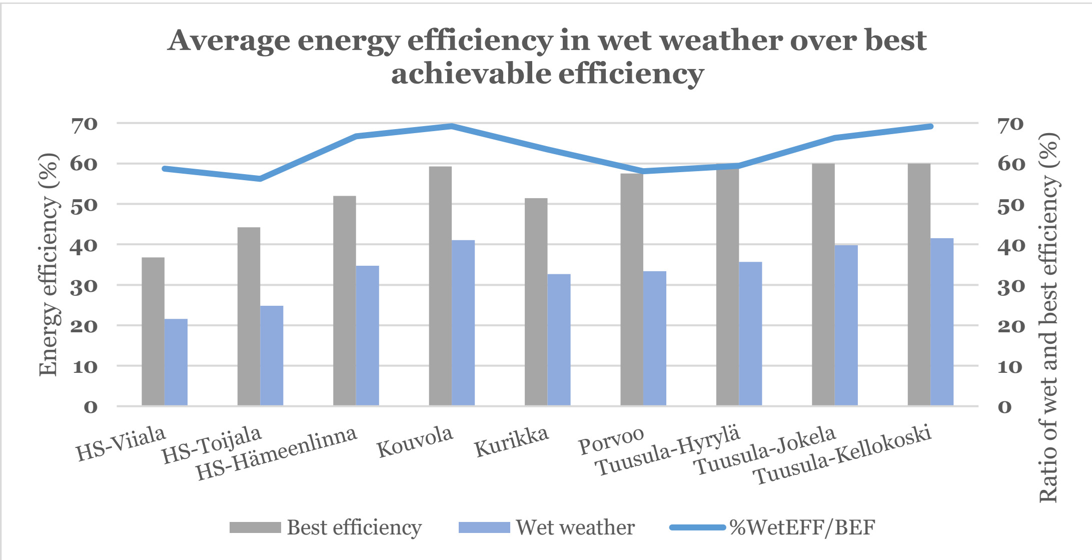

Figure 34. Average energy efficiency in wet weather over its best achievable efficiency

In both dry and wet scenarios, the average simulated efficiencies followed the same order of magnitude as their best efficiencies. In most of the region, the average efficiency was higher in the wet scenario, except for the Tuusula area. Kellokoski had the highest simulated efficiency in dry and wet weather, which was 40% and 41.5%. Following was Kouvola, with a value in dry and wet weather of 38% and 41% correspondingly. The percentage of average simulated value over the best achievable efficiency was the highest in the two areas. HS-Viiala had the lowest dry weather (21.6%) and wet weather average simulated efficiency (21.6%). However, HS-Toijala had the worst ratio of simulated efficiency over the best achievable, the result was under 60% in two scenarios.

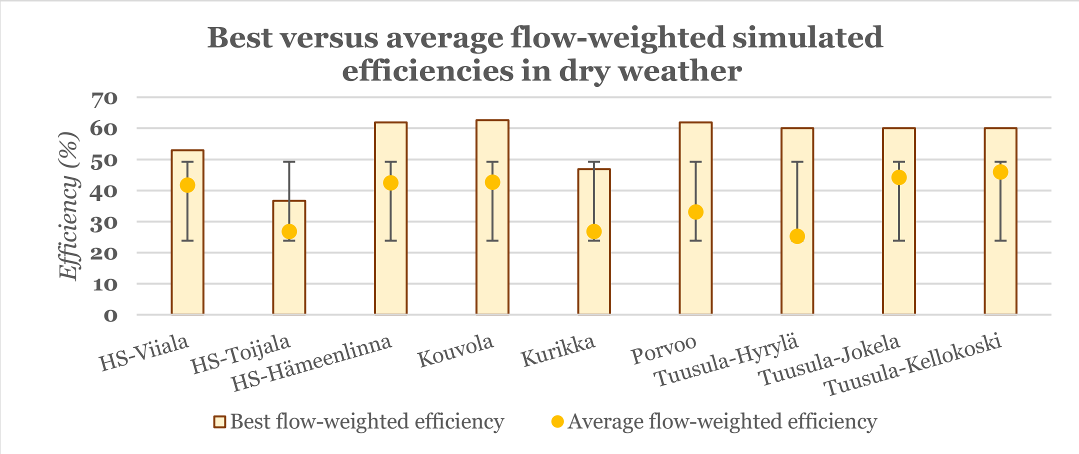

Figure 35. The best achievable flow-weighted efficiency and the average flow-weighted efficiency

The order of magnitude for the best achievable flow-weighted efficiency and the averaged flow-weighted value were different in comparison to the average result in the previous analysis. In Figure 35 and Figure 36, while Viiala had the lowest average best achievable efficiencies previously, its flow-weighted values were two times higher (53% in dry weather and 53.6% in wet weather), and Toijala's best flow-weight efficiencies were the lowest (37% in dry weather and 36% in wet weather). Hämeenlinna, Kouvola and Porvoo all had high flow-weight best efficiencies, which were higher than 60%. Among the three, Kouvola's best efficiencies were the highest: 61% in dry weather and 62% in wet weather.

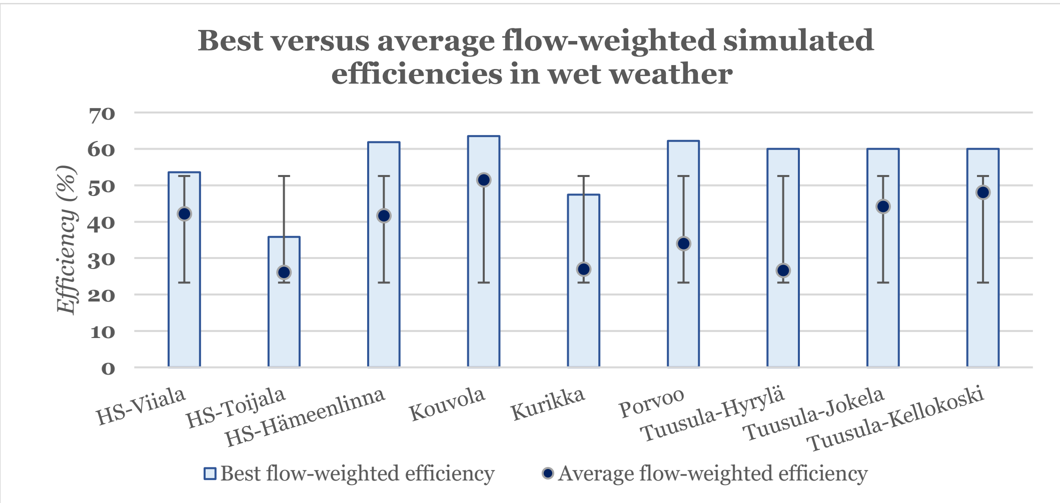

Figure 36. The best achievable flow-weighted efficiency and the average flow-weighted efficiency

As can be observed from Figure 35 and Figure 36, the average flow-weight efficiency with a standard deviation of 1.5 for observing the variation of the dataset was presented in all five regions. In dry weather, the value ranged from 26% to 41% and it was 28% to 44% in wet weather. The average flow-weighted value in wet weather was the highest in Kouvola, which was 51.5%. Besides, the average flow-weighted value in dry weather was the highest in Kellokoski with a value of 46%. Overall, the performance of Toijala, Kurikka, and Hyrylä was not as good as the other region, since their average flow-weighted efficiencies were under 30% in both the dry scenario and wet scenario.

From the five studied sites, there were recorded energy consumption measurements in Porvoo and Kurikka. The data was taken into account for calculating the actual energy efficiencies, as shown in Figures 37 and 38. In Porvoo, the average simulated and real efficiency in dry weather is 33% and 23%, while the average simulated value and real efficiency for the set of available energy measurements in wet weather is 34% and 18%. The highest difference between the efficiency from estimated records and the simulated results can be seen in JVP51 with almost 125% higher in reality for the dry scenario, which was because the actual energy consumption was far lower than the simulated value. On the other hand, the largest energy consumption differences were the wet weather energy consumption of JVP1, which was about 300 kWh/d higher than the value from the simulation, and the actual wet weather consumption of JVP100 should be approximately 600 kWh/d lower than the simulated value.

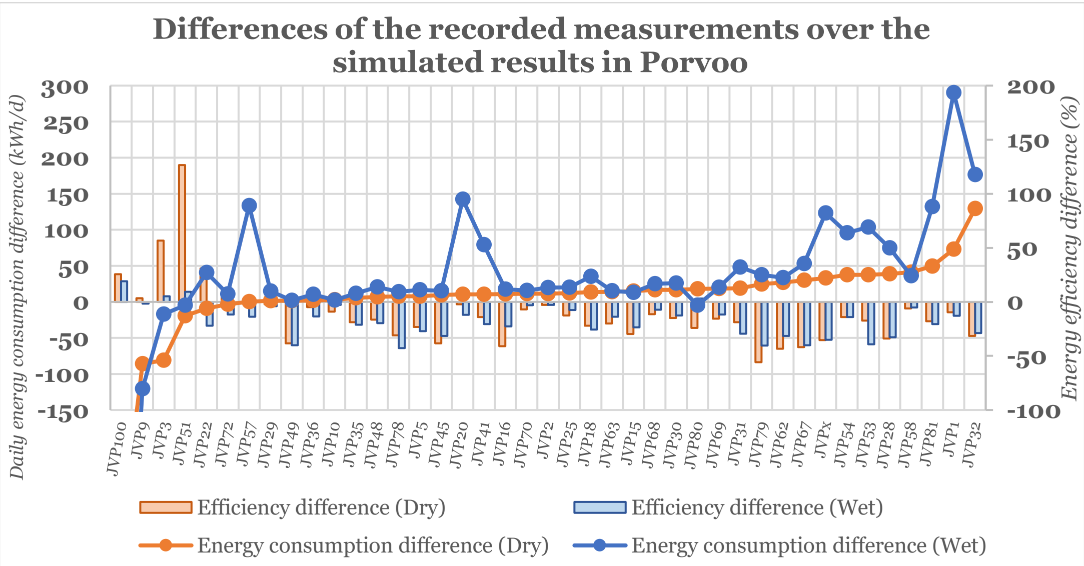

Figure 37. The simulated energy efficiencies in comparison to the actual efficiency in Porvoo

In Kouvola, the average simulated efficiency of the whole system was 29.3% in dry weather and 29% in wet weather. On the other hand, the real efficiency based on the set of available energy measurements is 12% in dry weather and 11% in wet scenario. Similar to Porvoo, the average simulated efficiency of the whole system was higher than the real efficiency.

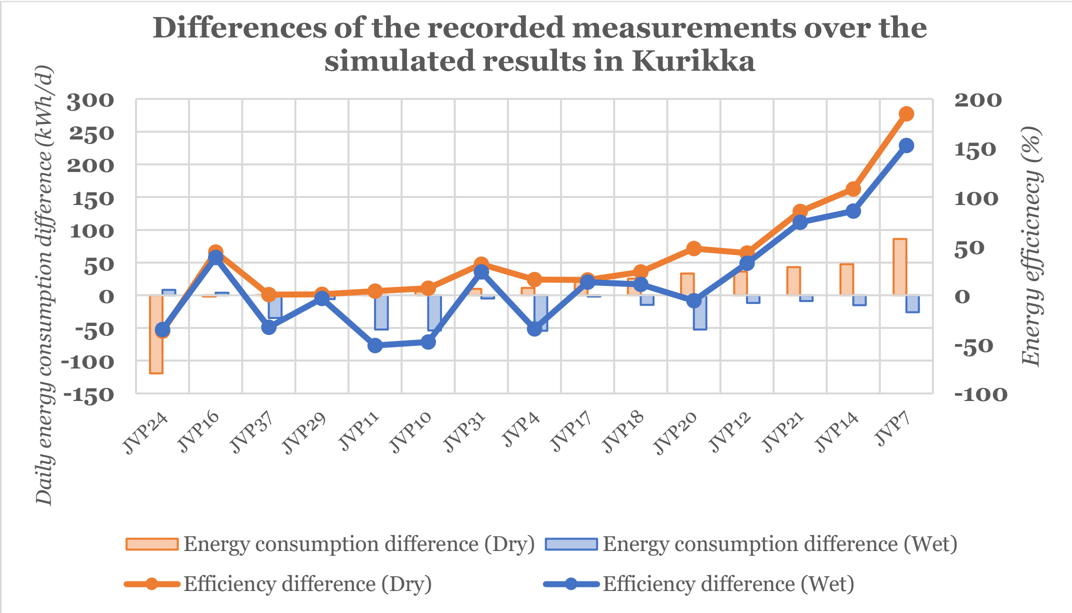

Figure 38. The simulated energy efficiencies in comparison to the actual efficiency in Kurikka

4.2.2 Energy balance

A more complete picture of the energy use of a sewer system can be shown in the energy balance in dry weather (Figure 39) and wet weather (Figure 40). The average percentage of each energy component was presented in the first bar to give a better comparison scale. The energy outflux intrinsic friction (around 0.01% in all regions), external friction, and overflow were too minimal which cannot be observed from the graph. Hence, in this section, the outflux external inefficiencies could be defined as the sum of the energy outfluxes.

For the dry weather study, the outflux external inefficiencies held the largest part of the total system in every region, which corresponded to the pump efficiency. Looking at the average bar, the energy outflux (53%) and energy influx (42%) were almost equivalent. Toijala and Jokela had the highest external inefficiencies, 60% and 64% respectively. On the other hand, external inefficiencies in Kellokoski and Viiala were around 40%. The least contributions to the system energy are the external undue and intrinsic parts from energy influx, referring to the energy used in pumping undue inflows and the energy produced by undue gravitational inflows. The values differed in every case, yet the lowest was observed in Kurikka, with 3.4% of intrinsic undue energy influx and 0.9% of external undue energy influx.

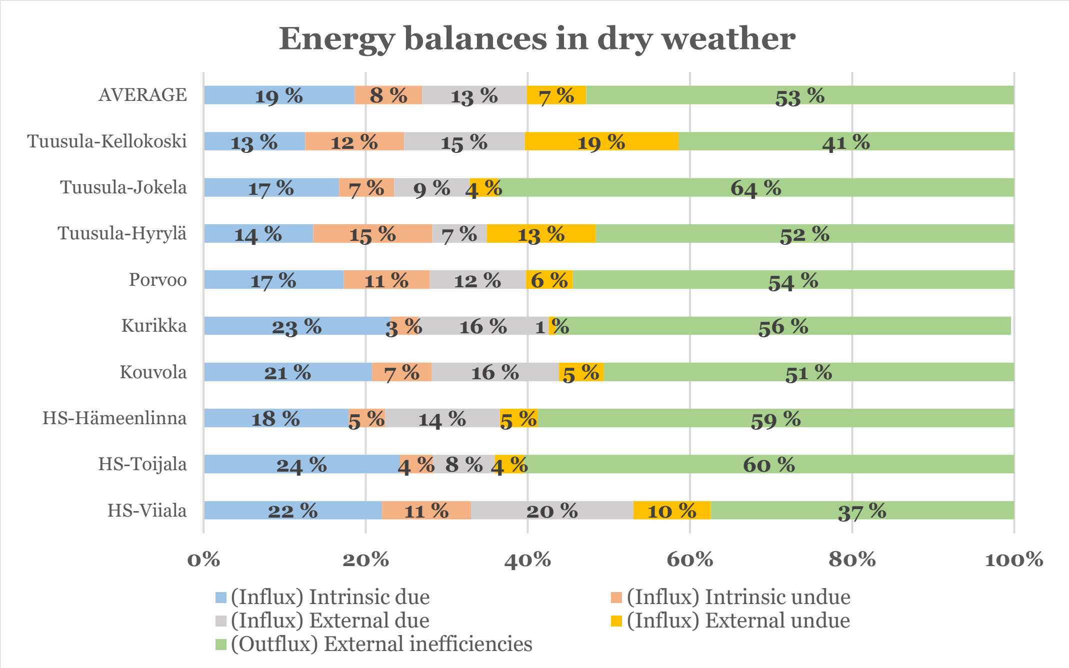

Figure 39. Energy balances in dry weather of all studied sites

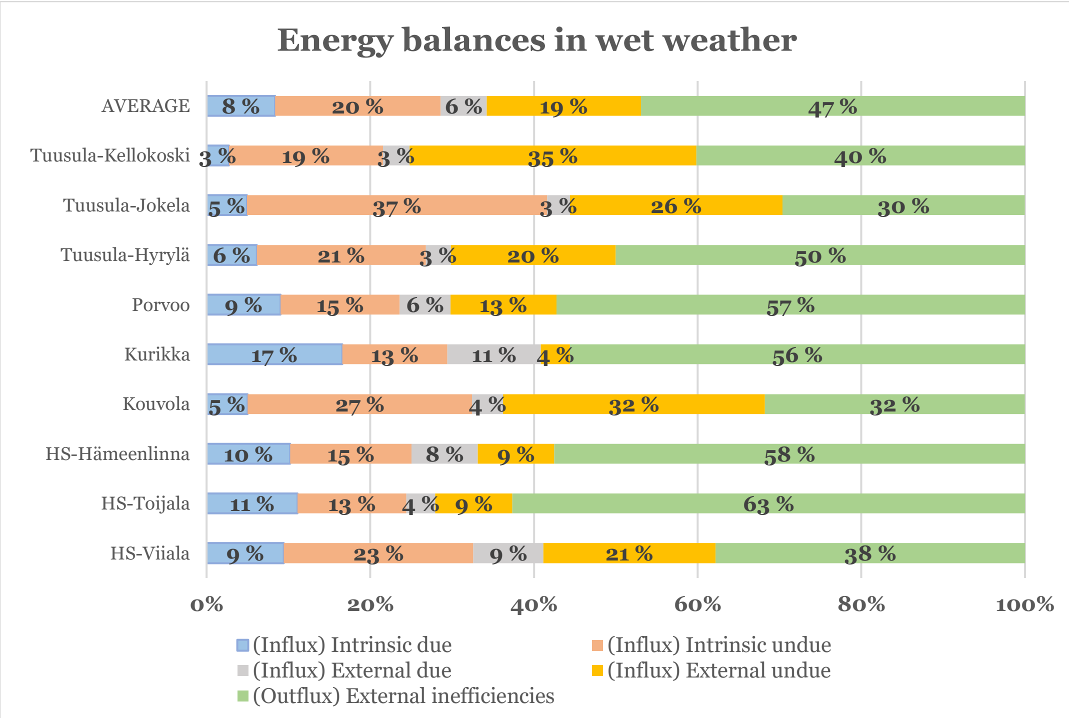

Figure 40. Energy balances in wet weather of all studied sites

Similar to the dry weather case, external inefficiencies percentage was the biggest part making up the energy system. Nonetheless, the energy outflux was slightly lower than energy inflows in this scenario, which was 47% and 53% respectively. Toijala also contained the highest external inefficiencies percentage of 63%. In contrast to the dry case, the second largest portions in wet weather were the external undue energy inflows and intrinsic undue energy inflows. Kelloskoski had the highest external undue energy influx of 35% and Jokela had the highest intrinsic undue energy influx of 37%. The energy influx external due was the lowest in both cases.

4.2.3 Relationship between the performance and characteristic

The relationship between four different pump parameters, which were the flow rate, the specific energy, the energy efficiency, and the electric power. With the following graphs, the result of every pump in five regions were combined for visualization with their 20th, 50th, and 80th percentile lines. From the total of 470 pumps, there were 217 pumps with actual head-flow and efficiency curves. The maximum flow rate that could be performed was 155 l/s, and the highest specific energy was over 40 kWh/m3. In this section, the pump flow rate and electrical energy were presented in logarithmic scale for better visualization and reading comprehension.

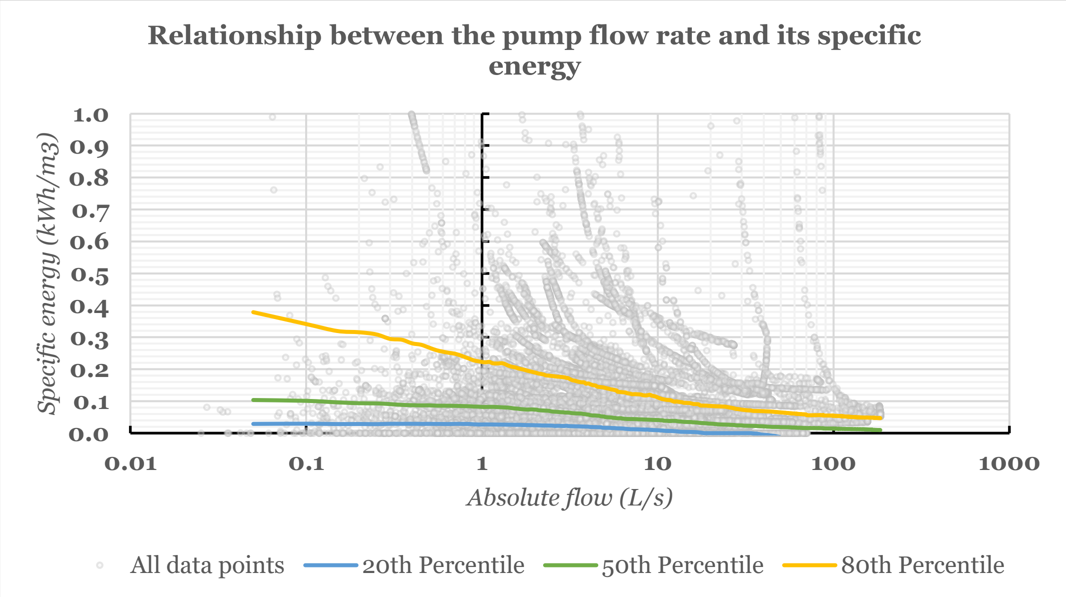

Figure 41. Relationship between the pump flow rate and its specific energy

In Figure 41, the relationship between the pump flow rate and its specific energy was presented. The specific energy increased with a flow rate lower than 5 l/s. Towards the higher flow rate, the specific energy kept decreasing. Most of the available pumps performed with the maximum absolute flow of 25 l/s and its specific energy mainly stayed under 1 kWh/m3.

The pump efficiency of all pumps remained below 70%. Mainly, efficiency ranged between 20% to 45%. The same tendency can be observed from Figure 42 of all pumps that the efficiencies increased with a higher flow rate. With the flow rate of under 5 l/s, the efficiency changed quite rapidly, while at a higher rate, the increase in efficiency was moderated toward its best achievable value.

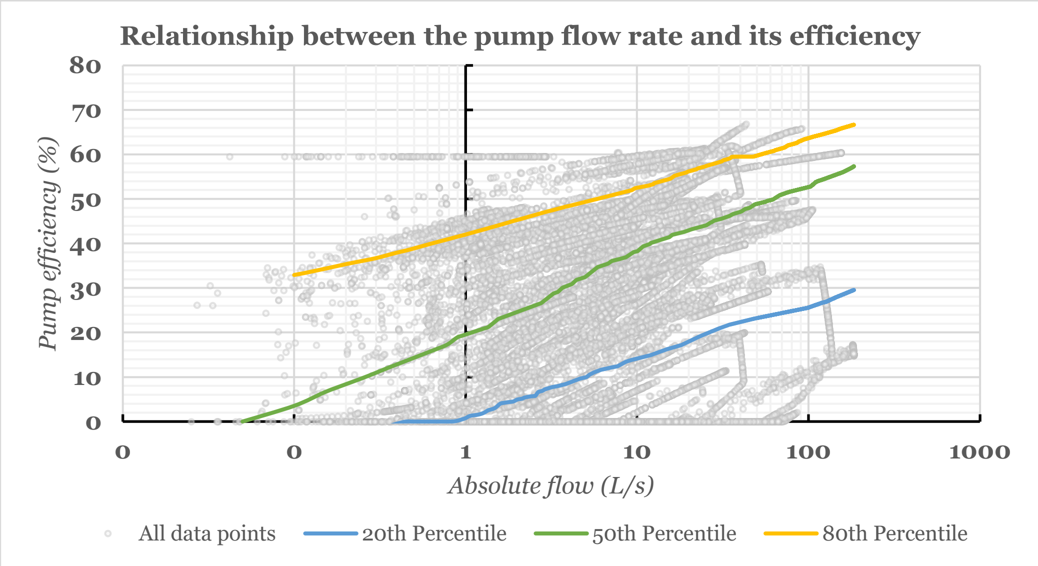

Figure 42. Relationship between the pump flow rate and its efficiency

Lastly, the relationship between electric energy consumption and its efficiency was shown in Figure 43. The electric power for the most part stayed under 10 kW with efficiency almost reaching its maximum. At the larger scale, the electric power could reach 100 kW and the corresponding efficiency higher than 60%.

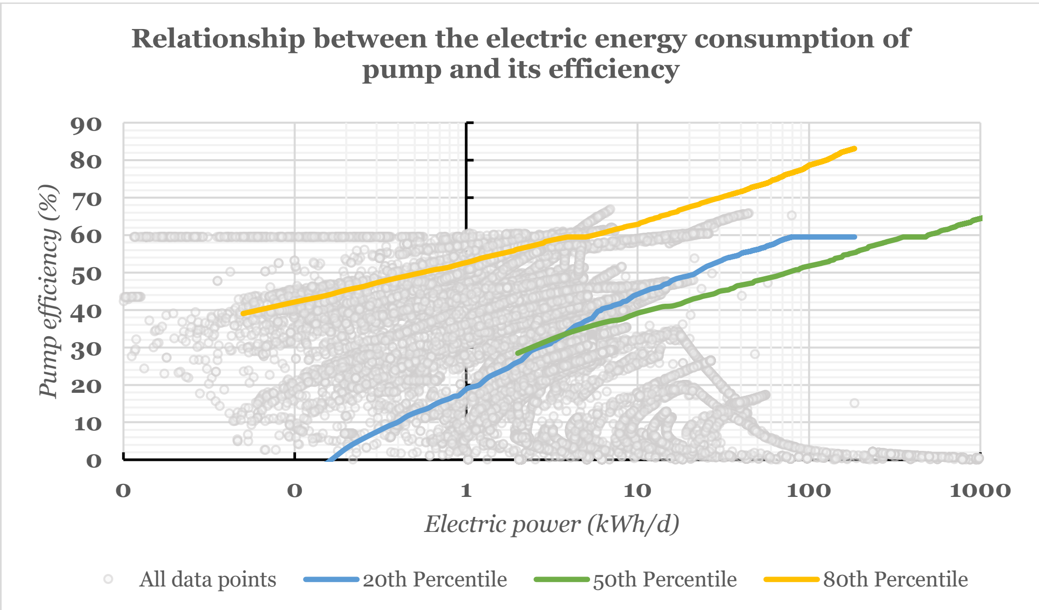

Figure 43. Relationship between the electric energy consumption of pump and its efficiency

4.3 Friction loss percentage in the pressure line

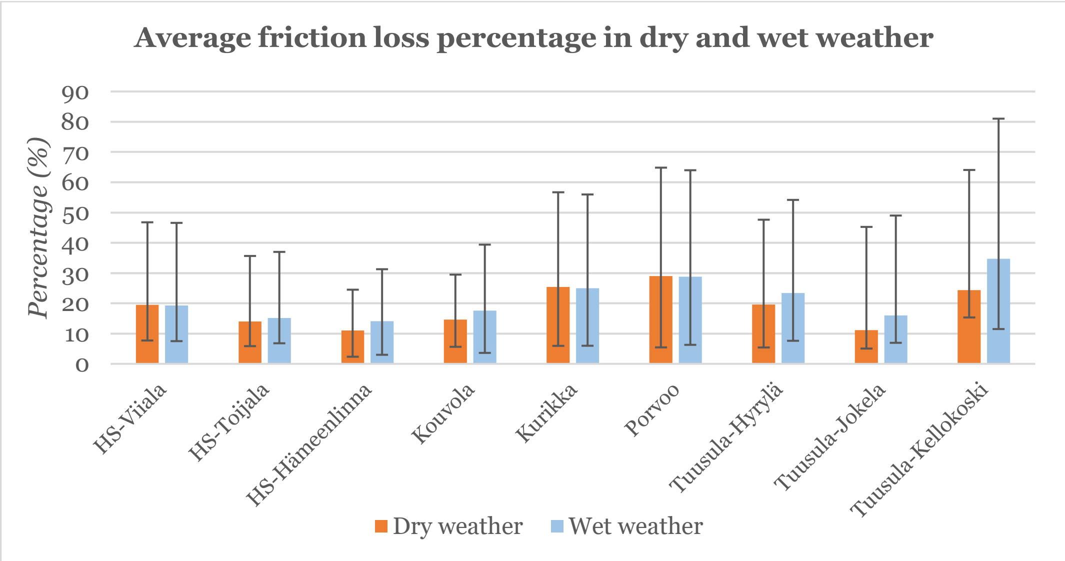

Figure 44. Average friction loss percentage in dry and wet weather

The average friction loss percentages in all five regions were presented in dry weather and wet weather, along with its 95% confidence interval to take in the range of the results. Hämeenlinna and Jokela had the lowest average friction loss percentages in dry weather, which were both around 11 %. The highest head loss percentage was 35 % in Kellokoski, during wet weather. In general, the average friction loss percentage remained under 40 % in wet weather and under 30 % in dry weather. The difference between dry weather and wet weather was not significant. The changes were approximately a-1.2-time increment in wet weather, nonetheless, the differences were more significant in Jokela and Kellokoski. The average friction loss percentage in wet weather was 1.4 times higher than the value in dry weather.

5 Smart control methods optimized results

In this section, the results of energy saving potential and overflow reduction after the applied smart control and using the suggested pump replacements are presented in three areas: HS regions (Viiala, Toijala, and Hämeenlinna), Porvoo and Tuusula (Hyrylä, Jokela, and Kellokoski). The best efficiency can be achieved from the current pump and the optimal pump taken from the dry weather scenario.

5.1 Hämeenlinna Region Water Utility

The selection of the optimal pump for HS regions will be presented in this part, along with the potential for energy consumption and overflows reduction and the corresponding repayment period.

5.1.1 Optimal pumps selection

From the pumping station chain in Viiala, there were 7 stations selected for a more suitable pump definition as listed in Table 23 below. JVP224, JVP220, JVP210, JVP240, and JVP230 were chosen for their high specific energy, while JVP222 had low energy efficiency and JVP223 had a friction loss percentage higher than 50% total static head. In the tables below, the best achievable efficiency with the current designed flow rate was compared with a more suitable pump definition.

Table 23. Optimal and current pumps selection for the Viiala region

Name	Current pump		Optimal pump	
	Name	Best efficiency	Name	Best efficiency
JVP224	S1034C1501P	37% at 28 l/s	SL1.80.80.30	53% at 12 l/s
JVP222	SV024B1D501P	5% at 7 l/s	SL1.50.65.09	35% at 6.5 l/s
JVP220	S1104AH6B511	48% at 50 l/s	SL1.80.80.40	56% at 31 l/s
JVP223	SV024CU50B	16% at 21 l/s	SL1.80.80.15	50% at 17 l/s
JVP240	SV044DHS50B	29% at 18 l/s	SL1.80.80.22	59% at 16 l/s
JVP210	S1404H3B511	50% at 90 l/s	S1.100.125.500	53% at 55 l/s
JVP230	S1054H3B511	37% at 58 l/s	SL.100.100.4	45% at 35 l/s

Similarly, in Table 24, JVP120 was selected for its high specific energy consumption and high head loss percentage in the Toijala area. The other pumps JVP130, JVP121, and JVP123 had low energy efficiency, and especially, JVP123 performed with a friction loss percentage higher than 50 %.

In Hämeenlinna (Table 25), the pumping stations with high specific energy were JVP01 – the pump with the highest energy consumption in the network, JVP101, JVP31 (also had low energy efficiency), JVP23, and JVP34 (Table 25). JVP02 was also selected for its high friction loss percentage.

Table 24. Optimal and current pumps selection for Toijala region

Name	**Current pump**		**Optimal pump**	
	Name	Best efficiency	Name	Best efficiency
JVP121	SLV.80.80.15	8% at 2 l/s	SLV.65.65.09	10% at 2 l/s
JVP130	PX3-150	37% at 13 l/s	SL1.50.65.15	65% at 12 l/s
JVP120	PX3-150	30% at 52 l/s	SL1.100.100.55	50% at 60 l/s
JVP123	SV014bliap	1% at 2 l/s	SLV.65.65.09	10% at 2 l/s

Table 25. Optimal and current pumps selection for the Hämeenlinna region

Name	**Current pump**		**Optimal pump**	
	Name	Best efficiency	Name	Best efficiency
JVP23	T6A-B	32% at 67 l/s	SL.100.220.4	65% at 28 /s
JVP31	K203TH-VB6323-26KW	17% at 129 l/s	SL2.110.250.130	48% at 43 l/s
JVP34	Px4-150	43% at 52 l/s	SL.100.240.2	58% at 30 l/s
JVP01	F06K-S	69% at 208 l/s	S2.110.200.850	59 % at 175 l/s
JVP02	Fluidit generated	45% at 82 l/s	S2.140.300.350	64% at 18 l/s
JVP101	Fluidit generated	48% at 81 l/s	S2.140.300.350	64% at 34 l/s

5.1.2 Energy saving potential

When replacing the current pump with a more suitable pump selection with a higher efficiency range in Viiala, the energy consumption was reduced in all three scenarios: dry, wet, and overflow cases. While the maximum reduction can be observed from pump JVP223 (more than 60%), pump JVP210 and JVP220 (up to 57% and 69% respectively in overflow scenario), nonetheless, some pumps had increased energy usage, for example, pump JVP221 and JVP222 in dry and wet weather. The energy reduction increased with increased inflows coming to the network, the maximum change could be observed was 69% in JVP220 and 99% in JVP222 in the overflow scenario. However, when applying the level control method, energy consumption intensively increased in dry weather. On the other hand, it decreased in the overflow scenario and kept reducing when applying both level control and using optimal pumps, as shown in Table 26.

Table 26. HS region total energy consumption of the chosen pumping chain

		Viiala	**Toijala**	**Hämeenlinna**
Dry weather	Original (kWh/d)	166	70	2763
	Optimal pump	-15 %	-46 %	67 %
	Original & control	609 %	105 %	-20 %
	Optimal pump & control	427 %	-38 %	3 %
Wet weather	Original (kWh/d)	395	166	4567
	Optimal pump	-12 %	-46 %	78 %
	Original & control	171 %	-6 %	-3 %
	Optimal pump & control	94 %	-21 %	15 %

Overflow scenario	Original (kWh/d)	4483	756	7196
	Optimal pump	-56 %	-41 %	17 %
	Original & control	-0.3 %	7 %	-37 %
	Optimal pump & control	-40 %	-34 %	-39 %

The energy consumption was successfully reduced in all selected pumps when the pump type was changed in the Toijala network. In all three scenarios, the optimal alteration helped reduce the energy usage by up to 98 % in wet weather, nevertheless, the energy consumption was not reduced as exceedingly in the overflow situation. In the case of using the smart control method without changing pump definition, JVP130 energy usage was increased in all three scenarios with the highest change in dry weather, approximately more than two times the original consumption. Likewise, the control did not perform well for this purpose in JVP156 and JVP122. The situation could not be improved even with the changed pump definition, regarding some individual stations, however, the total consumption of the whole chain did reduce by around 20% to 30%.

Similar outcomes as Toijala were observed in Hämeenlinna as can be seen in Table 26. The optimal pump successfully minimizes the energy consumption in the selected pumps. The energy usage of pumps JVP31 and JVP23, which originally consumes quite significant energy daily, with optimal pumps was reduced up to 80% for the three scenarios. However, the energy usage happened to increase in other areas (JVP13 for example with the increment of 2 to 5 times in dry and wet weather). The total energy consumption of the chosen chain was reduced by 20 % in dry weather, 3 % in wet weather, and 37 % in overflow cases when applying the level control without changing the optimal pumps. While making an additional change to the pump definition in combination with level control, only the overflow scenario brought benefits for energy-saving purposes, with a reduction of 39 %.

5.1.3 Overflow reduction

In Viiala's case, the additional flow was increased in every part of the network. The total overflow volume per day in the current situation was 232 m^3. The value can be reduced to zero only by changing to more suitable pump selections, while it can be reduced by only 19 % when applying the level control method.

The backflow scenario in Toijala would create 34 m^3 in the nearby manhole. The overflow could be reduced by 9 % with the applied control. On the other hand, the energy consumption increased by 20 times when changing the pump model, showing that the chosen pump definition was not suitable for higher inflows. Moreover, when pump replacement was taken into account, the total overflow volume increased significantly. When applying the control together with the optimal pumps, the reduction was minimal, which was around 2m^3.

Table 27. Daily total overflow volumes in the Hämeenlinna regions results

		Total overflow volume (m^3)	Percentage change from the original
Viiala *Demand multiplier*	Original	232	0 %
	Optimal pump	0	-100 %
	Original & control	189	-19 %
	Optimal pump & control	0	-100 %
Toijala *Backflow accident*	Original	34	0 %
	Optimal pump	753	2132 %
	Original & control	31	-9 %
	Optimal pump & control	750	2125 %
Hämeenlinna *Blockage accident*	Original	1986	0 %
	Optimal pump	1885	-5 %
	Original & control	1868	-6 %
	Optimal pump & control	1957	-1 %

Because of the blockage, there will be overflow from the overflow pipe of JVP01 in the Hämeenlinna area. The maximum overflow reduction was 6 % for the case of using the current pump and applying the level control method.

5.1.4 Estimation of cost

Based on Viiala's energy consumption result above, it is not beneficial to change the pump in this area. The estimation of cost was calculated for pump JVP120 and JVP123 in Toijala, together with pump JVP31 and JVP23 in Hämeenlinna.

Table 28. Repayment period for Hämeenlinna regions pumps' replacement

Region	Pump	Yearly energy consumption (kWh/a)	Yearly energy consumption with optimal pump (kWh/a)	Yearly total electric expenses reduction (euro)	Optimal pump price with one-year maintenance (euro)	Repayment time (year)
Toijala	**JVP120**	19 549	10 873	17 35	6 060	3.5
	JVP123	313	39	55	4 316	79.0
Hämeenlinna	**JVP31**	82 369	21 920	12 090	19 900	1.7
	JVP23	107 548	34 545	14 601	18 981	1.3

5.2 Porvoo

The study on the Porvoo pumping station chain will be shown in this section.

5.2.1 Optimal pumps selection

In the Porvoo area, six pumping stations were selected for changing with more suitable pump definitions, which were JVP04, JVP100, JVP01, JVP05, JVP18, and JVP09. In addition, JVP02 and JVP10 were also included for their high head loss percentage. The list can be seen in Table 29.

Table 29. Optimal and current pumps selection for the Porvoo region

Name	**Current pump**		**Optimal pump**	
	Name	Best efficiency	Name	Best efficiency
JVP05	Flygt NP 3102.181 LT 420	57% at 33 l/s	SL1.80.100.40	20% at 8 l/s
JVP02	S1.100.200.135.4	46% at 100 l/s	S2.140.300.350	44% at 41 l/s
JVP04	Gorman-Rupp T6A-B-4	2% at 84 l/s	SL.100.130.4	30% at 22 l/s
JVP18	Sarlin SV034CH6	1% at 11 l/s	SE1.80.100.15	40% at 64 l/s
JVP10	Flygt NP 3085.183 MT 460	49% at 30 l/s	SE1.80.100.22	55% at 6 l/s
JVP01	Gorman-Rupp T10-A-3AS-B	35% at 130 l/s	S2.145.300.200	64% at 68 l/s
JVP09	Gorman-Rupp T4A-3-B	18% at 42 l/s	SL.100.100.4	54% at 7 l/s
JVP100	Fluidit generated	17% at 184 l/s	S2.100.300.400	56 % at 122 l/s

5.2.2 Energy saving potential

From all of the scenarios, the energy consumption of pumps JVP4, JVP10, JVP8, JVP1, JVP9, and JVP100 had been reduced by applying the level control without changing the pump definition, or only changing the pump definition and with both the changed pump and level control. The detailed results of all pumps can be observed in Appendix 7.2.2. Their energy usage reduction was higher in dry and wet weather than in overflow scenarios, yet the results were remarkably significant with a reduction of up to 90% (pump P18, P9, and P4 for instance). On the other hand, the energy consumption of the remaining stations (JVP16, JVP73, JVP17, and JVP58) increased, especially, energy usage in JVP17 was more than 4000 % higher in wet weather when applying the level control method. A similar large increment can be observed in JVP58. Nonetheless, these stations originally consumed very low daily electrical energy, so the changes did not have an impact on the total energy use.

In overall, the sum of energy consumption of the whole chain was successfully reduced in all scenarios when applied any suggested changes. The highest change was obtained from using the optimal pumps in dry weather, the total energy consumption of the chain can be reduced by around 80%.

Table 30. Porvoo total energy consumption of the chosen pumping chain

		Total energy consumption
Dry weather	Original (kWh/d)	4640
	Optimal pump	-92 %
	Original & control	-68 %
	Optimal pump & control	-84 %
Wet weather	Original (kWh/d)	6615
	Optimal pump	-86 %
	Original & control	-55 %
	Optimal pump & control	-54 %
Backflow scenario	Original (kWh/d)	5520
	Optimal pump	-23 %
	Original & control	-29 %
	Optimal pump & control	-4 %
Blockage scenario	Original (kWh/d)	1246
	Optimal pump	151 %
	Original & control	-81 %
	Optimal pump & control	-74 %

5.2.3 Overflow reduction

With the backflow happening in JVP01, JVP02, and JVP16, overflow happens in the overflow pipe of pump JVP100 with a total overflow volume was 40 m^3. The overflow volume can be canceled when using the optimal pump and reduced by half with the level control method, shown in Table 31. If the control algorithm was built to signal all sets of upstream stations to react immediately to store more inflows when the main pump level reaches its level, then the overflow is reduced to 5 m^3, which is equal to a -87% percentage change. The case was tested using the same pump definition.

Table 31. Daily total overflow volumes in Porvoo

		Total overflow volume (m^3)	Percentage change from the original
Backflow accident	Original	39	0 %
	Optimal pump	0	-100 %
	Original & control	18	-54 %
	Optimal pump & control	0	-100 %
Blockage accident	Original	98	0 %
	Optimal pump	101	3 %
	Original & control	85	-14 %
	Optimal pump & control	81	-18 %

The blockage scenario happened causing an overflow volume of 98 m^3. When altering the pump definition, the total overflow slightly increased by 3%, however, it decreased up to 20% when applying the level control. In this scenario, if all upstream stations react immediately then the same result for total overflow was observed.

5.2.4 Estimation of cost

Besides the estimated yearly energy consumption from the simulation, the actual yearly recorded energy usages in JVP10, JVP1, JVP9, and JVP100 were available. Since the actual consumption was higher than the simulated result, the repayment time resulted in a little longer period.

Table 32. Repayment period for Porvoo region m s’ re la e ment

Pump	Yearly energy consumption (kWh/a)		Yearly energy consump-tion with optimal pump (kWh/a)	Yearly total electric expenses reduction (euro)		Optimal pump price with one-year mainte-nance (euro)	Repayment time (year)	
	Simu-lated	Actual		Simu-lated	Actual		Simu-lated	Actual
JVP4	953 860	No data	21 895	186 393	No data	17 083	0.1	No data
JVP10	4 704	5 680	3 052	330	526	6 183	18.7	11.8
JVP1	137 801	177 470	28 195	21 921	29 855	25 060	1.1	0.8
JVP9	70 594	42 202	3 808	13 357	7 679	13 665	1.0	1.8
JVP100	268 152	115 604	51 960	43 238	12 729	24 085	0.6	1.9

5.3 Tuusula

For Tuusula regions, the potential for energy usage and overflow reduction was studied in three areas: Hyrylä, Jokela, and Kellokoski. The estimation of cost will be presented in the end based on the fit of different weather scenarios and level control methods.

5.3.1 Optimal pumps selection

In the Tuusula area, all pumping stations with high energy consumption or specific energy were selected for changing with more optimal pumps. The following tables (Table 33, Table 34, and Table 35) presented the list of chosen pumps in Hyrylä (JVP22, JVP25, JVP13, JVP10, JVP1, and JVP14), Jokela (JVP12, JVP4, JVP8, and JVP1) and Kellokoski with only one pump, which was JVP1. The best achievable efficiency with the current designed flow rate was compared with a more suitable pump definition shown below.

Table 33. Optimal and current pumps selection for Hyrylä region

Name	Current pump		Optimal pump	
	Name	Best efficiency	Name	Best efficiency
JVP22	generated	45% at 19 l/s	SLV.100.100.75	17% at 3 l/s
JVP25	generated	48% at 43 l/s	S2.110.250.650	60% at 239 l/s
JVP13	generated	49% at 21 l/s	SE1.80.100.55	48% at 14 l/s
JVP10	generated	51% at 15.5 l/s	SLV.80.100.40	40% at 19 l/s
JVP1	generated	29% at 79 l/s	S2.105.250.500	60% at 203 l/s
JVP14	generated	19% at 36 l/s	SE1.80.100.15	31% at 35 l/s

Table 34. Optimal and current pumps selection for Jokela region

Name	Current pump		Optimal pump	
	Name	Best efficiency	Name	Best efficiency
JVP12	generated	50% at 27 l/s	SL1.80.100.75	57% at 10 l/s
JVP4	generated	45% at 46 l/s	S1.100.125.300	50% at 14 l/s
JVP8	generated	2% at 10 l/s	DPK.V.65.80.22	28% at 1.6 l/s
JVP1	generated	42% at 30 l/s	SL1.100.100.75.4	54% at 15 l/s

Table 35. Optimal and current pumps selection for Kellokoski region

Name	Current pump		Optimal pump	
	Name	Best efficiency	Name	Best efficiency
JVP1	generated	47% at 74 l/s	S2.100.200.650	65% at 218 l/s

5.3.2 Energy saving potential

For the Hyrylä region, the studied wet weather had already the peak scenario with overflow happening in several manholes. Therefore, the energy-saving potential study included only two cases in the region, which explains the similar results between the wet and overflow scenarios in Table 36. With the optimal pump, the total energy consumption of the whole chain was reduced by 70% in dry weather and 60% in wet weather. Particularly, JVP1 and JVP14 which were the highly consuming pumps, can be reduced by up to 97% in wet weather. Besides, almost all pump energy consumption would be reduced by more than 50% with optimal pumps, except for JVP10, JVP31, and JVP3 in dry weather, and JVP30 in wet weather with a massive increment of 17 025%. However, JVP30 had quite insignificant daily energy usage and was not chosen from the set of stations that need a change to a better pump. The increase in energy consumption was influenced by the changed pump model of nearby stations. On the other hand, the energy-saving potential did not perform well in Hyrylä, as can be observed with more detailed results in Appendix 7.2.3, nearly every pump consumed more energy with the smart control, especially in dry weather. The case improved modestly in wet weather and when combined with the changed pumps.

Table 36. Tuusula total energy consumption of the chosen pumping chain

		Hyrylä	Jokela	Kellokoski
Dry weather	Original (kWh/d)	1224	359	240
	Optimal pump	-70 %	-28 %	-9 %
	Original & control	239 %	1 %	-19 %
	Optimal pump & control	192 %	-46 %	-12 %
Wet weather	Original (kWh/d)	2830	1977	1099
	Optimal pump	-60 %	-35 %	-25 %
	Original & control	235 %	-46 %	-85 %
	Optimal pump & control	27 %	-52 %	107 %
Overflow scenario	Original (kWh/d)	2830	1362	264
	Optimal pump	-60 %	-27 %	11 %
	Original & control	235 %	-19 %	25 %
	Optimal pump & control	27 %	-30 %	19 %

All selected pumps in Section 5.3.1 had improved performance with more suitable pumps in Jokela. JVP8 and JVP1 were the two pumping stations with high daily electricity consumption that were intensively reduced, especially in dry weather, which was up to 94% reduction in JVP8 for all scenarios and more than 90% in JVP1 in dry weather with level control. Level control worsened the situation in Jokela energy usage in dry weather, for example in stations of low daily energy consumption JVP146 and JVP132. However, in total, the control reduced the consumption of the whole chain in wet weather by 46% and 19% in overflow cases. The effect from individual pumps was not clear to observe.

In Kellokoski, the change of pump definition in JVP1 could reduce energy consumption by 10% in dry weather and 24% in wet weather. The total energy usage would be reduced in dry and wet weather with optimal pump, level control method without optimal pump replacement. On the contrary, both the pump replacement and level control were not optimized in the overflow scenario, the daily electricity usage was increased in most parts.

5.3.3 Overflow reduction

The increase of inflows in every location in the network would cause a daily overflow volume of 17 624 m^3 in Hyrylä. The volume was increased slightly when replaced with the optimal pump, while again moderately decreased by only 1% with applying the smart control.

The overflow can be minimized by up to 60% when applying the level control for the Jokela chain, however, it could be increased somewhat with the optimal pump being installed. If the control algorithm was built to signal all sets of upstream stations to react immediately to store more inflows when the main pump level reaches its level, then the overflow is reduced to 106 m^3, which is equal to a -62% percentage change.

Table 37. Daily total overflow volumes in Tuusula

		Total overflow volume (m^3)	**Percentage change from the original**
Hyrylä	Original	17 624	0 %
Demand	Optimal pump	17 844	1 %
multiplier	Original & control	17 446	-1 %
	Optimal pump & control	17 921	2 %
Jokela	Original	281	0 %
Blockage	Optimal pump	305	9 %
accident	Original & control	117	-59 %
	Optimal pump & control	232	-18 %
Kellokoski	Original	101	0 %
Blockage	Optimal pump	112	11 %
accident	Original & control	75	-26 %
	Optimal pump & control	62	-39 %

The same result was shown in the Kellokoski blockage scenario. The total daily overflow was increased with the optimal pump; however, the control method could help reduce it by up to 40% when applying it together with the optimal pump.

5.3.4 Estimation of cost

Based on Kellokoski's energy consumption result above, it is not beneficial to change the pump in this area. The estimation of cost was calculated for pump JVP1 and JVP14 in Hyrylä, along with JVP8 and JVP1 in Jokela.

Ta le 33. Re ayment eriod for T s la regions m s' re la ement

Region	Pump	Yearly energy consumption (kWh/a)	Yearly energy consumption with optimal pump (kWh/a)	Yearly total electric expenses reduction (euro)	Optimal pump price with one-year maintenance (euro)	Repayment time (year)
Hyrylä	**JVP1**	428 680	40 893	77 557	4 290	0.1
	JVP14	21 098	9 851	2 249	5 885	2.6
Jokela	**JVP8**	64 321	4 271	12 010	4 211	0.4
	JVP1	86 235	45 519	8 143	7 725	1.0

6 Discussion

In the section, the uncertainties and assumptions made from the research was listed and mentioned. The outcomes from benchmarking phase were discussed to assess the performance of the Finnish sewerage network. Moreover, the applicability of the proposed level control method was defined.

6.1 Uncertainties

Before coming up with the conclusion, several assumptions made in the study need to be emphasized. In more than half of the cases, the storage volume was assumed to be 1 meter in diameter in most of the area, or based on the total incoming inflows if the station was a large one. Likewise, the elevation of the manhole, storage unit, and pump startup/shutoff depth was estimated based on the topography. Along with the share of generated pump curves overall, there is a certain degree of reliability in the outcomes but should not differ completely from reality. Furthermore, the suggested pumps for the better fit of the system were restricted to only the Grundfos database and their automated selection tool. While a manual search will yield a better result, it might be likely that more suitable candidates could be left out in this situation.

The overflow scenario was made entirely hypothetically. Extreme weather or accident could hardly occur in the near future since the total inflows were assigned to be massive in some locations in order to create an overflow in the system. It could be concluded that the capacity of the network in the five utilities was quite high so that a large amount of water could be retained. Since the scenario was imaginary, the result of the reduction of the overflow volume could change greatly depending on the duration of the accident and the location when it could happen.

The estimation of the cost for the replacement of the pump at the end of the study did not include the cost of installing the pump and other possible extra costs. The cost of the energy was assumed to be constant. Not to mention, most of the pump prices were collected from Grundfos' list price, except for Hämeenlinna pumps, Porvoo – JVP9 and Tuusula pumps' prices were taken from foreign websites (Russia Esmo Company for Hämeenlinna and ProFluid GmbH for the rest) when the official pump price is not available in Grundfos Finland's list price.

6.2 Benchmarking

In this discussion, the results of the studies will be compared with the result from other utilities in other countries, based on certain assessment schemes to evaluate the performance of the Finnish sewerage network. For instance, the performance assessment system (PAS) proposed by Jorge et al. (2021) for energy efficiency in wastewater systems could be used to evaluate several service objectives and criteria comprehensively. Because the study focused only on the collection and transportation of sewer systems, the standards Type B in PAS will be referred to in this section. The performance between the five areas will also be reviewed, together with a discussion on the variation and relationship of different parameters in dry and wet scenarios.

6.2.1 Flood analysis

According to Table 14, the result for the infiltration rate median was around 19% in dry weather (60% confidence interval range between 23 % to 27 %) and over 67% in wet weather (60% confidence interval range between 58 % to 63 %), noted that the infiltration rate was not calculated using the same source of measurement data and in different periods. In the UK, it has been observed that the infiltration rates range from 15% to 50% in average dry weather (White et al., 1997) and an addition of 10 to 20% more in wet weather scenarios (Heywood and Lumbers, 1997). The undue flows to Folhadela WWTP, Vila Real, Portugal in May 2014 and May 2015 can be detected up to 47% of infiltration inflows in dry weather and as a sum of 85% including rainwater flows in wet weather (Bentes et al., 2022). Another example is from Kuantan City, Malaysia, the average infiltration rate was 17% to 21% (Hiew and Su, 2017). To compare with the infiltration rates studied in other countries, it can be concluded that the level of I/I of the studied Finnish sewerage networks is average. However, it should be noted that the UK's result was taken from the late 20th century, the age of different networks should be considered as also the differences in the climate of different countries. Therefore, there should be more room and opportunities to decrease the infiltration rate in the sewer systems in Finland.

For the most part, the infiltration rate was calculated differently in the five studied zones, using different periods and different recorded measurement sources, hence, the comparison of leakage between the areas was only an approximation. In addition, wet weather scenarios would vary greatly in different years. Among the five utilities, Kurikka had the lowest infiltration rate, which was only 11%. Yet, the infiltration calculation was made with the assumption of the average and minimum flow in 2016. Contrasting to Kurikka, Porvoo had the hourly measurement of the flow rate of each pumping station, also the measurement was recorded recently, thus the result was more trustworthy. The infiltration rate in Porvoo was the second lowest (18%) of the five utilities, nonetheless, at the same time, their infiltration rate between dry and wet weather was the highest – the rate in the wet season was more than 3 times higher than in the dry season. Tuusula had the highest infiltration rate in both seasons. The reliability of wet weather would improve if the rainfall intensity and flows normalized based on it were also considered.

The flood analysis elevation map for heavy rainfall and possible lake flood happening had located the points where water usually accumulates. These locations happened to be in the same zones with high infiltration rates in wet weather since groundwater levels might increase in the site. While the flow measurement data was available, it was more accurate to determine the infiltration percentage of each smaller area in the network than using the elevation map. On the other hand, with the network capacity tested using Fluidit Sewer software, network bottlenecks were found, which was very efficient when creating the overflow scenario for applying the smart control method in the second phase.

6.2.2 Energy analysis

Overall, the performance of sewerage networks typically consumes less energy than water networks in terms of collecting and transporting (ERSAR, 2017). The specific energy consumption for the total amount of water pumped in the sewer network was relatively smaller than the water supply network. The median calculated from the five regions was 0.11 kWh/m^3, while the median in the drinking-water system was 0.37 kWh/m^3 (Saviranta, 2015). It can be explained that while the water supply needs to obtain certain pressure for the delivery point(s) with longer pipe lengths, in the sewer network, the flow is created to pump wastewater over difficult topography and lead to the treatment plant with the shorter pipeline. The specific energy per pumped total wastewater volume in the five studied regions ranged from 0.12 to 0.15 kWh/m^3 for the 60% confidence interval. Following the PAS (Jorge et al., 2021), since the value was higher than 0.09 kWh/m^3, it was considered to be in a fair to bad level of performance. However, the topography of the studied region holds an important part of the specific energy. Therefore, energy efficiency will be a better indicator for the energy assessment of the system.

Energy efficiency

On the other hand, the sewerage network typically has lower efficiency than the water supply network. Following ERSAR (2017) reference values for the standardized energy consumption and the corresponding efficiencies for water supply systems, pump efficiency between 68% and 100% represent a good service level, 50% to 68% efficiency is an acceptable level, and below 50% shows poor performance. While the median of electrical efficiency in the five studied areas was around 36%, it was significantly lower than the drinking water standard and slightly lower than the estimated range of wastewater pumps from Loureiro et al (2020), which is 40% to 60%. Moreover, to compare with the Finnish water supply system, according to Saviranta's study (2015), the observed energy efficiency in the water supply pumping system also had a median of 59%, with a 60% confidence interval range between 52% and 61%.

The difference between the energy efficiencies in dry and wet weather, the variation between the average efficiencies and flow-weighted efficiencies, and the difference between the recorded data and simulated results are also worth mentioning. During the wet season, the incoming flow to the pumping station increases which activates the additional pump(s) to work. Therefore, the efficiencies were lifted a little higher than the value in dry weather. Furthermore, the energy efficiency was improved when calculating by flow-weighted method than with the usual average value of all available pumps. Flow-weighted value had been influenced by efficiencies of stations with higher designed flows. This could be explained that at most of the large pumping stations, the pump definition was better selected, and at the same time, the pump data was well collected in those areas. It was assumed that in smaller pumping stations, the pump curve was not available or falsely documented. While the pump curve was generated in the simulation, it might result in lower or incorrect energy efficiencies. Lastly, the energy efficiencies were significantly reduced when comparing the recorded energy consumption with the simulated results due to the fact that the actual energy usage was higher than the estimation from the simulation. The differences were mostly under -20% for Porvoo pumping stations in actual cases, only a few stations have efficiency differences higher than -25%. In Kurikka, the large difference between the modeled energy efficiencies and the real values is due to the highly optimistic and unrealistic assumption of the 60% efficiency curves for the missing data pumping stations (22 pumps out of 56 pumps were generated instead of using their actual curves), as well as the roughly estimated energy consumption in 2016 given by the utility. The daily energy usage in dry and wet weather was estimated from the monthly minimum, maximum, and average of the year 2016, hence the reliability of the data might be incompetent.

Energy balance

In terms of energy balance in the system, an example from a wastewater utility in Lisbon, Portugal studied using the same energy balance assessment scheme from Jorge et al. (2021) could be used as a reference for review. In this situation, the pump efficiency was assumed to be 30% since no data was audited, while the average energy efficiency in all five studied regions was somewhat on a similar scale, which was around 33%. The total contribution of wet and dry weather inflows to the undue flow percentage was 43% in Portugal – the average for both seasons was 21%. While in our study, the average intrinsic and external energy flow undue was in total 15% in dry weather and 39% in wet weather. Hence, the Finnish value was marginally higher than Portugal, however, remains in the same range.

In the Lisbon system (Jorge et al, 2021), a major part of the energy consumption was associated with the total influx intrinsic energy because the system was composed of mainly gravity sewer and only one pumping station. On the other hand, from the average of all energy flow portion in the five Finnish utilities, the energy outflux – external inefficiencies held the largest percentage in both seasons, which were around 50% on average of the total energy incoming and outgoing fluxes. The studied regions had a larger scope than the Lisbon network that many pumping stations were included for total energy consumption used for elevation. Overall, the friction loss energy of both gravitational and pressurized lines contributed minimally to the energy loss of the system, but the pump energy inefficiencies made a major part, especially in dry weather. The percentage of energy inefficiencies was reduced in wet weather since the energy flux for undue inflows increased notably. The energy flux produced by the gravitational part of the system – incoming flux intrinsic due and undue – was in total about 27% in dry weather and 28% in wet weather. While the total volume was increased considerably in wet weather, the energy use for transportation and its pumping inefficiencies evened out the increment, which lead to a quite similar portion of all energy fluxes coming in and out of the system. According to PAS (Jorge et al., 2021), if the system can be self-produced by 20% to 100% of the total energy in the system, its performance can be evaluated at a good level. With the current value of over 27% intrinsic incoming energy flux, on average, it could be beneficial for the Finnish sewerage system to consider using energy-recovery equipment in the future for energy-saving potential and compensate for almost half of the inefficiencies. Especially, in wet weather when the total inflow is increased, in the Viiala region (the intrinsic energy incoming flux was over 30% in both seasons), Kouvola, and Jokela (32% and 42% in wet weather, respectively).

Friction loss percentage in the pressure line

The median friction loss percentage was calculated to be 10% in dry weather and a slightly higher value of 12% in wet weather. The head loss percentage was higher in the wet scenario because the higher flow induced the extra pump to start functioning in some areas while sharing the same pressure line. Yet, the increment was rather insignificant. On the other hand, the overall average head loss percentage was considerably lower than the median in the Finnish water supply system, which was 19% (Sunela, 2017). Referring to the Darcy-Weisbach formula (Equation 5), friction loss has a positive correlation with pipe length and fluid velocity, and an inverse relationship with the pipe's inner diameter. There is no audited data for pipe size diameter difference between sewer and water networks in Finland. In addition, flow velocities are lower on average in water supply than in pressure sewer – recommended values for maximum value are 0.6 to 1.2 m/s for water network and in pressure sewer, it should be 1 to 1.3 m/s (RIL, 2010). Therefore, it is then explained that due to the nature of the sewer pumping stations with short pressure lines and dominated geodetic head, the friction losses are lower than the water supply system. For pumping stations with large dynamic losses (more than 50%), adjusting the pump's rotational speed by a frequency converter will significantly improve pump performance and save energy (Pulli, 2009), since it is beneficial to weigh up the cost of purchasing VSD.

Summary

In general, based on the average and flow-weighted energy efficiencies in dry and wet weather, the percentage of energy fluxes in the system's energy balance, and the reliability of the collected data and simulated results, it can be concluded that the performance of the studied Finnish sewerage systems is in a "fair" to "poor" level when comparing with other situations all around the world. There is quite a limited amount of research on sewerage energy consumption that focuses mainly on transporting and collecting, since this sector only holds the share of around 10% in the total of wastewater management (depending on the share of gravity-induced collection), while aeration takes mostly 55% of the total energy (Liu et al., 2012). Therefore, the evaluation was made roughly based on available studies and the potential for further development.

When comparing the performance of all five utilities, Kouvola had the highest average efficiency in both seasons, also the ratio between the average efficiency and the best achievable efficiency was the highest in this case. With the flow-weighted efficiency, Kouvola did not have the highest result in dry weather, but it was again the highest in wet scenarios. In some cases, Tuusula – Kellokoski appeared to be a better candidate, however, all pump definition in Tuusula was generated by Fluidit software, hence, the results were not as reliable as Kouvola. Even though Kouvola also has a large amount of generated pump curve (75%), most of the large and main pumping stations were documented properly. If relying on the availability and the reliability of the given data, Hämeenlinna and Porvoo came in second place for areas with high performances (with approximately half of the pumping stations' data being audited). The two regions both had average and flow-weighted efficiencies between 30% to 40%. Regarding the friction loss percentage, Porvoo had the highest percentage on average, which was around 30%, followed were Kurikka and Tuusula. Based on the result of energy balance portions in the system, the energy flux going out of the system by friction loss was less than 0.01% in all regions and very minimal, the analysis on friction loss will only benefit individual pumps for further improvements, such as long-term energy usage by changing pump definition.

6.3 Smart control methods

In this part, the benefit and applicability of the level control method will be analyzed from the results of HS Vesi, Porvoo and Tuusula regions.

6.3.1 Energy saving potential

The selection of the optimal pump was restricted to only the Grundfos automatic selection tool, hence, there might be a better fit for the system. Furthermore, with pumping stations using generated curves in Fluidit Sewer, the highest achievable efficiency was assumed to be 60%. While it is considered a quite high efficiency for wastewater systems, in reality, the performance could result in lower efficiency, or there is a high chance that there is no available pump in the market to achieve that high efficiency to apply in this case. For the reasons above, some stations had an increment in energy consumption when using the optimal suggested pumps. Moreover, the change of pump definition affects the current flow rate in the originally designed system, therefore, within the same pumping station chain, for stations that did not have their pumps being replaced, the incoming flow to their reservoir might be increased and the stations need to pump more frequently. As a result, the daily energy consumption in these locations would increase, for example, pump JVP13 in Hämeenlinna. Apparently, pump JVP13's original daily energy consumption was one of the highest in the group, therefore it had a large impact on the total energy consumption of the whole chain. On the other hand, for stations with low energy usage, even though the energy can be increased excessively, the consumption of the whole chain would still decrease from the original setup (for example, pump JVP73, JVP17, and JVP16 in Porvoo).

When applying the level control method, the flow rate was alternated accordingly to maintain the desired water level inside the tank. To do so, most pumps need to reduce their pumping rate to its minimum. At the same time, efficiency would drop very low corresponding to the low flow rate, based on its pump curve. Hence, the daily energy consumption became enormous when applying the control setting in some areas such as Viiala, Toijala, or Hyrylä – a small network with low total inflows, especially in dry weather. Nonetheless, in situations when the inflows were higher, for instance in wet weather and overflow scenarios or networks with high designed flow rates such as Porvoo and Hämeenlinna, although the efficiency still be reduced using variable speed drive, the energy used to pump the small flow rate was not as high as the original on-off setting which required constant pumping during the peak scenario. In the end, the utilities will get the benefit from using the level control in high-demand situations. The control method benefit will be elevated when used in combination with the optimal pump. Since the efficiency range is higher, the energy loss from using variable speed drive modification will not be as large as in the original setup.

The pump speed adjusting method had been studied by other scholars for water supply pumping stations such as Eker and Kara (2003) with their optimization for water level control, or Abdulrahman and Nasher (2010) with their model predictive controller in manipulating pump speed. Nevertheless, the solutions were defined as too complicated to be implemented. Besides, Gao et al. (2016) studied the changes in real-time in water level upstream stations, yet the stability of the water level upstream of the pumping station was neglected. In order to achieve the best working point for all three scenarios when using the level control method, more thorough research should be done and tested in the future regarding the control setting, chosen pump type and the location to be applied. Moreover, given that the suggested method is merely a modest improvement over the existing on-off control, the control algorithm of this approach was relatively simple to implement with the communications and logic controller technologies already in place at the pumping stations.

6.3.2 Overflow reduction

Three different types of overflow scenarios were tested to observe the excess flow reduction by applying the proposed smart control. As noted above, these extreme scenarios were made only for the demonstration of the overflow reduction capability of the level control application.

For the scenario when the inflows were increased in every location (the demand multiplier was increased in the simulation), the overflow reduction capability was small because water could not be retained in other locations except for the storage units, but there was still potential. With the Viiala case, the overflow was not too high, and yet under control, the overflow could be prevented completely with level control in combination with using the optimal pump. On the other hand, in the Hyrylä case, the overflow volume was too high, which explained that the capacity of the network had been utilized fully and there was barely free volume for the application of the level control method.

For the backflow scenario, inflows were increased excessively in some specific locations. In this situation, reduction in overflow was not utilized. While Toijala and Porvoo scenarios had similar total daily overflow (around 30 to 40 m^3/d), Porvoo overflow volume can be reduced by up to 100%, and Toijala overflow volume can be reduced by 9% maximum. It can be concluded that the potential in decreasing the excess volume was highly dependent on the network design, its capacity, and the location where backflow happening.

Lastly, for the blockage scenario, the level control showed a quite clear result in reducing the excess flow, although the percentages of overflow decreasing were different in every case. In Hämeenlinna, the overflow was reduced by up to 6%, while in Jokela it could be decreased by up to 60%. Additionally, hypothetical blockage scenarios were created within a short period of time, which did not exceed three hours. For this reason, the flood reduction potential would not be utilized when the blockage happened for a longer period, in other words, when the capacity of the network had been fully used.

Generally, the proposed level control is certainly able to reduce the overflow volume to a definite level. When the network total capacity is exceeded, it is suggested to have another additional storage to store the overflow volume. Regarding time delay, if all target stations start to store more water immediately after the selected downstream station level surpasses the set limit (usually apply to blockage scenario), the approach will bring the benefit only when the length of the network is long, or in a large network. The same reduction will be observed in a small network regardless of time delay.

6.3.3 Estimation of cost

Based on the results of daily energy consumption of optimal pumping selection replacement in the network in different conditions: dry weather, wet weather, and overflow scenarios, with and without applying the level control, several pumping stations were carried out with the estimation of cost. Their repayment periods were calculated with only the price of the pump and an assumed 10% maintenance expenditure, while there can be several possible costs that did not include such as the installation cost, staff training, and certain adjustments needed when changing the pump. Most of the stations had quite short repayment times, except for Toijala - JVP123 and Porvoo - JVP10.

7 Conclusions

The aim of the thesis was to study the overall performance of several Finnish sewerage systems from the energy consumption and capacity during different conditions, and consequently, a smart control method was developed to improve the situation. The energy and flood analysis was carried out on five different water utilities: HS-Vesi (Viiala, Toijala, and Hämeenlinna), Porvoo, Kurikka, Kouvola and Tuusula (Hyrylä, Jokela, and Kellokoski) using Fluidit Sewer simulated results. The level control method was developed and applied using Python Control Stations available in Fluidit Sewer for the simulation of HS-Vesi, Porvoo, and Tuusula. The chosen pumping station chains in the three regions were selected based on the basis of energy and flood analysis from the previous phase.

The general picture of the Finnish sewer systems was assessed based on the results of five presentative utilities. On the whole, compared with other countries, the Finnish I/I level was found to be average, with the median infiltration rate being 19% in dry weather and 67% in wet weather conditions. Among the studied regions, Kurikka had the lowest I/I rate while the Tuusula infiltration rate was the highest. It is worth mentioning that Porvoo had the highest ratio between the I/I in the dry and wet seasons, which was 1:3. Regarding energy consumption in pumping stations, the sewer network typically consumes less energy than the water network in Finland, based on the simulated result of specific energy per pumped wastewater volume ranged from 0.12 to 0.15 kWh/m^3. However, the efficiency of 36% in the sewer network was typically at a lower level than in the water supply network, which was 59% for the median (Sunela, 2017). With this value of efficiency, it can be concluded as fair to a poor level, notably, most energy outflux in the system was lost because of pump ineffectiveness, as shown in the energy balance calculation. Luckily, the average energy flux produced by the gravitational part of the system was about 27% of the total incoming and outgoing flux, evaluated as a good level for applying energy recovery equipment in the future. Nevertheless, installing energy recovery equipment in sewers would necessitate a single location with a significant elevation difference. This location selection process would demand more attention in future studies. The friction loss in pressure sewers over the total head generated in the pumps was also slightly smaller than the water supply side and held a minimal impact on the energy consumption of the whole system. In five areas, Kouvola and Hämeenlinna appeared to have better performance than the rest based on the energy efficiency and the reliability of the given initial information for the study.

The level control method worked at its best during high inflow conditions. Since the pumping station flow rate was alternated accordingly to maintain the desired water level inside the wet well, efficiency could drop very low in some cases which eventually increased the daily energy consumption, nonetheless, could be easily avoided by the algorithm's future development. However, in the peak scenario, the original on-off setting would still consume higher energy than pumping minimum flow with low efficiency. In addition, the control method benefit will be higher when used in combination with the optimal pump model for the variable speed operation in each location. Hence, more thorough research should be done in the future on the energy-saving potential of using variable speed drives in combination with level control.

Regarding the excess volume reduction, while the effective level control in the backflow scenario depends highly on the network itself (overflow can be completely prevented in Porvoo but only a 9% reduction in Toijala), the blockage scenario and scenario using a higher demand multiplier demonstrated that the method could reduce flood to a definite level, within a certain period. The reduction was a maximum of 60% in Jokela. When the total capacity is exceeded, another additional storage is suggested to store the overflow.

After all, it should be mindful of the fact that several assumptions were created in the research. Several network variables were missing and had to be assumed based on the existing information. The infiltration rate was calculated using different measurement sources and different periods, hence, the comparison between the areas was only an approximation. The actual energy efficiency might be lower than the simulated results, as more than half of the pump curves were generated by Fluidit Sewer 2.2 with the assumption of 60% as the best achievable efficiency point. The proposed optimal pumps were restricted to only the Grundfos database. Last but not least, the overflow scenario of each region was made based on the previous accident that happened, yet the additional flow to the network was not recorded, hence the scenario details were made up only to observe overflow and therefore the functionality of the level control method can be demonstrated.

The network performance in the various utilities did not differ much from one another. It was discovered that the performance complied with the design principles. Nonetheless, there is still room for enhancement, especially, since the infiltration can be reduced in wet weather conditions and the energy efficiency of pumping stations can be improved. The energy efficiency would be lower in reality compared to the simulated results. In addition, although a smart control system has been found to have the ability to reduce floods and increase energy efficiency, more study and development are still needed in the future.

References

Aaltonen, J., Huokuna, M. (2017). Flood mapping of river ice breakup jams in River Jyrönjoki delta. CGU HS Committee on River Ice Processes and the Environment. 19th Workshop on the Hydraulic of Ice-Covered Rivers. Whitehorse, Yukon, Canada.

Aaltonen, J., Huokuna, M. (2017). Flood mapping of river ice breakup jams in River Jyrönjoki delta. CGU HS Committee on River Ice Processes and the Environment. 19th Workshop on the Hydraulic of Ice-Covered Rivers. Whitehorse, Yukon, Canada.

Abdulrahman, A., Nasher, N. (2010). Water supply network system control based on model predictive control. J. King Saud Univ.—Eng. Sci. 22, 119–126.

Åström, K. J., Hägglund, T. (1995). PID Controllers: Theory, Design, and Tuning, 2nd edition. Instrument Society of America, 1995.

Bentes, I., Silva, D., Vieira, C., Matos, C. (2022). Inflow Quantification in Urban Sewer Networks. Hydrology 9(4), 52. https://doi.org/10.3390/hydrology9040052

Berger, V., Niemann, A., Frehmann, T., Brockmann, H. (2013). Advanced energy recovery strategies for wastewater treatment plants and sew-er systems using small hydropower. Water Utility 5, 15-24.

Bulu, A. (2018). Specific Energy. Specific Energy. Lecture notes: Fluid Mechanics (CE5301). Istanbul Technical University.

Davis, M. L. (2020). Water and Wastewater Engineering: Design Principles and Practice. 2nd Edition. New York: McGraw-Hill Education. https://www.accessengineeringlibrary.com/content/book/9781260132274

Eker, I., Kara, T. (2003). Operation and control of a water supply system. ISA Trans. 42, 1–13.

Ellis, G. (2004). Control System Design Guide: Using Your Computer to Understand and Diagnose Feedback Controllers. Elsevier Science & Technology. ProQuest Ebook Central: https://ebookcentral.proquest.com/lib/aalto-ebooks/detail.action?docID=286665

ENPI. (2012). Kymenlaakso. Read on 21/5/2023. Retrieved from http://cliplive.infoeco.ru/index.php?id=31

ERSAR. (2017) Guide for the Assessment of the Quality of Service in Water and Wastewater Services. 3rd edition. Technical guide 22. Entidade Reguladora dos Serviços de Águas e Resíduos, Laboratório Nacional de Engenharia Civil: Lisbon, Portugal. Read on 15/10/2019. Retrieved from http://www.ersar.pt/pt/publicacoes/publicacoes-tecnicas/guias

Fair G.M. (1968). Water purification and wastewater treatment and disposal New York: Wiley.

Fecarotta, O., Carravetta, A., Morani, M. C., Padulano, R. (2018). Optimal Pump Scheduling for Urban Drainage under Variable Flow Conditions. Resources 2018, 7, 73. DOI:10.3390/resources7040073

Fischer, C., Stanchev, P. (2022). Flood hazard and risk maps: A key instrument for flood risk management. Read on 22/4/2023, Retrieved from https://blogs.worldbank.org/water/flood-hazard-and-risk-maps-key-instrument-flood-risk-management

Flygt. (2013). Variable speed wastewater pumping. Xylem. Read on 11/01/2022. https://www.xylem.com/siteassets/brand/flygt/flygt-resources/flygt-resources/variable-speed-wastewater-pumping-1894.pdf

Ganora, D., Isacco, S., Claps, P. (2017). Framework for Enhanced Storm-water Management by Optimization of Sewer Pumping Stations. Journal of Environmental Engineering. 143(8):04017025. DOI: 10.1061/(ASCE)EE.1943-7870.0001220. © 2017 American Society of Civil Engineers.

Gao, X., Nie, X., Sun, B., Zhang, C. (2016). Study on opening time difference of the adjacent multi-stages pump stations in water transfer projects. J. Hydraul. Eng. 47, 1502–1509.

Goodwin, G. C., Graebe, S. F., Salgado, M. E. (2000). Control system de-sign. Retrieved from https://shorturl.at/hstSV

Grundfos. (2023). https://product-selection.grundfos.com

Halonen, J. (1987). Energiankäytön vähentäminen teollisuuspumppauksess. Master's thesis. Lappeenranta University of Technology. Department of energy technology. 126 p.

Heywood, G., Lumbers, J. (1997). Infiltration to Sewers: Modelling and Management. Paper given at IWQA UK National Meeting, Leeds, November 1997.

Hiew, T. Y., & Su, K. N. (2017). Assessment on inflow and infiltration in sewerage systems of ahang, ahang. Water Science and Technology, 76(11), 2918-2927. https://doi.org/10.2166/wst.2017.463

Hydraulic Institute (U. S.). (2004). Variable Speed Pumping: A Guide to Successful Application. Elsevier. https://www1.eere.energy.gov/manufacturing/tech_assistance/pdfs/variable_speed_pumping.pdf

Jahai, J. S., Deflorio-Barker, S., Lin, C. J., Hilborn, E. D., Wade, T. J. (2017). Sanitary Sewer Overflows and Emergency Room Visits for Gastrointestinal Illness: Analysis of Massachusetts Data, 2006–2007. Environmental Health Perspectives. Vol. 125, No.11, https://doi.org/10.1289/EHP2048

James, B. R. (2003). Constant Wet Well Level Control Saves Cost and Energy. WaterWorld. PennWell Corporation. Read on 21/5/2023. Retrieved https://www.pattersonpumps.com/assets/pdf/constant.pdf

Jorge, C., Almeida, M. C., Covas, D. (2021). Performance Assessment System for Energy Efficiency in Wastewater Systems. Water 2021, 13(13), 1807. https://doi.org/10.3390/w13131807

Jorge, C., Almeida, M. d. C., Covas, D. (2021). Energy Balance in Wastewater System with Energy Recovery: A Portuguese Case Study. Infrastructures 2021, 6, 141. https://doi.org/10.3390/infrastructures6100141

Karassik, I. J., McGuire, T. (1998). Centrifugal pumps. 2nd Edition. New York: Chapman & Hall. 989 p. ISBN 0-412-06391-3.

Karttunen, E. (2004). Vesihuolto II. Tuhkanen Tuula, Kiuru Heikki. Helsinki: Suomen Rakennusinsinöörien Liitto TIL ry. ISBN 951-758-438-5.

Kuronen, M. (2022). Sewer network modeling. Lecture 22.3.2022. WAT-E2110 Design and Management of Water and Wastewater Networks. Aalto University.

Labadie, J. W., Morrow, D. M., Chen, Y. H. (1980). Optimal Control of Unsteady Combined Sewer Flow. Journal of the Water Resources Planning and Management Division, Proc ASCE 106:205-223

Liu, F., Ouedraogo, A., Manghee, S., Danilenko, A. (2017). A primer on energy efficiency for municipal water and wastewater utilities. Technical report 001/12. ESMAP (Energy Sector Management Assistance Program). https://www.esmap.org/sites/default/files/esmap-files/FINAL_EECI-WWU_TR001-12_Resized.pdf

Loureiro, D., Silva, C., Cardoso, M. A., Mamade, A., Alegre, H., Rosa, M. J. (2020). The development of a Framework for Assessing the Energy Efficiency in Urban Water Systems and Its Demonstration in the Portuguese Water Sector. Water 2020, 12(1), 134. https://doi.org/10.3390/w12010134

Malekpour, A., Karney, B. (2014). A Non-Oscillatory Preissmann Slot Method Based Numerical Model. 16th Conference on Water Distribution System Analysis, WDSA. Procedia Engineering 89. 1366-1373.

Marchis, M. D., Fontanazza, C. M., Freni, G., Messineo, A., Milici, B., Na-poli, E., Notaro, V., Puleo, V., Scopa, A. (2014). Energy recovery in water distribution networks. Implementation of pumps as turbines in a dynamic numerical model. Procedia Engineering 70, 439-448.

Marinaki, M., Papageorgiou, M. (2005). Optimal Real-time Control of Sewer Networks. Advances in Industrial Control series ISSM 1430-9491. Springer-Verlag London Limited.

Morante-Carballo, F., Montalvan-Burbano, N., Arias-Hidalgo, M., Dominguez-Granda, L., Apolo-Masache, B., Carrion-Mero, P. (2022). Flood Models: An Exploratory Analysis and Research Trends. Water. 14, 2488. https://doi.org/10.3390/w14162488

Munson, B., Young, D., Okiishi, T. (2005). Fundamentals of Fluid Mechanics. Hydraulic Institute. 5th Edition.

Nasik, R. (2010). Principles of Pumps and Pumping Installation. IREE. https://irieen.indianrailways.gov.in/uploads/files/1302522604445-Principles%20of%20Pumps%20....pdf

Pachaly, R. L., Vasconcelos, J. G., Allasia, D. G., Bocchi, J. P., (2021). Evaluating SWMM capabilities to simulate closed pipe transients. Journal of Hydraulic Research. DOI: 10.1080/00221686.2020.1866695

Pachaly, R. L., Vasconcelos, J. G., Allasia, D. G., Tassi, R., Bocchi, J. P. (2020). Comparing SWMM 5.1 calculation alternatives to represent unsteady stormwater sewer flows. Journal of Hydraulic Engineering. Volume 146 issue 7.

Pereira, A., Pinho, J. L. S., Faria, R., Vieira, J. M. P., Costa, C. (2019). Improving operation management of wastewater systems. A case study. Water Science & Technology. 80.1. DOI: 10.2166/wst.2019.264

Pohjola, M. (2006). PID Controller Design in Networked Control Systems. Master's thesis for the degree of Master of Science in Technology. Helsinki University of Technology.

RIL. (2010). RIL 237-2-2010. Vesihuoltoverkkojen suunnittelu – mitoitus ja suunnittelu. Helsinki: Suomen Rakennusinsinöörien liitto RIL ry. ISBN: 978-951-758-521-7.

ArcGIS. (2023). https://www.esri.com/en-us/arcgis/products/arcgis-pro/

Pulli, M. (2009). Flow Technology. Tammertekniikka, 1st edition.

Ruuskanen, A. (2007). Optimization of energy consumption in wastewater pumping. Master's Thesis. Lappeenranta University of Technology. https://lutpub.lut.fi/bitstream/handle/10024/30387/TMP.objres.519.pdf?sequence=1

Saviranta, S. (2015) Energy Audit of Finnish Water Distribution Networks. Master's thesis, Tampere University of Technology. URL http://urn.fi/URN:NBN:fi:tty-201511171722.

SCALGO. (2023). https://scalgo.com/live/

Spellman, F. R. (2003). Handbook of Water and Wastewater Treatment Plant Operations. Boca Raton: Lewis Publisher. 661 p. ISBN 1-56670-627-0.

Sunela, M. (2017). Real-Time Control Optimization of Water Distribution System with Storage. ISBN 978-9949-83-165-4. Tallinn University of Technology, School of Engineering, Department of Civil Engineering and Architecture.

United Nations. (2014). World Urbanization Prospects: The 2014 Revision. Department of Economic and Social Affairs, Population Division. Highlights (ST/ESA/SER.A/352). United Nations. Retrieved 01 July 2022 from http://esa.un.org/unpd/wup/Publications/Files/WUP2014-Highlights.pdf

United State Environmental Protection Agency (EPA). (1995). National Conference on Sanitary Sewer Overflows (SSOs office of Research and Development Washington DC. EPA/625/R-96/007. Read on

22/4/2023. Retrieved from https://citeseerx.ist.psu.edu/document?repid=rep1&type=pdf&doi=6b05a5e7aab2bbdc1c176f50a55901afa2a177b5#page=15
United State Environmental Protection Agency (EPA). (2000). Wastewater Technology Fact Sheet. Pipe Construction and Materials. EPA 832-F-00-068. Washington, D. C. https://www3.epa.gov/npdes/pubs/pipe_construction.pdf
United State Environmental Protection Agency (EPA). (2000). Why Control Sanitary Sewer Overflows? https://www.epa.gov/sites/production/files/2015-10/documents/sso_casestudy_control.pdf
United State Environmental Protection Agency (EPA). (2008). Review of Sewer Design Criteria and RDII Prediction Methods. EPA/600/R-08/010. Edison, New Jersey 08837.
United State Environmental Protection Agency (EPA). (2016a). National Pollutant Discharge Elimination System (NPDES). Sanitary Sewer Overflows (SSOs). Read on 22/4/2023. https://www.epa.gov/npdes/sanitary-sewer-overflows-ssos
Uponor. (2014). Material and service life. Technical handbook. Read on 12/04/2023. Retrieved from https://issuu.com/uponorfi/docs/02_materials_and_service_life_962477bb6fa2a3
Walski, T. M., Barnard, T. E., Harold, E., Merritt, L. B., Walker, N., Whitman, B. E. (2007). Wastewater collection system modeling and design. Haestad Methods, Inc. 1st edition. Exton, PA: Bentley Institute Press.
Wapro. (2020). Flooding: Cause and effect in sewer and stormwater systems. A brief overview of the reasons behind increased flooding and the consequences for municipalities. Read on 22/4/2023. Retrieved from https://wapro.com/en-gb/knowledge-bank/cvp/flooding-cause-and-affect-sewer-and-stormwater-systems
Weyrauch, P., Matzinger, A., Pawlowsky-Reusing, E., Plume, S., Seggern, D., Heinzmann, B., Schroeder, K., Rouault, P. (2010) Contribution of combined sewer overflows to trace contaminant loads in urban streams. Water Research. Volume 44, Issue 15, Pages 4451-4462. ISSN 0043-1354. https://doi.org/10.1016/j.watres.2010.06.011.
Whitehead, E., Hiscock, K.M and Dennis, P.F. (1999). Evidence for Sewage Contamination of the Sherwood Sandstone Aquifer Beneath Liverpool, UK. In: J.B. ELLIS, J.B (ed), Impacts of Urban Growth on Surface Water and Groundwater Quality. Pub No.259, IAHS Press Ltd, Wallingford, UK, 179-185.
Wirzenius, A. (1978). KeskiJVPopumput. Third edition. Tampere: Kustannusyhtymä. 323p.
Wood, D. J, Heitzman, G. C. (1983). Hydraulic Analysis of Surcharged Storm Sewer Systems. KWRRI Research Reports. 66.

YLE (Yleisradio Oy). (2004). Critcal Flood Situation in Southern Finland. Read on 21/5/2023. Retrieved from https://yle.fi/a/3-5160638

YLE (Yleisradio Oy). (2012). Floods result from heavy downpours. Read on 21/5/2023. Retrieved from https://yle.fi/a/3-6324320

YLE (Yleisradio Oy). (2017). Flooding in Southern Finland – but no records broken yet. Read on 21/5/2023. Retrieved from https://yle.fi/a/3-9874649

A. APPENDICES

7.1 Energy analysis and friction loss result

7.1.1 HS-Vesi Region

Viiala

Zone	Name	Best eff (%)	Specific energy (kWh/m3)	NRW (%)		Dry weather Head (m)		Wet weather Head (m)		Dry weather Energy	Dry weather EFF	Wet weather Energy	Wet weather EFF
				Dry	Wet	Total H (m)	Friction (%)	Total H (m)	Friction (%)	kWh/d	(%)	kWh/d	(%)
1	JVP224	45.50	0.12	0.43	41.30	5.66	17.31	5.76	18.06	2.05	30.83	3.65	30.17
	JVP264	38.60	0.01			2.34	1.85	3.93	14.78	0.05	10.09	0.29	14.78
	JVP225	40.70	0.11			8.76	2.64	8.77	2.69	3.14	20.42	5.03	20.30
2	JVP260	37.60	0.04	21.33	51.70	7.77	6.25	7.82	6.85	3.55	18.42	7.67	18.16
	JVP261	29.40	0.04			4.29	18.94	4.27	19.00	0.42	15.11	0.74	14.48
	JVP262	28.60	0.04			12.59	1.93	12.59	1.99	3.64	11.85	5.00	11.51
3	JVP220	56.80	0.17	41.19	77.90	7.74	20.51	7.70	19.79	20.85	47.47	53.32	47.53
	JVP221	31.80	0.14			2.68	5.32	2.70	5.46	0.15	13.23	0.56	13.05
	JVP222	26.70	0.14			1.86	26.55	2.12	10.04	0.24	2.51	1.90	3.90
	JVP223	35.40	0.13			1.07	71.00	1.11	71.84	0.91	13.29	2.22	13.46
	JVP226	35.40	0.11			2.55	10.75	2.55	10.95	0.06	15.84	0.12	16.92
	JVP263	35.40	0.03			3.38	4.62	3.38	4.72	0.27	19.00	1.00	18.94
4	JVP250	23.00	0.06	2.55	16.50	5.42	3.81	5.44	3.84	1.71	22.22	1.91	22.58
	JVP251	18.00	0.06			3.03	48.16	3.50	50.81	0.08	12.00	0.09	11.28
	JVP252	18.00	0.06			2.67	57.02	2.81	53.42	0.06	15.04	0.06	15.05
	JVP253	44.00	0.06			5.65	13.55	5.67	13.62	1.08	24.67	1.23	23.75
	JVP254	23.00	0.05			0.65	15.87	0.65	16.85	0.02	18.30	0.06	18.43
	JVP255	45.50	0.04			0.60	18.20	1.23	5.73	0.01	27.16	0.02	26.69
5	JVP240	47.90	0.07	36.86	83.6	7.23	5.20	7.25	5.53	4.37	24.12	17.25	24.47
	JVP241	37.00	0.06			9.87	3.15	9.88	3.18	0.49	27.29	1.62	25.87
	JVP242	44.00	0.06			1.24	18.77	1.31	23.22	0.07	15.31	0.47	14.31
	JVP243	23.00	0.06			6.24	1.15	6.25	1.18	0.23	15.21	0.78	14.46
6	JVP230	44.90	0.10	2.29	37.8	5.92	69.32	6.08	69.37	4.57	33.94	6.98	33.80
	JVP231	47.90	0.09			1.37	60.29	1.39	61.21	1.70	27.12	2.53	27.01
	JVP232	39.60	0.08			5.86	9.27	5.84	9.41	0.61	27.20	0.85	28.69
	JVP233	47.90	0.07			3.29	31.43	3.31	30.65	1.66	38.15	3.00	38.28
	JVP234	23.00	0.07			3.80	3.66	3.80	3.70	0.45	12.95	0.98	12.98
7	JVP210	58.40	0.36	68.84	68.20	31.03	15.03	31.22	15.44	129.66	48.92	303.30	48.77
	JVP212	39.60	0.18			3.25	19.96	3.24	20.06	0.19	17.89	0.26	16.59

Toijala

Zone	Name	Best eff (%)	Specific energy (kWh/m3)	NRW (%)		Dry weather Head (m)		Wet weather Head (m)		Dry weather Energy	Dry weather EFF	Wet weather Energy	Wet weather EFF
				Dry	Wet	Total H	Friction (%)	Total H	Friction (%)	kWh/d	(%)	kWh/d	(%)
1	JVP101	49.20	0.04	0.00	5.59	1.98	3.51	1.86	3.16	0.54	22.58	0.53	23.14
2	JVP150	47.20	0.07	1.08	54.82	1.73	46.87	2.28	57.25	28.72	13.35	80.87	16.93
3	JVP140	24.80	0.15	46.83	76.59	4.15	17.88	4.55	16.68	18.27	15.53	21.51	18.28
	JVP141	56.60	0.06			3.90	4.00	3.67	4.42	1.02	19.33	1.46	19.19
	JVP142	47.20	0.17			7.56	3.24	7.08	3.75	1.04	20.10	1.75	16.56

4	JVP164	51.50	0.02	17.25	67.53	3.90	9.48	3.57	2.10	1.57	44.20	3.99	44.33
	JVP111	47.20	0.06			7.30	0.18	7.00	0.57	1.72	35.18	5.00	35.53
	JVP112	23.40	0.07			0.75	65.73	0.74	64.68	1.35	17.26	3.44	15.13
5	JVP130	60.00	0.06	24.89	63.41	8.27	1.42	8.19	0.61	29.89	36.93	64.54	37.37
	JVP133	47.20	0.28			9.69	0.99	9.60	0.34	4.73	10.39	5.28	8.99
	JVP134	55.40	0.17			11.78	4.16	11.46	1.48	5.08	17.24	20.21	18.42
	JVP135	60.00	0.08			2.81	17.91	2.81	18.38	0.41	18.43	1.03	18.66
	JVP165	51.50	0.05			2.86	6.52	2.66	0.24	0.11	29.85	0.45	23.51
	JVP131	26.70	0.06			2.80	5.64	2.65	5.55	1.60	23.57	2.59	20.63
	JVP132	33.60	0.06			4.27	0.47	6.51	7.98	0.06	33.45	0.24	35.11
	JVP340	32.30	0.14			24.16	1.63	23.28	0.39	6.82	37.24	10.17	46.00
	JVP341	60.00	0.13			1.72	2.81	6.15	0.09	1.19	32.94	5.65	27.03
	JVP342	60.00	0.13			4.50	9.11	6.28	7.60	0.13	13.71	1.61	13.77
	JVP343	36.60	0.13			5.12	1.25	9.24	1.02	1.02	4.55	1.49	33.56
	JVPK301	60.00	0.04			3.76	3.57	5.28	0.28	0.11	24.58	0.23	45.47
6	JVP122	23.40	0.02	32.29	72.89	1.41	14.93	1.10	9.10	0.24	22.78	0.61	21.71
	JVP123	26.70	0.12			2.72	47.69	3.20	62.52	0.21	4.93	0.12	10.33
	JVP156	35.30	0.03			2.84	2.32	4.11	0.04	0.02	24.89	0.05	42.27
7	JVP120	41.10	0.06	32.25	65.55	4.59	48.77	5.49	56.48	29.85	28.51	76.68	35.98
	JVP126	35.30	0.04			2.77	23.28	6.57	67.30			0.01	34.47
	JVP125	53.32	0.05			2.20	2.24	2.20	2.54	0.04	45.83	0.03	36.34
	JVP121	49.20	0.06			4.17	3.65	4.01	0.18	0.45	9.57	0.49	16.16
	JVP124	41.10	0.06			4.13	4.40	3.93	4.58	1.30	15.87	2.18	16.27
8	JVP330	38.90	0.09	0.43	14.42	8.19	4.18	7.87	2.54	5.19	21.04	7.21	21.10
	JVP331	38.90	0.07			9.23	4.40	8.86	0.25	1.73	51.91	2.23	51.91
	JVP332	38.90	0.09			1.68	12.50	2.16	18.48	0.91	23.44	0.80	13.00
	JVP333	77.00	0.06			2.09	24.93	2.03	23.48	0.31	17.19	0.35	16.93
9	JVP320	39.90	0.15	0.40	29.94	8.32	10.68	7.93	6.33	20.79	11.36	30.75	11.88
	JVP321	26.70	0.08			3.95	4.21	4.29	0.47	0.05	12.01	0.23	15.06
	JVP322	38.90	0.09			1.75	12.38	1.38	3.76	4.42	24.67	5.61	20.14
10	JVP310	39.90	0.14	82.82	84.87	24.37	2.16	22.10	0.69	43.24	28.54	65.04	29.60
	JVP311	39.90	0.14			6.89	7.98	6.69	5.20	3.38	33.15	3.27	30.18
	JVP312	60.00	0.07			3.19	13.66	2.75	0.68	0.64	35.73	0.76	35.49
	JVP313	36.60	0.10			1.19	27.03	0.96	34.90	0.20	11.36	0.31	11.98
	JVP314	33.60	0.16			0.94	51.47	0.92	50.57	2.10	26.47	1.96	22.72
11	JVP110	51.50	0.04	8.84	57.49	2.34	13.71	2.56	20.94	23.88	13.48	54.31	16.02
	JVP113	47.20	0.04			2.25	39.66	2.31	39.57	0.45	19.51	1.87	21.26
	JVP114	53.32	0.10			4.34	10.71	4.08	6.93	0.97	9.05	5.31	8.68
12	JVP167	39.90	0.02	1.48	67.58		0.00		0.00	0.00	4.93	5.59	32.57
	JVP166	51.50	0.05			5.67	22.68	7.74	51.44	28.46	10.66	46.89	27.58
	JVP156	35.30	0.03			2.84	2.32	4.11	0.04	0.02	24.89	0.05	42.27

Hämeenlinna						Dry weather		Wet weather		Dry weather		Wet weather	
Zone	Name	Best eff (%)	Specific energy (kWh/m3)	NRW (%)		Head (m)		Head (m)		Energy	EFF	Energy	EFF
				Dry	Wet	Total H	Friction (%)	Total H	Friction (%)	kWh/d	(%)	kWh/d	(%)
1	JVP60	60.00	0.06	7.89	11.62	2.85	13.02	3.20	22.29	0.47	40.61	3.73	39.71
	JVP64	43.00	0.16			1.69	16.31	1.77	19.59	2.92	48.07	0.15	29.28
2	JVP22	49.40	0.09	6.05	51.11	5.47	7.61	5.92	14.71	61.03	20.32	107.71	30.24
	JVP46	60.00	0.11			4.55	8.04	4.75	11.45	1.23	33.57	2.21	35.30

3	JVP34	51.81	0.20	2.64	45.29	28.30	1.77	28.36	1.98	252.78	42.12	427.75	42.01
	JVP36	60.00	0.08			2.88	20.84	3.02	24.21	0.49	31.54	0.88	31.54
	JVP39	60.00	0.13			10.88	2.97	10.96	3.61	1.04	40.52	2.67	40.53
4	JVP04	47.00	0.06	43.54	76.66	7.57	10.46	7.90	13.56	31.22	39.85	85.88	39.68
	JVP43	60.00	0.04			4.10	5.33	4.22	7.14	0.42	40.77	1.24	40.80
	JVPA110	47.20	0.08			3.69	12.74	3.75	14.26	1.60	23.37	2.76	23.58
5	JVP33	53.32	0.08	7.45	58.96	7.66	18.43	7.62	16.03	20.72	40.94	48.70	41.11
	JVP35	39.90	0.18			20.28	1.28	20.34	1.54	13.10	33.72	39.40	33.74
	JVP109	60.00	0.07			4.34	8.15	4.63	13.53	2.11	34.87	5.30	36.62
6	JVP02	60.00	0.04	21.56	45.58	6.07	44.04	6.64	46.78	23.72	42.83	36.66	44.66
	JVP29	44.40	0.04			2.88	10.78	3.21	19.84	5.31	30.71	8.99	30.71
	JVP38	60.00	0.04			7.54	9.84	7.76	12.35	10.41	49.30	15.42	49.71
	JVP40	47.20	0.08			3.07	19.09	3.22	22.53	1.12	22.64	2.08	22.64
	JVP56	60.00	0.02			2.31	14.25	2.34	15.00	0.06	44.00	0.18	44.85
7	JVP68	60.00	0.12	0.13	39.51	15.05	4.91	15.04	4.79	2.62	42.39	129.02	35.75
	JVP51	33.90	0.13			5.46	7.62	5.51	8.38	3.16	14.26	9.28	14.28
	JVP54	60.00	0.09			13.38	13.86	13.43	14.04	37.95	33.92	56.66	34.19
	JVP58	60.00	0.00										
	JVP04	47.00	0.06			7.57	10.46	7.90	13.56	31.22	39.85	85.88	39.68
	JVP80	34.60	0.21			11.09	12.69	11.11	12.79	0.04	40.66	2.12	29.15
	JVP111	49.20	0.08			5.00	4.08	5.65	14.80	0.00	0.00	0.73	28.26
8	JVP01	81.30	0.11	38.33	65.74	24.81	20.59	24.85	20.81	993.60	65.97	1307.4	68.07
	JVP03	60.00	0.05			4.47	8.46	4.88	14.27	40.94	14.15	64.52	14.68
	JVP07	42.60	0.21			17.21	1.57	17.37	2.40	11.93	34.62	27.98	34.72
	JVP08	48.00	0.19			3.83	33.62	3.99	36.34	0.19	33.92	0.78	34.23
	JVP09	60.00	0.02			2.19	10.28	2.29	13.04	0.05	42.72	0.11	43.46
	JVP11	49.20	0.22			14.55	0.48	14.96	1.06	0.41	39.13	1.14	30.44
	JVP15	39.90	0.56			9.29	0.46	12.85	1.31	0.42	19.75	0.96	19.67
	JVP83	47.20	0.07			1.52	28.99	1.53	29.23	1.53	17.99	0.81	22.64
	JVP101	60.00	0.05			7.56	34.51	8.03	38.03	75.05	45.03	152.43	46.42
	JVP107	47.20	0.06			6.86	2.86	6.86	2.94	0.23	39.99	0.50	39.90
9	WWTP	47.20		30.10	58.03		0.00		0.00				
	JVP06	49.70	0.08			8.84	7.40	9.61	14.63	26.94	28.93	58.80	29.52
	JVP20	60.00	0.00			4.96	6.34	5.53	15.52	1.95	41.43	5.22	42.39
	JVP24	60.00	0.15			11.02	4.50	11.61	8.99	7.35	40.49	14.43	40.56
	JVP25	39.90	0.18			10.44	4.58	10.95	8.55	18.19	13.37	16.59	14.61
	JVP27	60.00	0.80			17.79	0.60	17.84	0.80	4.51	7.01	8.69	7.01
	JVP66	60.00	0.03			3.65	16.38	3.80	19.62	0.19	29.32	5.20	42.92
	JVP88	60.00	0.03			1.21	16.53	1.23	11.38	0.29	41.40	0.97	40.13
10	JVP31	59.20	0.08	42.74	77.42	3.90	62.32	6.14	78.50	119.26	15.88	392.15	17.34
11	JVP13	60.00	0.24	25.67	68.47	21.86	26.67	21.63	26.04	922.15	10.79	1466.56	10.58
	JVP14	60.00	0.02			2.03	12.83	2.18	17.95	0.12	42.72	0.25	44.03
	JVP17	60.00	0.05			7.18	8.21	7.24	9.01	6.55	48.83	11.83	48.90
	JVP18	26.70	0.10			5.62	4.21	5.80	7.10	0.47	19.06	1.19	19.32
	JVP21	60.00	0.02			2.55	23.60	2.73	26.06	1.26	46.10	2.52	47.71
	JVP103	35.50	0.11			5.05	4.45	5.08	5.02	1.26	28.24	2.99	29.73
12	JVP23	58.00	0.12	45.47	74.10	17.81	26.10	18.11	26.89	311.99	21.19	485.51	25.95
	JVP49	60.00	0.08			8.08	8.30	8.32	10.78	26.66	11.68	55.76	11.68
	JVP63	60.00	0.08			12.46	1.68	12.66	3.02	4.74	24.91	7.53	48.34
	JVP73	60.00	0.03			4.37	4.53	4.46	6.39	84.04	19.26	0.69	44.33
	JVP108	60.00	0.09			7.45	1.97	7.61	3.61	1.11	48.48	1.74	49.10
13	JVPT19	51.50	0.06	16.28	87.59	6.97	14.93	7.26	16.16	23.12	33.58	35.25	34.77
	JVP96	60.00	0.04			4.21	4.86	4.30	6.38	0.14	41.40	0.29	41.41

	PT18	51.50	0.11			11.06	12.69	11.19	13.69	26.33	42.64	28.77	42.75
	JVP92	35.50	0.02				0.00		0.00	0.63	41.23	0.72	45.90
14	JVP52	60.00	0.14	25.73	70.57	18.06	2.55	18.98	7.08	265.93	27.30	489.84	29.48
	JVP28	60.00	0.02			1.92	21.98	2.01	25.02	1.58	40.16	2.97	40.25
	JVP30	60.00	0.05			7.74	3.63	7.90	5.55	3.23	48.71	4.81	48.92
	JVP47	60.00	0.03			3.46	11.34	4.26	26.87	0.15	42.66	0.76	46.17
	JVP48	47.20	0.06			4.42	14.49	4.32	12.55	0.09	28.99	0.16	25.17
	JVP26	29.18	0.43			6.66	26.19	6.71	26.82	0.43	20.89	1.71	20.65
	JVP61	29.90	0.19			13.39	3.62	13.36	3.25	3.47	39.62	9.45	24.95
	JVP75	60.00	0.43			9.65	13.51	9.76	14.35	0.41	43.88	1.18	28.67
	JVP84	49.20	0.14			11.81	3.57	11.81	3.45	0.38	22.64	4.13	33.80
	JVP85	60.00	0.11			12.50	3.49	12.35	2.24	2.35	33.81	1.06	41.47
15	JVP44	60.00	0.11	18.59	50.61	19.33	3.73	19.55	4.68	18.56	50.66	33.11	50.70
	JVP45	60.00	0.05			2.55	23.33	3.70	47.52	0.20	39.64	0.44	40.06
	JVP59	49.70	0.10			6.07	6.18	6.10	6.50	0.80	37.89	0.95	40.62
	JVP82	39.50	0.11			6.60	4.31	6.61	4.47	16.50	47.06	2.90	18.53
	JVP99	38.90	0.17			12.42	3.74	12.47	3.88	0.87	31.25	1.62	32.42
16	JVP53	60.00	0.10	6.29	53.45	15.34	8.56	15.40	8.85	53.29	36.15	103.10	37.33
	JVP19	41.00	0.20			14.17	1.35	14.26	1.90	4.96	34.12	8.43	34.16
	JVP71	36.50	0.15			11.72	1.59	11.78	1.99	0.64	19.58	2.32	31.02
	JVP81	55.40	0.12			16.83	3.63	17.16	5.29	0.47	29.19	30.70	47.01
	JVP91	34.31	0.06			6.61	11.70	6.65	12.14	0.41	40.11	0.96	41.24
17	JVP10	60.00	0.26	0.00	11.33	19.38	3.20	20.14	6.92	10.97	40.64	17.55	40.69
	JVP50	46.80	0.16			12.06	1.75	12.12	2.13	1.92	39.54	2.04	39.54
	JVP70	31.30	0.10			4.83	12.36	5.02	15.22	86.03	35.82	2.08	19.86
18	JVP72	36.70	0.57	57.75	90.83	18.08	6.36	19.46	13.05	1.27	31.02	183.20	20.59
	PR03	60.00	0.25			25.46	5.28	25.54	5.59	49.27	41.00	50.35	41.00

7.1.2 Porvoo

						Dry weather		Wet weather		Dry weather		Wet weather	
Zone	Name	Best eff (%)	Specific energy (kWh/m3)	NRW (%)		Head (m)		Head (m)		Energy	EFF	Energy	EFF
				Dry	Wet	Total H	Friction (%)	Total H	Friction (%)	kWh/d	(%)	kWh/d	(%)
1	JVP29	60.00	0.05	0.00	50.50	3.50	24.54	2.93	7.66	7.83	5.33	12.57	5.52
	JVP62	60.60	0.08			1.01	48.75	1.86	52.72	3.21	48.57	11.23	42.87
	JVP63	60.50	0.16			8.26	94.78	11.82	97.36	1.42	22.01	10.96	24.13
	JVP64	60.00	0.46			1.89	95.30	3.86	66.17	0.54	46.85	0.60	46.54
	JVP66	60.00	0.15							0.00	0.00	0.00	0.00
	JVP67	60.60	0.16			7.59	80.27	8.13	82.88	0.52	42.58	3.10	42.53
	JVP68	33.00	0.17			5.17	47.03	5.17	47.03	9.18	17.67	26.32	16.78
	JVP69	41.00	0.24			3.88	10.79	9.46	14.14	0.48	15.95	8.43	16.92
	JVP70	30.00	0.31			6.50	73.44	6.50	73.44	13.34	14.93	29.26	12.11
	JVP71	41.00	0.21			5.50	36.36	5.50	36.36	0.18	14.24	0.28	14.76
2	JVP32	77.60	0.09	85.93	70.77	9.79	54.48	9.11	50.44	105.19	58.33	176.98	58.70
	JVP30	60.00	0.08			3.13	59.88	3.19	58.74	2.15	18.46	6.33	15.83
	JVP60	36.90	0.09			1.62	40.96	1.97	50.83	0.69	23.17	0.75	23.18
	JVP49	60.00	0.48			2.70	15.49	2.59	15.00	0.05	39.56	0.05	41.09
	JVP31	60.00	0.12			16.77	1.79	17.03	3.27	24.30	45.31	24.89	45.39
	JVP39	60.00	0.06			6.73	11.84	6.62	10.41	3.04	32.38	3.18	32.29
	JVP50	60.00	0.03			3.83	14.20	3.55	7.92	2.07	38.50	2.15	38.56

3	JVP79	72.90	0.06	11.02	75.64	12.93	82.63	11.79	80.87	2.05	60.34	17.52	59.83
	JVP33	65.00	0.05			6.05	4.70	5.88	2.34	0.49	49.40	0.72	49.50
	JVP43	60.00	0.05			7.27	4.98	7.03	2.35	0.55	39.09	0.83	37.80
	JVP48	35.40	0.15			11.15	1.92	11.00	0.56	2.38	22.72	3.14	23.06
	JVP55	60.00	0.04			3.05	0.87	3.42	5.99	0.04	38.85	0.05	38.82
	JVP80	39.70	0.14			12.80	45.08	13.15	14.27	0.71	24.97	39.04	20.07
	JVP81	39.30	0.20			13.70	11.10	16.55	16.37	13.17	23.08	22.71	24.54
	JVPz	39.00	0.10			7.06	6.43	6.86	4.14	1.35	27.29	2.31	27.44
	JVPm	60.50	0.14			12.67	33.59	5.01	67.90	0.21	19.19	0.43	18.39
4	JVP35	74.60	0.03	0.00	46.12	6.64	31.53	5.98	22.63	9.61	54.46	18.17	55.55
	JVP28	70.00	0.04			3.42	20.28	3.17	13.96	0.45	34.25	0.77	33.16
	JVP36	73.00	0.09			14.91	23.18	14.59	21.51	19.31	52.20	27.71	51.68
	JVP61	60.00	0.00			10.30	2.99	10.17	2.13	2.08	33.28	4.81	31.36
5	JVP100	60.00	0.07	74.06	79.30	4.69	48.72	9.75	75.85	520.36	14.65	1181.00	17.55
	JVP3	74.30	0.15			15.91	2.52	16.30	6.14	124.76	30.75	123.75	31.25
	JVP8	60.50	0.04			3.39	46.90	3.90	53.02	127.31	27.17	140.36	27.85
	JVP12	59.20	0.08			12.09	0.91	12.00	0.23	3.13	45.01	3.47	44.69
	JVP13	73.00	0.03			4.93	9.25	4.54	2.10	0.96	49.19	1.09	48.62
	JVP21	60.90	0.08			6.19	10.23	6.54	14.78	11.10	33.06	12.92	32.31
	JVP22	61.50	0.08			7.29	33.26	7.63	35.44	21.76	36.12	24.64	36.66
	JVP72	60.00	0.15			24.00	2.44	23.83	1.80	21.42	40.91	23.56	40.89
	JVPy	60.50	0.14			18.01	3.72	17.61	1.38	0.43	35.59	0.48	28.63
6	JVP78	60.00	0.08	11.30	56.50	4.14	14.50	12.30	52.36	1.36	36.36	0.82	45.21
	JVP77	60.00	0.07			1.42	84.51	1.40	78.75	0.19	33.81	0.17	37.42
7	JVP18	60.00	0.04	0.05	46.86	3.13	21.76	3.62	31.97	11.72	41.38	21.58	41.36
	JVP6	68.40	0.05			8.57	4.79	8.38	2.59	8.42	47.32	13.62	47.61
	JVP7	73.00	0.03			5.96	12.20	5.44	6.87	1.73	57.67	4.17	56.78
	JVP15	61.50	0.09			11.37	14.60	10.89	10.83	7.60	45.38	11.09	45.19
	JVP23	39.50	0.10			4.71	44.30	4.60	42.71	2.22	16.34	5.27	16.36
	JVP75	39.60	0.10							0.00	0.00	0.00	0.00
	JVP76	40.40	0.17							0.00	0.00	0.00	0.00
8	JVP9	60.00	0.09	2.23	70.35	10.65	15.02	10.95	17.19	151.24	12.22	338.59	19.17
	JVP11	60.00	0.04			5.04	81.37	5.78	84.99	0.11	45.74	0.13	45.05
	JVP16	60.00	0.10			11.62	0.16	17.13	0.29	1.24	45.93	16.63	45.65
	JVP17	44.60	0.05			5.15	23.72	5.09	22.96	0.42	28.02	1.76	26.77
	JVP19	60.00	0.01			0.52	66.70	0.50	50.44	0.01	42.93	0.01	42.77
	JVP20	31.70	0.33			27.00	28.69	26.66	27.62	51.13	22.30	113.49	22.56
	JVP57	29.90	0.33			0.21	0.04	11.38	92.03	14.14	15.33	21.45	16.19
	JVP58	60.00	0.10			12.54	2.85	12.40	1.41	13.74	7.83	61.16	9.40
	JVP59	61.50	0.10			13.09	4.66	12.95	3.59	3.27	45.53	8.02	45.23
	JVP65	40.40	0.12			8.50	1.74	15.39	4.23	0.63	31.91	1.24	31.51
	JVP73	61.00	0.11			2.10	85.67	6.27	4.46	0.11	30.95	1.86	30.92
9	JVP1	60.00	0.06	3.72	56.39	5.02	41.76	4.95	37.38	277.72	24.31	472.59	27.90
	JVP2	60.00	0.04			6.98	79.48	6.75	78.29	101.14	43.35	198.07	44.20
	JVP4	60.00	0.27			5.98	31.55	5.91	30.76	147.19	21.39	511.98	20.79
	JVP5	76.00	0.02			4.49	58.50	4.19	55.09	9.86	53.98	15.34	54.27
	JVP10	73.00	0.02			4.38	27.03	4.04	21.20	9.25	42.30	20.22	43.59
	JVP14	70.00	0.04			3.17	44.45	3.18	43.39	0.15	35.98	0.20	35.36
	JVP34	60.50	0.10			15.55	2.18	15.47	2.50	5.39	47.61	15.73	48.14
	JVP41	37.90	0.14			13.14	24.59	13.00	23.82	7.31	25.35	17.35	25.43
	JVP44	23.40	0.06			1.82	20.74	1.75	17.86	2.02	13.62	2.68	13.76
	JVP51	75.50	0.09			16.13	6.71	16.08	6.41	28.67	59.14	39.91	59.43
	JVP52	76.10	0.08			9.41	21.79	10.32	28.59	70.96	15.61	141.42	16.15
	JVP53	75.00	0.07			5.53	80.75	5.47	80.18	23.81	28.06	57.23	48.64

	JVP54	33.20	0.18			10.18	1.77	10.13	1.28	1.79	14.90	4.16	14.67
	JVP302	60.00	0.12			8.45	24.03	7.79	17.57	20.66	35.56	20.92	35.97
10	JVP25	73.70	0.04	5.41	71.23	7.96	20.13	7.96	19.97	26.08	45.56	70.05	47.48
	JVP40	64.30	0.03			4.22	13.33	4.05	9.87	1.13	50.13	5.08	50.68
	JVP42	74.60	0.11			9.70	35.74	11.48	2.44	0.26	58.78	1.26	38.03
	JVP45	60.00	0.05			5.97	59.65	6.11	60.44	2.02	46.56	6.72	46.22
	JVP56	60.00	0.05			6.65	6.29	6.41	2.96	0.97	40.30	1.60	40.24
11	JVP27	60.00	0.05	0.00	49.33	5.59	70.69	4.42	63.05	19.20	31.94	37.15	32.06
	JVP38	34.60	0.08			7.63	5.00	7.28	0.53	6.08	20.84	7.66	20.78
	JVP24	74.60	0.05			6.50	8.20	6.32	5.63	0.64	55.94	2.33	55.82
	JVPx	60.00	0.03			3.23	17.25	3.13	14.64	0.25	35.51	0.32	35.30

Actual recorded energy consumption and its efficiency

		Dry weather				Wet weather			
	Best EFF	Pumping energy	Real energy consumption	EFF	Hydraulic/Real	Pumping energy	Real energy consumption	EFF	Hydraulic /Real
Name	(%)	kWh/d	kWh/d	(%)		kWh/d	kWh/d	(%)	
JVP1	60.00	277.72	350.84	24.31	14.59 %	472.59	762.62	27.90	14.93 %
JVP2	60.00	101.14	112.67	43.35	40.59 %	198.07	217.96	44.20	41.49 %
JVP3	74.30	124.76	43.94	30.75	87.34 %	123.75	106.66	31.25	36.34 %
JVP5	76.00	9.86	17.81	53.98	30.79 %	15.34	31.79	54.27	27.05 %
JVP9	60.00	151.24	65.34	12.22	15.61 %	338.59	218.28	19.17	17.59 %
JVP10	73.00	9.25	12.16	42.30	33.39 %	20.22	22.51	43.59	40.86 %
JVP15	61.50	7.60	22.63	45.38	15.78 %	11.09	24.08	45.19	21.68 %
JVP16	60.00	1.24	12.26	45.93	4.82 %	16.63	34.28	45.65	23.00 %
JVP18	60.00	11.72	25.2	41.38	19.26 %	21.58	56.86	41.36	15.90 %
JVP20	31.70	51.13	61.37	22.30	20.02 %	113.49	255.89	22.56	10.68 %
JVP22	61.50	21.76	12.49	36.12	67.14 %	24.64	65.11	36.66	14.75 %
JVP25	73.70	26.08	38.51	45.56	33.12 %	70.05	90.43	47.48	39.96 %
JVP28	70.00	0.45	39.11	34.25	0.39 %	0.77	75.69	33.16	0.35 %
JVP29	60.00	7.83	9.41	5.33	3.03 %	12.57	27.46	5.52	1.47 %
JVP30	60.00	2.15	18.85	18.46	3.57 %	6.33	32.30	15.83	3.22 %
JVP31	60.00	24.30	43.33	45.31	26.49 %	24.89	73.16	45.39	16.06 %
JVP32	77.60	105.19	234.61	58.33	26.76 %	176.98	353.37	58.70	29.94 %
JVP35	74.60	9.61	14.98	54.46	35.82 %	18.17	29.94	55.55	34.52 %
JVP36	73.00	19.31	21.51	52.20	47.43 %	27.71	38.02	51.68	38.27 %
JVP41	37.90	7.31	17.9	25.35	11.19 %	17.35	96.6	25.43	4.94 %
JVP45	60.00	2.02	11.77	46.56	8.31 %	6.72	22.21	46.22	14.60 %
JVP48	35.40	2.38	9.21	22.72	6.40 %	3.14	23.93	23.06	3.27 %
JVP49	60.00	0.05	1.82	39.56	1.18 %	0.05	2.01	41.09	1.08 %
JVP51	75.50	28.67	9.31	59.14	185.63 %	39.91	35.09	59.43	68.88 %
JVP53	75.00	23.81	61.41	28.06	10.80 %	57.23	160.99	48.64	9.50 %
JVP54	33.20	1.79	39.11	14.90	0.72 %	4.16	100.07	14.67	0.60 %
JVP57	29.90	14.14	14.50	15.33	14.95 %	21.45	154.84	16.19	2.34 %
JVP58	60.00	13.74	54.69	7.83	1.83 %	61.16	97.19	9.40	4.13 %
JVP62	60.60	3.21	29.94	48.57	5.20 %	11.23	44.77	42.87	11.30 %
JVP63	60.50	1.42	15.28	22.01	2.13 %	10.96	26.09	24.13	10.51 %
JVP67	60.60	0.52	30.30	42.58	0.76 %	3.10	56.18	42.53	2.44 %
JVP68	33.00	9.18	25.66	17.67	6.32 %	26.32	51.36	16.78	9.55 %
JVP69	41.00	0.48	19.01	15.95	0.41 %	8.43	28.82	16.92	5.28 %
JVP70	30.00	13.34	24.52	14.93	8.12 %	29.26	45.19	12.11	9.13 %
JVP72	60.00	21.42	18.10	40.91	50.31 %	23.56	34.31	40.89	29.18 %
JVP78	60.00	1.36	9.15	36.36	5.52 %	0.82	14.95	45.21	2.56 %
JVP79	72.90	2.05	26.8	60.34	4.69 %	17.52	55.17	59.83	19.39 %
JVP80	39.70	0.71	18.93	24.97	0.94 %	39.04	34.31	20.07	23.26 %

JVP81	39.30	13.17	62.57	23.08	5.25 %	22.71	154.84	24.54	4.07 %
JVPx	60.00	0.25	33.53	35.51	0.27 %	0.32	123.37	35.30	0.10 %
JVP100	60.00	520.36	189.6	14.65	40.41 %	1181.00	576.27	17.55	36.78 %

7.1.3 Kurikka

Zone	Name	Best eff (%)	Specific energy (kWh/m³)	NRW (%)		Dry weather Head (m)		Wet weather Head (m)		Dry weather Energy	Dry weather EFF	Wet weather Energy	Wet weather EFF
				Dry	Wet	Total H	Friction (%)	Total H	Friction (%)	kWh/d	(%)	kWh/d	(%)
1	JVP1	60.00	0.01	50.69	63.38	0.85	98.54	0.90	96.76	0.06	16.87	0.05	24.93
	JVP2	60.00	0.03			3.59	24.78	3.59	24.87	0.10	59.50	0.26	59.50
	JVP3	60.00	0.01			2.19	34.39	2.19	34.41	0.03	59.50	0.12	59.50
2	JVP4	60.00	0.03	13.34	44.71	5.63	8.26	5.65	8.63	0.90	59.50	2.93	59.50
	JVP5	60.00	0.10			3.31	0.16	3.32	0.16	1.25	9.19	2.36	9.20
	JVP6	60.00	0.13			14.94	7.47	15.13	5.68	2.25	59.50	2.66	59.50
3	JVP7	65.00	0.21	1.07	3.00	28.24	4.44	28.56	5.48	60.25	46.16	74.03	46.08
	JVP8	60.00	0.06			3.95	21.60	3.93	21.50	1.30	19.62	1.39	18.96
	JVP9	60.00	0.02			2.28	56.78	2.27	56.87	0.60	33.16	0.60	33.05
	JVP10	60.00	0.02			4.18	47.65	4.20	47.82	0.62	59.50	0.61	59.50
	JVP11	60.00	0.04			7.70	8.44	7.69	8.45	0.31	59.50	0.32	59.50
4	JVP12	67.60	0.08	2.98	23.77	7.10	55.94	7.27	57.00	5.26	15.19	26.06	17.13
	JVP13	38.20	0.05			2.57	29.19	2.62	30.73	4.96	4.96	50.16	5.54
	JVP14	68.20	0.16			25.11	2.24	25.38	3.29	81.40	30.68	78.54	38.89
	JVP15	65.00	0.20			29.91	8.18	30.10	8.74	69.25	43.25	87.21	43.07
	JVP16	65.00	0.31			37.19	6.94	37.22	7.03	120.01	30.45	148.92	30.67
5	JVP17	45.00	0.16	33.88	54.89	9.83	10.38	9.88	10.81	27.98	17.02	64.42	17.12
	JVP18	35.60	0.08			7.30	31.88	7.32	32.01	9.21	24.11	18.51	23.71
	JVP19	60.00	0.04			2.13	43.29	2.14	42.00	0.22	59.50	0.23	59.50
	JVP20	60.00	0.07			9.42	12.26	9.44	12.43	3.32	59.50	5.88	59.50
6	JVP21	45.00	0.11	2.20	6.71	7.13	6.65	7.12	6.18	23.17	14.23	24.83	14.32
	JVP22	60.00	0.01			0.53	70.26	0.53	70.94	0.18	59.50	0.17	59.50
	JVP23	60.00	0.10			13.02	6.98	13.01	7.01	5.71	33.95	5.57	34.05
7	JVP24	19.80	0.32	3.12	22.50	12.40	8.65	12.42	8.85	169.74	11.60	123.71	12.12
	JVP25	23.20	0.14			2.51	24.12	2.64	27.93	4.45	11.01	4.45	11.01
	JVP26	60.00	0.01			1.00	40.05	1.02	49.18	0.03	59.50	0.05	59.50
	JVP27	23.50	0.05			1.32	78.58	1.32	78.75	4.55	1.88	59.03	1.93
	JVP28	60.00	0.08			8.01	14.28	8.09	14.72	0.99	59.50	1.04	59.50
	JVP29	36.30	0.22			11.72	3.95	11.80	4.59	1.75	18.42	2.99	18.46
	JVP30	60.00	0.12										
8	JVP31	48.00	0.32	0.83	2.19	11.95	6.71	11.93	6.47	30.67	10.20	23.13	12.09
	JVP32	60.00	0.10			19.39	4.58	19.37	4.52	3.47	59.50	3.45	59.50
9	JVP33	60.00	0.02	15.06	50.69								
	JVP34	60.00	0.02										
	JVP35	23.50	0.10			2.68	19.23	2.70	19.55	0.78	6.63	1.19	8.79
	JVP36	60.00	0.05			3.70	21.04	3.69	21.07	0.11	20.43	0.24	18.42
	JVP37	60.00	0.08			10.47	7.74	10.50	7.94	0.20	47.32	0.35	48.61
	JVP38	60.00	0.04			4.41	22.17	4.45	22.75	0.22	59.50	0.62	59.50
	JVP39	36.40	0.10			4.86	26.12	4.82	25.43	6.85	17.49	6.85	17.43
10	JVP40	60.00	0.02	0.46	1.80	3.12	25.62	3.13	25.70	0.33	59.50	0.32	59.50
	JVP41	36.30	0.11			1.90	43.92	1.88	43.30	0.19	7.71	0.18	8.32

	JVP42	60.00	0.08			8.01	10.81	8.04	10.93	1.32	59.50	1.32	59.50
	JVP43	60.00	0.10			2.08	6.08	2.11	7.36	0.04	5.18	0.06	34.45
	JVP44	60.00	0.00			2.52	43.39	2.42	40.82	0.06	12.77	0.06	12.01
	JVP45	60.00	0.10			2.08	37.98	2.04	2.96	0.27	59.50	0.28	59.50
	JVP46	60.00	0.08			7.10	51.56	7.05	51.71	0.86	59.50	0.85	59.50
	JVP47	35.60	0.07			6.79	6.54	6.80	6.66	22.35	21.85	24.42	21.59
11	JVP48	34.70	0.09	0.43	8.41	8.33	18.43	8.32	18.19	2.14	26.17	2.17	25.19
	JVP49	36.30	0.16			3.88	30.24	3.88	29.93	2.63	11.65	2.90	11.75
	JVP50	36.30	0.16			3.79	27.48	3.78	27.29	2.20	11.56	2.42	11.71
	JVP51	36.30	0.16			4.64	58.09	4.64	58.17	1.95	12.45	2.32	12.65
	JVP52	36.30	0.16			2.07	48.80	2.07	48.36	0.71	8.30	0.85	8.34
	JVP53	36.30	0.18			8.81	10.14	8.81	10.10	1.68	15.05	1.74	14.33
	JVP54	48.00	0.08			4.83	16.12	4.79	15.37	83.43	3.73	223.39	3.46
12	JVP55	40.00	0.17	3.09	21.48	13.27	11.62	13.45	12.76	174.75	17.64	206.63	17.84
	JVP56	56.80	0.08			10.63	24.32	10.72	24.97	92.97	30.55	109.78	30.39

Actual recorded energy consumption and its efficiency

		Dry weather				Wet weather			
	Best EFF	Pumping energy	Real energy consumption	EFF	Hydraulic/Real	Pumping energy	Real energy consumption	EFF	Hydraulic /Real
Name	(%)	kWh/d	kWh/d	(%)		kWh/d	kWh/d	(%)	
JVP4	60.00	0.90	12.37	59.50	5.19	2.93	18.85	59.50	9.24
JVP7	65.00	60.25	146.48	46.16	20.40	74.03	258.80	46.08	13.81
JVP9	60.00	0.60	10.07	33.16	2.05	0.60	15.38	33.05	1.35
JVP10	60.00	0.62	6.43	59.50	5.52	0.61	7.87	59.50	4.63
JVP11	60.00	0.31	2.60	59.50	7.13	0.32	4.58	59.50	4.11
JVP12	67.60	5.26	41.33	15.19	3.34	26.06	69.08	17.13	6.64
JVP14	68.20	81.40	128.70	30.68	15.71	78.54	186.93	38.89	16.18
JVP16	65.00	120.01	118.30	30.45	34.17	148.92	192.80	30.67	25.26
JVP17	45.00	27.98	53.14	17.02	14.87	64.42	80.08	17.12	14.87
JVP18	35.60	9.21	34.75	24.11	9.23	18.51	42.21	23.71	10.99
JVP20	60.00	3.32	36.51	59.50	7.06	5.88	53.35	59.50	6.56
JVP21	45.00	23.17	66.21	14.23	5.33	24.83	110.16	14.32	3.40
JVP24	19.80	169.74	50.27	11.60	19.72	123.71	87.20	12.12	13.67
JVP29	36.30	1.75	2.87	18.42	12.57	2.99	4.10	18.46	13.99
JVP31	48.00	30.67	40.31	10.20	5.15	23.13	54.85	12.09	4.13
JVP35	23.50	0.78	2.82	6.63	3.07	1.19	4.35	8.79	1.99
JVP37	60.00	0.20	0.81	47.32	12.54	0.35	1.16	48.61	15.10

7.1.4 Kouvola

						Dry weather		Wet weather		Dry weather		Wet weather	
Zone	Name	Best eff (%)	Specific energy (kWh/ m3)	NRW (%)		Head (m)		Head (m)		Energy	EFF	Energy	EFF
				Dry	Wet	Total H	Friction (%)	Total H	Friction (%)	kWh/d	(%)	kWh/d	(%)
1	JVP1	38.00	0.20	0.00	83.07	9.66	10.28	17.46	44.58	54.01	11.82	310.81	20.63
	JVP2	60.00	0.10			17.24	0.35	17.37	1.10	1.75	48.44	10.50	48.71
	JVP3	60.00	0.05			7.95	3.54	7.95	3.57	0.37	49.06	1.38	48.96
	JVP4	60.00	0.04			4.15	1.86	4.23	3.41	1.06	21.08	8.63	20.61
2	JVP5	60.00	0.23	2.23	79.92	7.29	22.86	7.60	25.71	111.31	4.10	140.38	11.93
	JVP6	60.00	0.05			5.24	20.51	5.29	20.74	0.09	35.65	0.44	35.17
	JVP7	24.50	0.27			1.02	55.64	4.30	89.79	28.66	17.66	143.24	19.12
	JVP8	60.00	0.08			12.92	0.15	13.00	0.86	0.85	46.10	9.49	46.35
	JVP9	60.00	0.14			26.08	1.06	25.87	0.42	1.44	48.85	3.75	48.48
3	JVP10	75.00	0.13	29.35	91.55	33.89	3.22	37.31	6.98	619.41	64.83	1614.61	70.26
	JVP11	60.00	0.08			14.96	1.29	14.76	15.74	360.33	46.03	1150.97	50.81
	JVP12	60.00	0.04			6.42	0.43	6.60	2.87	1.07	45.28	9.29	45.88
	JVP13	60.00	0.04			7.74	4.92	7.75	5.05	0.53	49.50	1.57	49.58
	JVP14	60.00	0.02			4.31	4.70	4.03	1.48	1.16	46.53	7.96	45.84
4	JVP15	82.10	0.05	9.77	82.57	11.61	6.35	15.04	22.99	92.61	66.04	496.15	71.51
	JVP16	60.00	0.08			9.99	3.71	13.95	33.43	17.26	36.84	110.68	48.89
	JVP17	59.00	0.06			10.66	13.06	10.62	15.63	71.79	41.37	422.29	46.53
	JVP18	60.30	0.13			14.40	12.79	19.53	30.60	29.83	30.66	199.12	40.92
	JVP19	60.00	0.03					3.27	16.04			0.12	37.40
	JVP20	60.00	0.03			5.07	1.10	5.28	4.56	0.76	47.08	5.70	47.41
	JVP21	60.00	0.05			7.66	0.50	7.90	3.32	1.71	46.77	12.92	46.83
	JVP22	71.00	0.11			9.58	34.47	18.07	65.23	13.20	43.31	143.03	49.51
	JVP23	60.00	0.04			3.98	19.46	6.46	50.08	1.11	24.51	5.93	40.94
	JVP24	60.00	0.05			8.83	3.47	9.07	5.90	2.86	46.81	17.73	47.60
	JVP25	70.00	0.08			9.69	17.66	15.17	47.09	16.65	36.59	132.98	52.50
	JVP26	60.00	0.04			5.63	8.89	5.67	7.39	1.24	36.25	9.08	37.88
5	JVP27	60.00	0.10	44.88	78.56	18.55	1.67	18.64	2.17	24.33	47.91	49.61	47.93
	JVP28	60.00	0.05			4.95	6.63	4.91	6.19	0.14	28.87	0.30	28.82
	JVP29	60.00	0.02			3.23	9.36	3.36	10.08	0.44	47.97	1.84	48.27
	JVP30	60.00	0.11			19.41	1.33	19.43	1.40	4.68	49.76	6.23	49.46
	JVP31	60.00	0.07			8.82	9.81	8.81	9.86	0.70	37.85	1.77	37.40
	JVP32	60.00	0.03			3.55	12.94	3.64	13.33	0.39	43.48	1.09	43.46
	JVP33	60.00	0.02			3.62	11.54	3.80	15.55	2.49	47.99	4.25	48.64
	JVP34	60.00	0.11			20.95	0.27	20.98	0.43	2.97	49.45	8.14	49.28
	JVP35	60.00	0.02			2.93	5.22	2.95	5.92	0.41	47.12	0.97	47.32
	JVP36	60.00	0.10			16.77	0.62	17.81	0.57	1.77	48.27	7.53	49.02
	JVP37	60.00	0.07			8.37	2.07	8.53	2.09	0.75	41.53	2.73	41.57
	JVP38	60.00	0.07			10.54	3.80	10.68	5.17	4.38	47.43	10.41	47.27
	JVP39	60.00	0.07			13.12	3.92	12.83	1.91	4.51	48.33	8.37	47.92
6	JVP40	52.00	0.02	15.96	84.82	2.17	19.14	3.39	24.44	17.60	32.58	111.91	36.41
	JVP41	60.00	0.04			6.22	17.08	6.53	19.76	0.88	48.21	6.65	48.04
7	JVP42	62.00	0.10	58.41	98.16	18.03	6.67	18.22	8.14	17.83	40.24	351.97	48.89
	JVP43	60.00	0.04			7.33	5.87	7.49	7.80	0.25	48.86	5.98	49.21
	JVP44	60.00	0.09			8.54	2.45	8.42	0.82	1.16	21.26	18.05	21.41
8	JVP45	67.00	0.04	26.81	92.17	4.26	11.79	6.18	28.70	47.02	22.99	366.88	48.51

	JVP46	62.00	0.13			26.01	0.88	26.69	3.55	53.07	47.19	423.60	54.49
	JVP47	60.00	0.08			15.39	1.95	15.22	0.55	0.98	48.41	16.50	48.19
	JVP48	60.00	0.02			3.45	3.25	3.50	3.92	0.03	48.42	0.65	46.36
	JVP49	60.00	0.05			8.90	27.28	8.98	27.89	0.26	48.52	4.21	48.21
	JVP50	60.00	0.02			3.82	2.79	3.83	3.33	0.04	48.34	0.46	47.95
	JVP51	67.00	0.13			11.53	0.89	20.79	45.28	32.13	44.51	471.17	49.35
	JVP52	60.00	0.02			3.11	6.59	2.83	4.23	0.19	46.97	1.73	46.21
	JVP53	60.00	0.03			5.34	62.85	5.20	61.52	0.53	46.58	5.78	46.57
	JVP54	52.00	0.06			6.17	10.73	6.47	15.40	16.78	18.39	114.89	21.19
	JVP55	60.00	0.03			5.85	4.91	5.76	0.44	0.72	48.23	3.69	47.74
	JVP56	60.00	0.13			6.42	1.33	6.42	1.64	0.40	14.11	21.57	10.21
	JVP57	60.00	0.05			8.00	1.00	8.95	1.59	0.04	21.73	0.72	48.05
9	JVP58	52.70	0.07	42.20	86.80	10.47	45.24	10.52	45.45	3.08	35.60	13.42	36.06
	JVP59	60.00	0.30			7.97	12.34	7.83	8.78	0.20	9.22	0.69	10.14
	JVP60	24.50	0.05			2.13	10.10	2.12	9.76	0.17	9.56	0.73	9.48
10	JVP61	60.00	0.03	55.64	84.82	5.88	9.04	6.38	16.15	21.30	48.51	38.09	48.68
	JVP62	60.00	0.04			4.84	11.12	4.84	11.02	0.07	38.33	0.07	38.73
	JVP63	60.00	0.04			5.83	25.88	5.81	25.64	0.49	44.36	0.95	44.34
	JVP64	60.00	0.08			13.65	2.14	13.66	2.21	0.97	47.78	3.01	47.00
11	JVP65	58.00	0.09	10.48	74.09	14.41	20.49	15.81	28.33	232.31	41.26	483.34	46.47
	JVP66	60.00	0.08			11.79	68.50	11.74	68.67	0.11	43.37	0.14	44.49
	JVP67	67.00	0.07			5.95	21.89	10.76	57.39	51.18	32.67	292.33	46.33
	JVP68	60.00	0.04			6.07	1.59	6.13	2.46	0.76	48.75	3.23	49.10
	JVP69	60.00	0.08			10.83	4.78	12.68	14.54	0.45	42.85	0.46	45.82
	JVP70	58.00	0.25			25.94	1.36	27.42	6.52	56.55	29.96	250.72	28.94
	JVP71	60.00	0.03			4.19	3.47	4.30	5.78	0.66	46.65	3.62	47.12
	JVP72	60.00	0.05			8.93	0.45	8.59	0.94	0.49	48.08	1.42	46.94
	JVP73	60.00	0.04			6.24	1.93	6.54	2.29	0.69	47.54	2.34	47.68
	JVP74	60.00	0.04			5.99	4.58	6.06	4.42	0.26	40.66	1.17	41.29
	JVP75	60.00	0.04			7.21	47.14	10.73	68.24	56.14	44.53	153.81	49.45
	JVP76	60.00	0.14			25.06	1.16	24.92	0.64	7.72	48.39	31.80	48.05
	JVP77	60.00	0.03			4.10	0.98	4.34	6.25	1.73	45.60	8.03	46.68
	JVP78	78.50	0.03			6.99	6.71	6.85	5.89	20.73	50.06	46.39	49.07
	JVP79	60.00	0.07			11.84	3.84	12.05	5.02	26.48	46.59	96.83	49.02
	JVP80	60.00	0.06			10.42	6.50	10.20	8.39	2.67	48.90	20.38	50.11
	JVP81	60.00	0.02			4.01	1.24	4.03	1.86	0.12	48.73	0.64	48.58
	JVP82	60.00	0.16			29.11	64.70	29.13	64.71	2.77	48.58	2.92	48.54
	JVP83	56.00	0.11			15.16	7.60	15.58	10.30	15.49	41.06	11.85	34.15
	JVP84	60.00	0.07			6.61	17.28	6.60	15.16	1.45	36.27	75.65	22.98
	JVP85	60.00	0.35			29.53	0.51	29.45	0.93	9.38	22.88	86.03	41.65
	JVP86	60.00	0.05			8.40	5.91	8.41	6.00	2.00	48.89	5.71	49.42
	JVP87	60.00	0.12			22.61	1.09	22.65	1.29	2.09	48.30	12.68	47.92
	JVP88	60.00	0.06			5.62	6.12	6.35	8.22	0.13	32.26	0.26	34.84
	JVP89	60.00	0.03			4.89	2.96	4.97	4.44	0.11	46.74	1.11	46.38
	JVP90	60.00	0.05			7.65	5.43	7.82	7.32	13.38	46.17	41.73	46.59
	JVP91	60.00	0.12			9.29	5.45	9.60	8.49	13.95	16.59	75.74	18.52
	JVP92	60.30	0.20			28.42	5.10	31.86	15.37	34.23	48.45	120.13	49.03
	JVP93	62.00	0.09			11.70	4.27	14.72	20.61	89.35	33.53	278.59	40.01
12	JVP94	60.00	0.12	37.00	38.88	10.26	1.95	10.31	3.82	38.14	39.01	50.83	36.93
13	JVP95	52.70	0.07	36.81	93.27	14.50	12.34	19.04	37.65	131.68	49.55	593.02	60.84
	JVP96	60.00	0.22			30.01	0.91	29.77	0.17	3.42	34.89	34.87	34.84
	JVP97	60.00	0.08			8.44	1.36	8.50	2.26	0.74	34.78	7.37	34.60
	JVP98	60.00	0.03			5.03	8.88	6.45	52.41	3.54	44.94	30.70	49.91
	JVP99	52.00	0.09			10.92	26.85	10.60	24.76	45.67	31.94	62.80	30.86

	JVP100	64.00	0.11			13.20	6.77	17.44	29.32	85.36	41.49	377.94	50.48
	JVP101	60.00	0.03			4.32	10.76	4.37	11.91	0.11	46.33	0.77	46.41
	JVP102	60.00	0.08			3.98	35.38	4.94	48.19	72.07	26.98	103.50	27.91
	JVP103	58.00	0.11			9.37	24.22	15.35	53.34	64.72	29.99	258.44	42.01
	JVP104	60.00	0.05			1.48	20.70	1.50	24.40	0.11	6.60	78.44	5.34
	JVP105	60.00	0.15			26.11	1.42	26.38	2.46	6.38	47.98	70.78	48.94
	JVP106	58.00	0.12			15.82	40.25	19.49	51.40	85.66	41.01	297.33	47.72
	JVP107	60.00	0.15			5.10	8.88	5.75	18.08	1.48	10.59	2.75	10.63
	JVP108	56.00	0.09			3.77	68.29	9.69	88.05	69.82	10.57	208.56	26.81
	JVP109	52.00	0.07			4.51	39.30	4.95	44.70	201.76	9.41	717.54	16.36
	JVP110	52.00	0.11			14.54	3.36	14.29	1.87	5.46	32.17	67.44	31.54
	JVP111	60.00	0.05			8.79	0.71	8.81	0.99	0.25	48.95	1.84	49.18
	JVP112	60.00	0.04			6.83	7.52	6.86	8.08	0.32	48.42	1.97	48.31
	JVP113	60.00	0.26			15.15	0.47	15.22	0.99	2.44	13.46	29.69	14.54
	JVP114	60.00	0.07			1.69	50.08	1.88	54.29	1.45	3.75	13.03	18.60
	JVP115	29.50	0.34			16.74	11.73	17.93	17.56	3.62	13.93	59.32	15.20
	JVP116	60.00	0.16			19.68	8.91	21.89	18.27	101.74	35.42	9.43	24.07
	JVP117	61.00	0.07			5.69	7.85	5.59	6.29	1.18	23.95	206.46	39.73
14	JVP118	60.00	0.01	18.92	88.00	1.17	50.67	2.94	81.63	5.92	26.82	49.11	45.35

7.1.5 Tuusula

Hyrylä						Dry weather		Wet weather		Dry weather		Wet weather	
Zone	Name	Best eff (%)	Specific energy (kWh/ m3)	NRW (%)		Head (m)		Head (m)		Energy	EFF	Energy	EFF
				Dry	Wet	Total H	Friction (%)	Total H	Friction (%)	kWh/d	(%)	kWh/d	(%)
1	JVP1	60.00	0.14	54.21	90.12	17.05	0.16	0.93	17.23	0.70	4.07	895.06	24.42
	JVP2	60.00	0.05			8.50	0.72	8.42	8.49	0.73	8.62	0.33	43.40
	JVP3	60.00	0.13			6.27	0.65	10.33	6.64	0.12	1.86	0.72	12.60
	JVP4	60.00	0.01			2.33	0.84	36.06	2.07	0.71	34.27	0.14	36.15
	JVP5	60.00	0.05			4.41	1.42	32.10	7.87	0.28	3.55	0.01	45.58
2	JVP6	60.00	0.03	29.68	44.72	4.46	1.19	26.58	5.00	1.87	37.40	0.09	44.71
	JVP7	60.00	0.05			11.75	0.22	1.84	11.57	0.13	1.16	20.36	49.00
	JVP8	60.00	0.12			8.86	5.74	64.76	15.16	12.52	82.59	1.28	15.92
	JVP9	60.00	0.04			5.35	1.21	22.66	6.00	1.50	25.00	0.27	33.14
3	JVP10	60.00	0.06	45.26	86.31	10.41	1.12	10.74	10.43	1.11	10.67	34.36	50.27
	JVP11	60.00	0.03			3.33	0.83	24.99	3.49	1.00	28.70	0.52	43.14
	JVP12	60.00	0.08			10.72	0.86	8.05	11.19	1.25	11.13	8.99	41.87
4	JVP13	60.00	0.05	63.37	92.74	9.31	3.86	41.48	8.62	4.51	52.30	61.39	46.18
5	JVP14	60.00	0.04	60.84	79.50	1.87	0.09	4.95	2.49	0.56	22.28	41.52	11.24
	JVP15	60.00	0.13			9.58	1.61	16.84	4.47	0.08	1.84	0.78	16.67
	JVP16	60.00	0.04			3.57	0.83	23.21	3.71	0.94	25.47	1.91	26.65
	JVP17	60.00	0.04			5.14	0.71	13.83	4.89	0.43	8.86	0.26	37.27
6	JVP18	60.00	0.05	28.00	44.62	7.58	0.89	11.78	6.00	0.77	12.87	0.89	43.28
	JVP19	60.00	0.07			11.10	0.92	8.27	13.08	2.93	22.40	28.13	44.04
	JVP20	60.00	0.06			2.41	2.00	83.02	1.23	1.00	81.01	0.93	38.07
	JVP21	60.00	0.11			14.23	0.02	0.16	3.29	0.05	1.42	0.01	40.16
7	JVP22	60.00	0.06	56.19	86.41	9.39	5.27	56.15	10.96	6.73	61.36	5.53	41.00
	JVP23	60.00	0.02			3.35	0.75	22.49	3.32	0.74	22.36	0.13	47.08
	JVP24	60.00	0.03			4.74	0.06	1.23	4.68	0.06	1.32	0.09	41.51
8	JVP25	60.00	0.11	61.47	88.80	19.09	1.15	6.03	19.86	2.24	11.30	123.86	46.58

	JVP26	60.00	0.03			4.80	0.55	11.51	5.90	1.57	26.59	2.27	43.45
	JVP27	60.00	0.10			13.42	0.33	2.48	13.23	0.03	0.22	6.69	31.91
	JVP28	60.00	0.04			4.15	0.25	5.97	4.34	0.40	9.16	1.09	27.52
	JVP29	60.00	0.02			3.41	0.23	6.73	3.72	0.45	12.09	0.08	37.93
	JVP30	60.00	0.03			5.58	1.22	21.87	5.57	1.28	22.97	5.39	49.10
9	JVP31	60.00	0.15	66.56	93.51	21.89	0.45	2.08	22.26	0.84	3.77	3.00	32.51
	JVP32	60.00	0.09			15.20	0.16	1.06	27.73	12.17	43.89	1.46	45.15
10	JVP33	60.00	0.14	79.80	88.72	23.06	0.12	0.51	8.36	0.27	3.18	9.15	35.76
	JVP34	60.00	0.02			2.34	0.90	38.38	2.47	0.93	37.52	0.84	43.55

Jokela

Zone	Name	Best eff (%)	Specific energy (kWh/m3)	NRW (%)		Dry weather Head (m)		Wet weather Head (m)		Dry weather Energy	EFF	Wet weather Energy	EFF
				Dry	Wet	Total H	Friction (%)	Total H	Friction (%)	kWh/d	(%)	kWh/d	(%)
1	JVP1	60.00	0.08	51.70	89.04	12.07	1.28	10.61	15.53	4.82	31.07	65.70	43.55
	JVP132	60.00	0.05			8.98	0.67	7.43	8.99	0.68	7.52	1.86	42.29
	JVP3	60.00	0.14			4.86	0.23	4.77	9.77	0.14	1.41	0.68	27.73
	JVP4	60.00	0.11			16.26	1.46	9.00	20.12	5.32	26.44	99.72	44.24
	JVP5	60.00	0.06			8.55	0.21	2.42	8.57	0.23	2.67	0.47	41.58
	JVP6	60.00	0.08			9.44	0.08	0.80	13.19	0.80	6.09	1.23	42.29
	JVP7	60.00	0.04			3.49	1.10	31.52	3.50	1.11	31.68	4.04	26.20
	JVP8	60.00	0.18			7.83	1.78	22.75	8.26	2.13	25.79	9.06	27.69
	JVP9	60.00	0.11			5.80	0.15	2.65	14.34	0.76	5.32	0.85	39.34
	JVP176	60.00	0.04			4.05	0.17	4.14	4.05	0.17	4.23	0.53	39.77
2	JVP11	60.00	0.15	25.80	93.72	15.74	3.80	24.12	19.14	7.10	37.07	21.18	41.02
3	JVP147	60.00	0.07	23.59	87.57	12.42	1.90	15.31	13.42	3.14	23.39	45.36	48.29
	JVP146	60.00	0.00			0.60	0.03	4.66	0.65	0.04	5.56	0.14	45.00
	JVP14	60.00	0.01			1.95	0.32	16.33	1.97	0.31	15.90	0.28	42.49

Kellokoski

Name	Best eff (%)	Specific energy (kWh/m3)	NRW (%)		Dry weather Head (m)		Wet weather Head (m)		Dry weather Energy	EFF	Wet weather Energy	EFF
			Dry	Wet	Total H	Friction (%)	Total H	Friction (%)	kWh/d	(%)	kWh/d	(%)
JVP1	60.00	0.13	63.70	92.49	22.02	9.72	28.27	29.27	192.82	47.32	985.40	50.82
JVP2	60.00	0.09	64.00	92.50	8.79	38.30	9.83	44.70	14.55	12.34	59.37	17.19
JVP3	60.00	0.03	55.96	89.73	5.97	33.86	7.33	44.85	11.83	49.47	30.26	49.53
JVP4	60.00	0.03	5.63	40.78	4.48	13.97	5.52	29.35	7.53	41.30	11.74	39.65
JVP5	60.00	0.01	51.37	87.97	2.64	26.01	2.64	25.64	1.73	50.10	4.51	50.26

7.2 Smart control results

7.2.1 HS-Vesi Region

Viiala		P224	P225	P264	P220	P222	P223	P221	P210	P240	P230
Dry weather	Original (kWh/d)	2.04	3.19	0.04	20.85	0.25	0.95	0.16	129.66	4.34	4.57
	Optimal pump	-31 %	7 %	-75 %	-13 %	-40 %	-62 %	34 %	-13 %	-58 %	-36 %
	Original &control	6842 %	12040 %	350 %	205 %	128 %	-51 %	25 %	321 %	56 %	561 %
	Optimal pump &control	-7 %	12033 %	275 %	68 %	60 %	-91 %	31 %	206 %	1077 %	-35 %
Wet weather	Original (kWh/d)	3.65	5.06	0.3	53.32	2.01	2.26	1.00	303.30	17.15	6.98
	Optimal pump	-33 %	-4 %	-7 %	-11 %	379 %	-61 %	-40 %	-11 %	-56 %	-35 %
	Original &control	2136 %	3917 %	-45 %	298 %	-86 %	-62 %	-72 %	73 %	41 %	223 %
	Optimal pump &control	-24 %	3918 %	-43 %	103 %	-21 %	-80 %	-73 %	41 %	2 %	-36 %
Overflow scenario	Original (kWh/d)	187.19	96.8	61.37	650.2	25.26	21.92	21.49	3208.48	144.55	66.05
	Optimal pump	-64 %	6 %	7 %	-69 %	-99 %	-67 %	4 %	-57 %	-32 %	-37 %
	Original &control	0 %	-26 %	-90 %	9 %	-78 %	-63 %	-86 %	3 %	-32 %	20 %
	Optimal pump &control	-48 %	6 %	-90 %	-64 %	-99 %	-83 %	-84 %	-36 %	-47 %	63 %

Toijala		P120	P130	P121	P122	P123	P156
Dry	Original (kWh/d)	34.04	33.15	1.42	0.34	0.65	0.02
	Optimal pump	-43 %	-48 %	-58 %	-6 %	-75 %	50 %
	Current & control	-18 %	241 %	-68 %	311 %	-62 %	-100 %
	Optimal pump & control	-40 %	-40 %	-45 %	356 %	-46 %	-100 %
Wet	Original (kWh/d)	93.41	64.36	2.99	3.67	1.28	0.07
	Optimal pump	-45 %	-42 %	-76 %	-76 %	-98 %	-14 %
	Current & control	-39 %	46 %	-82 %	-9 %	-73 %	-59 %
	Optimal pump & control	-52 %	-51 %	1714 %	-77 %	-98 %	-63 %
Overflow	Original (kWh/d)	512.45	228.37	2.35	12.39	0.34	0.07
	Optimal pump	-36 %	-56 %	-17 %	1 %	-65 %	0 %
	Current & control	0 %	23 %	-69 %	-8 %	-35 %	2743 %
	Optimal pump & control	-36 %	-56 %	2142 %	-7 %	-77 %	2729 %

Hämeenlinna

		P34	P01	P31	P23	P13	P101	P04	P05	P02	P38
Dry weather	Original (kWh/d)	252.77	993.60	119.26	311.99	939.09	75.05	31.22	6.13	23.72	10.41
	Optimal pump	-27 %	14 %	-70 %	-76 %	228 %	-37 %	24 %	21 %	-21 %	15 %
	Original &control	107 %	16 %	-76 %	-61 %	-81 %	1 %	90 %	364 %	51 %	134 %
	Optimal pump &control	-28 %	107 %	-78 %	-65 %	-81 %	69 %	90 %	363 %	128 %	183 %
Wet weather	Original (kWh/d)	487.70	2067.78	442.92	259.25	960.48	167.90	93.98	18.92	48.68	19.37
	Optimal pump	-39 %	-19 %	-76 %	-47 %	487 %	-38 %	-10 %	-8 %	-44 %	-19 %
	Original &control	20 %	16 %	-75 %	-32 %	-22 %	-2 %	58 %	58 %	-4 %	44 %
	Optimal pump &control	-39 %	61 %	-70 %	-29 %	-22 %	56 %	58 %	60 %	39 %	44 %
Overflow scenario	Original (kWh/d)	432.16	1696.64	494.98	684.26	3586.21	145.92	85.56	17.50	36.93	15.43
	Optimal pump	-29 %	15 %	-78 %	-80 %	57 %	-28 %	0 %	1 %	58 %	3 %
	Original &control	107 %	37 %	-77 %	-66 %	-85 %	12 %	70 %	69 %	147 %	105 %
	Optimal pump &control	-31 %	69 %	-74 %	-73 %	-90 %	80 %	73 %	71 %	99 %	81 %

7.2.2 Porvoo

		P2	P4	P5	P18	P10	P1	P9	P16	P73	P17	P58	P100
Dry weather	Original (kWh/d)	101.16	2109.12	9.85	1425.80	9.30	330.98	122.30	1.23	0.11	0.42	13.52	516.05
	Optimal pump	-30 %	-98 %	209 %	-99 %	-37 %	-85 %	-89 %	597 %	8173 %	2029 %	116 %	-85 %
	Original &control	621 %	-98 %	25 %	-100 %	-17 %	-68 %	-77 %	357 %	-22 %	204 %	117 %	4 %
	Optimal pump &control	-44 %	-99 %	18 %	-100 %	-19 %	-19 %	-77 %	355 %	-27 %	205 %	2114 %	-90 %
Wet weather	Original (kWh/d)	198.06	3642.72	15.34	665.18	20.21	472.59	338.59	16.63	1.85	1.76	61.15	1181
	Optimal pump	-38 %	-97 %	188 %	-98 %	-34 %	-72 %	-99 %	60 %	50 %	483 %	154 %	-77 %
	Original &control	181 %	-78 %	29 %	-98 %	-30 %	-44 %	-80 %	146 %	6 %	4093 %	154 %	-15 %
	Optimal pump &control	930 %	-98 %	7 %	-98 %	-24 %	-46 %	-80 %	146 %	6 %	4093 %	154 %	-78 %
Backflow sce-	Original (kWh/d)	386.55	1567.30	25.57	73.16	30.65	729.07	252.22	128.37	4.66	3.85	330.50	1987.72
	Optimal pump	-11 %	-88 %	230 %	-62 %	-17 %	-37 %	-38 %	0 %	0 %	201 %	-12 %	28 %
	Original &control	20 %	-91 %	-8 %	-67 %	-17 %	-15 %	-31 %	3 %	-32 %	17 %	-12 %	1 %

	Optimal pump &control	159 %	-93 %	3 %	-76 %	-24 %	0 %	-29 %	6 %	-32 %	2103 %	-12 %	35 %
Blockage scenario	Original (kWh/d)							1150.62	24.79	4.67	3.82	61.67	
	Optimal pump							-93 %	56 %	0 %	204 %	4750 %	
	Original &control							-90 %	220 %	-32 %	29 %	-55 %	
	Optimal pump &control							-87 %	368 %	-32 %	285 %	-36 %	

7.2.3 Tuusula

Hyrylä	Dry weather				Wet weather			
Pump	Original (kWh/d)	Optimal pump	Original & control	Optimal pump & control	Original (kWh/d)	Optimal pump	Original & control	Optimal pump & control
JVP25	96.16	1 %	306 %	364 %	400.75	0 %	56 %	503 %
JVP30	5.39	-96 %	93 %	94 %	0.12	17025 %	4858 %	4858 %
JVP26	8.15	-82 %	79 %	79 %	45.41	-71 %	-67 %	-39 %
JVP27	41.94	-85 %	1635 %	1614 %	19.76	-12 %	-100 %	-57 %
JVP22	14.82	-46 %	30 %	-7 %	82.94	116 %	-54 %	-6 %
JVP13	64.91	-77 %	-21 %	-12 %	159.61	78 %	0 %	78 %
JVP10	19.69	248 %	86 %	254 %	145.35	-51 %	-13 %	66 %
JVP31	3.00	42 %	753 %	701 %	117.30	-96 %	-77 %	-97 %
JVP3	0.81	279 %	8860 %	7969 %	45.70	0 %	-61 %	-47 %
JVP1	895.27	-84 %	209 %	137 %	1744.49	-97 %	382 %	-74 %
JVP14	53.34	-69 %	-80 %	-75 %	66.91	-28 %	6 %	-27 %
JVP7	20.3	-93 %	10 %	-2 %	2.12	-100 %	-100 %	-100 %

Jokela		JVP12	P146	P147	JVP4	JVP11	JVP8	P176	JVP1	P132	JVP7
Dry weather	Original (kWh/d)	42.50	0.24	0.00	99.48	16.97	111.50	0.54	86.67	1.15	0.24
	Optimal pump	-30 %	-29 %	-78 %	-5 %	425 %	-92 %	481 %	-65 %	159 %	-100 %
	Original & control	27 %	12066 %	-97 %	115 %	-16 %	-93 %	33 %	-92 %	3034 %	-100 %
	Optimal pump &control	-3 %	12070 %	-99 %	-54 %	-16 %	-83 %	15 %	-93 %	3013 %	-100 %
Wet weather	Original (kWh/d)	275.40	1.99	0.02	648.83	194.66	308.36	1.37	541.67	4.50	0.00
	Optimal pump	-16 %	1 %	-3 %	-23 %	9 %	-94 %	183 %	-41 %	33 %	-72 %
	Original &control	-31 %	218 %	-54 %	-40 %	-24 %	-96 %	-3 %	-43 %	429 %	-100 %
	Optimal pump &control	-30 %	218 %	-67 %	-48 %	-24 %	-93 %	-6 %	-57 %	432 %	-100 %
Ov	Original (kWh/d)	200.40	1.36	0.00	439.18	181.72	220.99	3.50	309.32	5.04	0.27

	Optimal pump	-3 %	1 %	-67 %	-16 %	0 %	-94 %	2 %	-28 %	-1 %	-6 %
	Original &control	-5 %	363 %	-53 %	1 %	-19 %	-94 %	-62 %	-17 %	748 %	-88 %
	Optimal pump &control	-4 %	363 %	-70 %	-24 %	-19 %	-91 %	-63 %	-32 %	848 %	-87 %

Kellokoski		JVP1	JVP2	JVP3	JVP4	JVP5
Dry weather	Original (kWh/d)	205.65	14.39	11.08	7.31	1.57
	Optimal pump	-10 %	-7 %	3 %	0 %	-54 %
	Original & control	-19 %	-71 %	33 %	0 %	101 %
	Optimal pump & control	-12 %	-70 %	39 %	0 %	101 %
Wet weather	Original (kWh/d)	994.25	58.02	30.15	12.04	4.30
	Optimal pump	-24 %	-1 %	-91 %	0 %	-13 %
	Original & control	-88 %	-73 %	-21 %	-55 %	45 %
	Optimal pump & control	124 %	-73 %	-21 %	-54 %	44 %
Overflow sce-.	Original (kWh/d)	220.72	18.27	14.42	9.34	1.38
	Optimal pump	17 %	-3 %	0 %	-97 %	1 %
	Original & control	33 %	-70 %	16 %	4 %	233 %
	Optimal pump & control	30 %	-71 %	17 %	-94 %	229 %